Doctor of Philosophy

A study on the synthesis of carbon dots by the bottom-up approach for various color emission

The Graduate School of the University of Ulsan

Department of Chemical Engineering and Bioengineering

Dang Dinh Khoi

A study on the synthesis of carbon dots by the bottom-up approach for various color emission

Supervisor: Professor Eui Jung Kim

A Dissertation

Submitted to

the Graduate School of the University of Ulsan

in partial Fulfillment of the Requirements

for the Degree of

Doctor of Philosophy

by

Dang Dinh Khoi

Department of Chemical Engineering

Ulsan, Korea

November 2017

A study on the synthesis of carbon dots by the bottom-up approach for various color emission

This certifies that the dissertation

of Dang Dinh Khoi is approved

Committee Chair Prof Seung Hyun Hur

Committee Member Prof Eui Jung Kim

Committee Member Prof Jin Suk Chung

Committee Member Prof Won Mook Choi

Committee Member Prof Mun Ho Kim

Department of Chemical Engineering

Ulsan, Korea

November 2017

Acknowledgements

First and foremost, I would like to express my extreme gratitude to my supervisor Professor Eui Jung Kim for giving me the opportunity to work in his lab with generous guidance, encouragement and support throughout the course of this work. Thanks to his kindly support, now I have overcome hard times in my research and finished the Ph.D. program here in the University of Ulsan.

I am very grateful to Professor Sung Hyun Hur for spending his valuable time and warm heart in guiding me for the final step of my study. His constructive suggestions, insightful advices and also his kindly support are a great help for me to complete my Ph.D. program.

I would like to thank all the members of my committee: Professor Jin Suk Chung, Professor Won Mook Choi, and Professor Mun Ho Kim for taking the time to read this dissertation, doing me the honor of serving on my committee, and providing the endless helpful suggestions and advices on the work.

A special thanks to Dr. Chandrasekaran Sundaram for his favorable helps and collaboration in experiments during my study. My gratitude is extended to Pham Thanh Truc, Nguyen Phu Huy, Do Thi Lien and Ngo Thi Yen Linh for all their helps, support and friendship. I would also like to thank all Vietnamese students in UOU in general and in the School of Chemical Engineering and Bioengineering in particular for their support and friendship.

I would like to acknowledge Ms. Kyoung Cho Lim for her kindly helps in the usage of many instruments in our department, and I also wish to thank the staff of the School of Chemical Engineering and Bioengineering for their support and helps.

Finally, I would like to express my deeply thank to my parents and my beloved family for their love and unconditional support throughout my graduate study.

Abstract

Carbon dots that exhibited various color emission including blue, cyan, and multicolor emission (blue, cyan, yellow and red) were successfully synthesized via bottom-up approach. In addition, the as-prepared carbon dots were applied as chemical sensing of heavy metal ion and toxic organic compound. There were also proposed mechanisms for the formation of carbon dots, mechanism for quenching effect, and photoluminescence of multicolor emission.

First, highly fluorescent N and S co-doped carbon dots (CDs) were synthesized in one pot using caffeine as a raw material via a facile, green and cost-effective solid-state method. It is found that when caffeine and a mixture of caffeine and urea were heated, the CDs were not produced. However, when a mixture of caffeine and ammonium persulfate was heated, the CDs were fabricated exhibiting blue fluorescence with a quantum yield of 38%. In addition, the formation of CDs was enhanced with excellent optical properties when urea was added to the mixture of caffeine and ammonium persulfate. Without further chemical modification, the CDs emitted bright blue fluorescence with a high quantum yield as high as 69% due to the enhancement effect of N and S co-dopants on the surface of the CDs. Owing to the strong blue fluorescence, the CDs fabricated in this study could be used effectively as a fluorescence probe for Ag^{+} ions that exhibited high sensitivity and selectivity.

Then, a green, facile, and one pot hydrothermal process was employed for fabricating highly fluorescent N-doped carbon dots (NCDs) using pyromellitic acid (PA) as a novel precursor. It is found that under hydrothermally treatment process of a solution of PA and ethylenediamine (EDA), the NCDs were successfully fabricated exhibiting brightly pure cyan color emission. Due to the enhancement effect of N dopant on the surface of the NCDs, it exhibited an excellent fluorescent property with a quantum yield of 75%. Moreover, owing to its highly cyan fluorescence, the newly synthesized NCDs could be effectively applied as a fluorescence platform for sensitive and selective determination of 4-nitrophenol (4-NP) without further chemical modification. Our experiments shown that the calibration curve, obtained from a Stern-

Volmer semilog plot, was linear within the range 0.1 to 100 μM 4-NP ($R^2 = 0.9993$), and the limit of detection (LOD) was calculated to be 17 nM 4-NP following IUPAC standard (3.3σ).

Lastly, multicolor emission carbon dots are fabricated via solvothermal method at mild temperature. In this process, pyromellitic acid is employed as a novel precursor and various diamines including aliphatic diamines (ethylenediamine; EDA) and aromatic diamines (ortho, meta, and para phenylenediamine; 2-, 3-, 4-PD) are employed as nitrogen sources. The synthesized carbon dots are exhibited multicolor emission including blue, cyan, yellow and red with a maxima PL emission at 409, 486, 554, and 615 nm when the additives changes from EDA to 3-, 2-, and 4-PD, respectively. The properties of these prepared carbon dots are studied and a hypothesis of their photo-luminescence is proposed.

Table of Contents

List of Figures

List of Schemes

List of Tables

Nomenclature

Abbreviations

0D	Zero-dimensional
1D	One-dimensional
2D	Two-dimensional
CDs	Carbon dots
CQDs	Carbon quantum dots
CNTs	Carbon nanotubes
CFs	Carbon nanofibers
D.I. water	Distilled water
DWNTs	Double-walled carbon nanotubes
EDTA	Ethylenediaminetetraacetic acid
E_m	Emission
E_x	Excitation
fcc	face-centered cubic lattice
F_0	The fluorescent intensity of blank CDs sample
F	The fluorescent intensity of CDs samples with the presence of heavy metal ions or toxic organic compounds
FTIR	Fourier-transform Infrared Spectra
FWHM	Full width at haft maximum
GO	Graphene oxide
hcb	honeycomb lattice
HOMO	Highest occupied molecular orbital
HR-TEM	High-resolution transmission electron microscopy
IUPAC	International Union of Pure and Applied chemistry
LCD	Liquid-crystal display
LEDs	Light-emitting diodes
LOD	Limit of detection
LOMO	Lowest unoccupied molecular orbital

MWCO	Molecular weight cut-off
MWNTs	Multi-walled carbon nanotubes
NHS	N-hydroxysuccinimide
nM	Nanomol L^{-1} (10^{-9} mol L^{-1})
NCDs	N doped carbon dots
NDs	Nanodiamonds
o-CDs	Carbon dots synthesized without urea
OLC	Onion-like carbon nanospheres
Para nitrophenol	4-NP
PEG-diamine	Polyoxyethylenebis (amine)
(m -, o -, p- PD)	(m -, o -, p - Phenylenediamine)
PL	Photoluminescence
PLE	Photoluminescence excitation
PA	Pyromellytic acid
QY	Quantum yield
RPM	Round per minute
SWNHs	Single-walled carbon nanohorns
SWNTs	Single-walled carbon nanotubes
TEM	Transmission electron microscopy
Tris-HMA	Tris (hydroxymethyl) aminomethane
u-CDs	Carbon dots synthesized with urea
UV	Ultraviolet
UV-vis	Ultraviolet-visible
XPS	X-ray photoelectron spectroscopy

Roman and Greek letters

E_g	Optical band gap energy (eV)
R^2	A correlation coefficient
σ	Standard deviation
λ	Wavelength (nm)
λ_{em}	Emission wavelength
λ_{ex}	Excitation wavelength
μM	Micromole L^{-1} (10^{-6} mol L^{-1})
Φ	Quantum yield

Chapter 1

Introduction

1.1 Background

Carbon is found to be the 4th most abundant element in the universe, the 15th most abundant element in the Earth's crust, and the 2nd most abundant element in the human being body by mass after oxygen [1]. In nature, carbon could be found in various forms or allotropes depending on its electronic configuration that enable it to hybridize three possible orbital hybridizations that are sp, sp^2, and sp^3 [2, 3]. Based on these distinct hybridizations, diverse unique combinations of chemical and physical properties are intrinsic to carbon-based materials i.e. high mechanical strength, low toxicity, thermal and electrical conductivity, good optical properties, and physicochemical properties [4]. Up to now, massive research have been dedicated to this field and various carbon-based materials have been investigated including graphene and graphene nanoribbons, carbon nanotubes (CNTs) and carbon nanofibers (CFs), single-walled carbon nanohorns (SWNHs), fullerenes and onion-like carbon nanospheres (OLC), nanodiamonds (NDs), and carbon dots (CDs), a new rising member in the carbon family. Due to their unique properties, these carbon-based materials have been applied in energy conversion and storage, catalysis, sensors, bioimaging, drug delivery and cancer therapy, optoelectronics, electrochemistry and so on [5-14].

Carbon nanoallotropes can be divided into two general groups based on the basis of the predominant types of covalent bonds linking their C atoms [15]. The first group includes the graphenic nanostructures, which are primarily made up of sp^2 carbon atoms that are densely packed in a hexagonal honeycomb crystal lattice. They may also involve some sp^3 carbon atoms at defect sites or edges. This group includes graphene, CNTs, SWNHs, OLC nanospheres, and CDs. The second group of carbon nanostructures contain both sp^3 and sp^2 carbon atoms in various ratios and have mixtures of amorphous and graphitic regions, or consist predominantly of sp^3 carbon atoms. Up to now, nano-diamond is the only known member of this group. However, some types of carbon dots with non-graphitic structures could also be regarded as

members. The key characteristic property of these nanostructures is that they are not built from graphene parts or monolayers such as CNTs or SWNHs.

It is also possible to classify carbon nanostructures depending on their morphological characteristics. The first category in this classification scheme would be nanostructures with empty internal spaces such as fullerene, CNTs, and SWNHs. These hollow nanostructures contain internal voids that can accommodate guest molecules, metals, atoms, or other nanostructures. In some special cases, they can even provide environments which could facilitate specific reactions. The second category is robust nanostructures which contain no internal spaces. Some carbon nanoallotropes such as NDs, OLC spheres, and CDs would belong to a separate second category under this scheme. In addition, graphene could also be added to this category because it has no internal spaces too.

A final approach for categorizing carbon nanostructures that is used in this dissertation is based on their dimensional structures. This scheme separates carbon nanoallotropes into (i) Two-dimensional (2D) carbon nanoallotropes such as graphene, and graphene nanoribbons. (ii) One-dimensional (1D) nanoallotropes such as carbon nanotubes (CNTs), carbon nanofibers (CFs), and single-walled carbon nanohorns (SWNHs), and (iii) Zero-dimensional (0D) carbon nanostructures such as fullerenes, onion-like carbon (OLC) structures, nanodiamonds, and carbon dots (CDs).

1.1.1 2D carbon nanoallotropes

1.1.1.1 Graphene

Graphene is a very abundant material because it is the building block of graphite which is one of the oldest materials and most widely used natural materials. In a graphene sheet every carbon atom is connected to three neighboring carbon atoms by covalent σ bonds, constructing a robust honeycomb lattice (hcb). It is found that the unhybridization p orbitals of the carbon atoms are oriented perpendicularly to the planar structure of the graphene sheet and interact with one another to form the half-full π band that gives graphene its aromatic character [16]. The quality of a synthesized graphene product depends on the method by which it was produced [17]. Usually methods that yield higher quality of graphene sheets are generally more expensive. Lower quality of

graphene sheets normally show poor electrical conductivity or mechanical strength due to defects or oxygen sites that are dispersed in the graphenic lattice [18]. More importantly, its nanoplatelets are usually limited in size, and it is often mixed with multilayered graphenic nanosheets.

Multilayer graphitic nanosheets (MGNs) consist of between 2 and 10 graphene monolayers [19]. Their properties are similar to those of graphene. MGNs can be dispersed in organic solvents, forming stable transparent suspensions.

1.1.1.2 Graphene nanoribbons

An alternative form of graphene monolayers is thin graphene ribbons that are currently receiving significant research attention. These thin elongated graphene monolayer strips that can be produced by "unzipping" CNTs have attracted numerous attention in research [20, 21]. Usually, graphene nanoribbons are described as a one-dimensional sp^2-hybridized carbon strip of finite dimension with defined edges. There are three types of graphene nanoribbons which are currently recognized depending on the edge termination: (i) armchair, (ii) zigzag, (iii) and chiral nanoribbons [22]. In some cases, graphene nanoribbons exhibit combination of different edges, which are termed hybrid graphene nanoribbons, mostly heterojunctions of armchair and zigzag patterns [23]. Similar to graphene, graphene nanoribbons can exhibit bilayered or few-layered arrangements in which more layers of finite graphene strips are stacked together. These carbon nanostructures are considered graphitic nanoribbons [22].

1.1.2 1D carbon nanoallotropes

1.1.2.1 CNTs and CFs

Carbon nanotubes, a general term that refers to a wide range of tubular carbon nanoallotropes with similar structures and shapes, were discovered and characterized several years before the isolation of graphene [24]. Ideally, they are based on a hexagonal lattice of sp^2 carbon atoms similar to that of graphene. However, in nanotubes, the edges of the graphene sheet are fused to form a cylindrical tube with a high aspect ratio. The simplest CNT has a single graphenic wall and is capped at both ends. Single-walled carbon nanotubes (SWNTs) have diameters of around 0.4–2 nm and are several micrometers long, with an empty internal space. CNTs can also be double-

walled (DWNTs) or multi-walled (MWNTs) carbon nanotubes depending on the number of graphenic layers in the walls of their cylindrical structure [25]. The aspect ratio (i.e. length-to-diameter ratio) of CNTs frequently exceeds 10 000, and therefore, carbon nanotubes are regarded as the most anisotropic materials ever produced. Besides diameter and length, chirality (the angle between the hexagons and the nanotube axis) is another important characteristic of the CNTs. Depend on the chirality, carbon atoms around the nanotube circumference can be organized into several structures that are armchair, zigzag, and chiral patterns, the most common examples.

Carbon nanofibers are described as a noncontinuous 1D carbon nanoallotrope of cylindrical or conical shape that are composed of stacked and curved graphene sheets arranging in various ways [26-28]. Long before the discovery of CNTs, they have been identified and extensively studied. They are frequently described as sp^2-based linear filaments with a diameter ranging from 50 to 200 nm and a high aspect ratio exceeding 100. Depend on the internal structure of them, several types of CFs have been recognized so far, that are [26, 27]: (i) platelet carbon nanofibers with graphene layers lying in a perpendicular manner with respect to the fiber axis; (ii) herringbone (or fishbone) CFs consisting of graphene sheets tilted to the fiber axis; (iii) ribbon (or tubular) CFs with graphene layers forming a stacked organization parallel to the fiber axis; (iv) stacked-up and cone-stacked carbon nanofibers with similar structure composed of truncated cones arranged to leave a hollow core; (v) cone-helix carbon nanofibers with a graphite layer forming a continuous helix-spiral architecture and with an internal hollow core. The main difference from CNTs is that CFs lack of hollow cavity in its structures.

1.1.2.2 Single walled nanohorns (WNHs)

SWNHs were discovered by Iijima in 1999 while studying the formation of CNT [29]. Nanohorns are tubule-like or cone-like structures that are made from graphene monolayer. Frequently, they appear in large spherical aggregates which are resembled dahlia flowers with diameter is around 80-100 nm. Individual nanohorns have diameters of 4-5 nm at the base of the cone and 1-2 nm at the tips. The distance between adjacent walls in SWNHs is measured to be around 0.4 nm. There are also other types of SWNH aggregations which are appeared in features of buds and seeds [30].

1.1.3 0D carbon nanoallotropes

1.1.3.1 Fullerenes and onion-like carbon (OLC)

Since the fullerenes were discovered, the study of carbon nanostructures was commenced. Generally, fullerenes are closed cages made of sp^2-hybridized carbon atoms arranged into 12 pentagons and a calculable number of hexagons that depends on the total number of carbon atoms. A fullerene with $20 + 2n$ carbon atoms will have n hexagons. C_{60} is a simple spherical molecule which takes the form of a truncated icosahedron containing 12 pentagons and 20 hexagons and all of its carbon atoms are sp^2-hybridized. Although its chemical properties are very similar to those of an organic molecule, C_{60} can be regarded as the smallest carbon nanostructure and a representative 0D carbon nanoallotrope. C_{60} can exist either as aggregates forms or a crystalline structure with a face-centered cubic (fcc) lattice in solid phase [15].

In addition, previous publications have discussed a fullerene-type graphitic nanoallotrope, a multi-shell spherical carbon nanostructure that is often called onion-like carbon (OLC) [31-33]. OLC structures consist of concentric graphenic shells such as giant fullerenes that enclose a series of progressively smaller fullerenes. They were first discovered by Ugarte [34] in a mixture of CNTs after irradiation with strong electron beam.

1.1.3.2 Nano diamonds (NDs)

Nanodiamonds are sp^3 carbon nanoparticles that consist of crystal domains with a diamond-like morphology and diameters which are greater than 1-2 nm but less than 20 nm [35]. Nanostructures of this type which have diameters above 20 nm behave like bulk diamonds. Conversely, sp^3 carbon nanostructures with diameters of less than 1 nm are usually called diamondoids and occur naturally in petroleum deposits [36]. The sp^3-hybridized surface-bound carbon atoms of these small diamondoids are normally bonded to hydrogen or other non-carbon atoms. As a consequence, their properties resemble those of organic molecules rather than bulk diamonds. However, they are often dominated by intense signals arising from impurities containing sp^2-hybridized carbon atoms; therefore, extremely purify nanodiamond samples are needed [15].

1.1.3.3 Carbon dots

Carbon dots (also referred to as carbon quantum dots or carbon nanodots, abbreviated as C-dots or CDs) are a class of carbon based fluorescent nanomaterials [37]. The discovery of CDs can be traced back to a 2004 report on the component of fluorescent nanoparticles derived from the single-wall carbon nanotubes (SWNTs) and separated by gel electrophoresis [38]. Till 2006, Sun et al. [39] produced fluorescent carbon nanoparticles by chemical synthesis via laser ablation of a carbon target and surface passivation. These nanoparticles were endowed with their proper name of ‘‘carbon dots’’ for the first time. After that, there have been extensive investigations by many research groups around the globe and publications on this topic are progressively increasing [40-42].

Generally, CDs are spherical (quasi-spherical) or disk like carbon nanoparticles that comprise amorphous to nanocrystalline core with the average size has been reported to be usually less than 10 nm [43]. It has been demonstrated that the inner part of CDs is primarily composed of sp^2-hybridized carbon atoms while in the outer part sp^3-hybridized carbon atoms are presented, as inferred from nuclear magnetic resonance (NMR) measurements [44].

In recent years, CDs have attracted highly interesting of the research community for their high performance, easily available and cheap precursors, facile synthesis approaches, and potential applications in a wide area. The high performances of CDs are universally believed to include excellent photostability, favorable biocompatibility, low toxicity, outstanding water solubility, high sensitivity and excellent selectivity to target analytes, tunable fluorescence emission and excitation, high quantum yield (QY) [44-46]. Therefore, CDs are promising as a competitive alternative for heavy metal based quantum dots (QDs) and organic dyes.

1.2 Motivation

It is noticeable that although extensive investigation on the synthesis and application of carbon dots can be found in literature since its first discovery in 2004, the photoluminescence of these reported synthesized carbon dots are usually in blue color emission and also exhibited low quantum yields. Furthermore, most of these reported carbon dots are fabricated using carbohydrates, citric acid and its relatives, and natural organic materials as precursors. More importantly, it has been noticed that there were just a few papers reported synthesis of multicolor emission carbon dots and their photoluminescence mechanisms.

1.3 Objectives

It was interesting and also challenging for synthesizing highly photoluminescence carbon dots which are exhibited longer wavelength excitation and emission, especially multicolor emission carbon dots. Therefore, the first objective of the research described in this dissertation is to synthesize carbon dots by employing novel precursors via various approaches such as solid-state, hydrothermal and solvothermal methods. The second objective is to fabricate newly carbon dots which possess highly quantum yields and ideally exhibited longer photoluminescence emission and excitation. Those as-prepared carbon dots then applied as chemical sensor for detection of heavy metal ions or toxic organic compounds. The third objective of this dissertation is to synthesize multicolor emission carbon dots using new precursor and propose their photoluminescence mechanism.

1.4 Organization of dissertation

The following chapters delineate the results undertaken to achieve the objectives of this dissertation:

In chapter 2, the overview of luminescent carbon dots including “bottom-up” synthesis approaches, properties and sensing applications is presented.

In chapter 3, highly fluorescent N and S co-doped carbon dots were fabricated by a facile, one pot solid-state approach using caffeine as a new precursor. These as-prepared carbon dots exhibited bright blue color emission and were applied as a selective and sensitive fluorescence platform for the detection of Ag^{+} in aqueous media. The chapter has been accepted to publish as a full research article in a peer review journal of Sensor and Actuator B: Chemical.

In chapter 4, highly fluorescent N doped carbon dots were fabricated by a green, facile, one pot hydrothermal method using a novel precursor, pyromellitic acid. These synthesized carbon dots exhibited highly pure cyan color emission and were employed as nanoprobes for sensitive and selective determination of 4-nitrophenol. The chapter has been finished in manuscripts and is projected to submit as a full research article in a peer review journal of Sensor and Actuator B: Chemical.

In chapter 5, multicolor emission carbon dots are synthesized via solvothermal method at mild temperature in which pyromellitic acid is employed as a novel precursor and various diamines including aliphatic diamines (ethylenediamine; EDA) and aromatic diamines (ortho, meta, and para phenylenediamine; 2-, 3-, 4-PD) are employed as nitrogen sources. This paper is preparation and data are collecting to fully characterize properties of the multicolor CDs and also propose its photoluminescence mechanism.

In chapter 6, the findings of the work undertaken in this dissertation were summarized. Also, suggestions on future directions of the carbon dots research were outlined.

1.5 References

[1] Reece, J. B., Urry, L. A., Cain, M. L. 1., Wasserman, S. A., Minorsky et al., Campbell Biology. Tenth edition. Boston: Pearson, 2014.

[2] Y. Su, Y. Zhang, Carbon nanomaterials synthesized by arc discharge hot plasma, Carbon, 83(2015) 90-9.

[3] J.-T. Wang, C. Chen, Y. Kawazoe, New Carbon Allotropes with Helical Chains of Complementary Chirality Connected by Ethene-type π-Conjugation, 3(2013) 3077.

[4] B.-T. Zhang, X. Zheng, H.-F. Li, J.-M. Lin, Application of carbon-based nanomaterials in sample preparation: A review, Analytica Chimica Acta, 784(2013) 1-17.

[5] E. Frackowiak, F. Béguin, Carbon materials for the electrochemical storage of energy in capacitors, Carbon, 39(2001) 937-50.

[6] F. Bonaccorso, L. Colombo, G. Yu, M. Stoller, V. Tozzini, A.C. Ferrari, et al., Graphene, related two-dimensional crystals, and hybrid systems for energy conversion and storage, Science, 347(2015).

[7] J.L. Figueiredo, M.F.R. Pereira, Carbon as Catalyst, Carbon Materials for Catalysis, John Wiley & Sons, Inc.2008, pp. 177-217.

[8] M.D. Angione, R. Pilolli, S. Cotrone, M. Magliulo, A. Mallardi, G. Palazzo, et al., Carbon based materials for electronic bio-sensing, Materials Today, 14(2011) 424-33.

[9] A.K. Wanekaya, Applications of nanoscale carbon-based materials in heavy metal sensing and detection, Analyst, 136(2011) 4383-91.

[10] S.C. Ray, A. Saha, N.R. Jana, R. Sarkar, Fluorescent Carbon Nanoparticles: Synthesis, Characterization, and Bioimaging Application, The Journal of Physical Chemistry C, 113(2009) 18546-51.

[11] A. Bianco, K. Kostarelos, M. Prato, Applications of carbon nanotubes in drug delivery, Current Opinion in Chemical Biology, 9(2005) 674-9.

[12] Z. Liu, J.T. Robinson, S.M. Tabakman, K. Yang, H. Dai, Carbon materials for drug delivery & cancer therapy, Materials Today, 14(2011) 316-23.

[13] P. Avouris, Z. Chen, V. Perebeinos, Carbon-based electronics, 2(2007) 605.

[14] D. Chen, L. Tang, J. Li, Graphene-based materials in electrochemistry, Chemical Society Reviews, 39(2010) 3157-80.

[15] V. Georgakilas, J.A. Perman, J. Tucek, R. Zboril, Broad Family of Carbon Nanoallotropes: Classification, Chemistry, and Applications of Fullerenes, Carbon Dots, Nanotubes, Graphene, Nanodiamonds, and Combined Superstructures, Chemical Reviews, 115(2015) 4744-822.

[16] J.C. Meyer, C. Kisielowski, R. Erni, M.D. Rossell, M.F. Crommie, A. Zettl, Direct Imaging of Lattice Atoms and Topological Defects in Graphene Membranes, Nano Letters, 8(2008) 3582-6.

[17] Y. Hernandez, V. Nicolosi, M. Lotya, F.M. Blighe, Z. Sun, S. De, et al., High-yield production of graphene by liquid-phase exfoliation of graphite, 3(2008) 563.

[18] G. Wang, J. Yang, J. Park, X. Gou, B. Wang, H. Liu, et al., Facile Synthesis and Characterization of Graphene Nanosheets, The Journal of Physical Chemistry C, 112(2008) 8192-5.

[19] A.B. Bourlinos, T.A. Steriotis, R. Zboril, V. Georgakilas, A. Stubos, Direct synthesis of carbon nanosheets by the solid-state pyrolysis of betaine, Journal of Materials Science, 44(2009) 1407-11.

[20] D.V. Kosynkin, A.L. Higginbotham, A. Sinitskii, J.R. Lomeda, A. Dimiev, B.K. Price, et al., Longitudinal unzipping of carbon nanotubes to form graphene nanoribbons, Nature, 458(2009) 872-6.

[21] A. Sinitskii, A. Dimiev, D.V. Kosynkin, J.M. Tour, Graphene Nanoribbon Devices Produced by Oxidative Unzipping of Carbon Nanotubes, ACS Nano, 4(2010) 5405-13.

[22] M. Terrones, A.R. Botello-Méndez, J. Campos-Delgado, F. López-Urías, Y.I. Vega-Cantú, F.J. Rodríguez-Macías, et al., Graphene and graphite nanoribbons: Morphology, properties, synthesis, defects and applications, Nano Today, 5(2010) 351-72.

[23] X. Jia, M. Hofmann, V. Meunier, B.G. Sumpter, J. Campos-Delgado, J.M. Romo-Herrera, et al., Controlled Formation of Sharp Zigzag and Armchair Edges in Graphitic Nanoribbons, Science, 323(2009) 1701-5.

[24] S. Iijima, Helical microtubules of graphitic carbon, Nature, 354(1991) 56-8.

[25] Y.A. Kim, H. Muramatsu, T. Hayashi, M. Endo, M. Terrones, M.S. Dresselhaus, Fabrication of High-Purity, Double-Walled Carbon Nanotube Buckypaper, Chemical Vapor Deposition, 12(2006) 327-30.

[26] M. Inagaki, Y. Yang, F. Kang, Carbon Nanofibers Prepared via Electrospinning, Advanced Materials, 24(2012) 2547-66.

[27] A. Ramos, I. Cameán, A.B. García, Graphitization thermal treatment of carbon nanofibers, Carbon, 59(2013) 2-32.

[28] P. Serp, M. Corrias, P. Kalck, Carbon nanotubes and nanofibers in catalysis, Applied Catalysis A: General, 253(2003) 337-58.

[29] S. Iijima, M. Yudasaka, R. Yamada, S. Bandow, K. Suenaga, F. Kokai, et al., Nano-aggregates of single-walled graphitic carbon nano-horns, Chemical Physics Letters, 309(1999) 165-70.

[30] Yudasaka, M.; Iijima, S.; Crespi, V. H. In Carbon Nanotubes; Jorio, A.; Dresselhaus, G.; Dresselhaus, M. S., Eds.; Topics in Applied Physics, Vol. 111, Springer-Verlag: Berlin, Heidelberg, Germany, (2008) 605-29.

[31] D. Pech, M. Brunet, H. Durou, P. Huang, V. Mochalin, Y. Gogotsi, et al., Ultrahigh-power micrometre-sized supercapacitors based on onion-like carbon, 5(2010) 651.

[32] Y.V. Butenko, S. Krishnamurthy, A.K. Chakraborty, V.L. Kuznetsov, V.R. Dhanak, M.R.C. Hunt, et al., Photoemission study of onionlike carbons produced by annealing nanodiamonds, Physical Review B, 71(2005) 075420.

[33] F. Banhart, P.M. Ajayan, Self-compression and diamond formation in carbon onions, Advanced Materials, 9(1997) 261-3.

[34] D. Ugarte, Curling and closure of graphitic networks under electron-beam irradiation, Nature, 359(1992) 707-9.

[35] O.A. Williams, Nanocrystalline diamond, Diamond and Related Materials, 20(2011) 621-40.

[36] J.E. Dahl, S.G. Liu, R.M.K. Carlson, Isolation and Structure of Higher Diamondoids, Nanometer-Sized Diamond Molecules, Science, (2002).

[37] W. Liu, C. Li, Y. Ren, X. Sun, W. Pan, Y. Li, et al., Carbon dots: surface engineering and applications, Journal of Materials Chemistry B, 4(2016) 5772-88.

[38] X. Xu, R. Ray, Y. Gu, H.J. Ploehn, L. Gearheart, K. Raker, et al., Electrophoretic Analysis and Purification of Fluorescent Single-Walled Carbon Nanotube Fragments, Journal of the American Chemical Society, 126(2004) 12736-7.

[39] Y.-P. Sun, B. Zhou, Y. Lin, W. Wang, K.A.S. Fernando, P. Pathak, et al., Quantum-Sized Carbon Dots for Bright and Colorful Photoluminescence, Journal of the American Chemical Society, 128(2006) 7756-7.

[40] P.G. Luo, S. Sahu, S.-T. Yang, S.K. Sonkar, J. Wang, H. Wang, et al., Carbon "quantum" dots for optical bioimaging, Journal of Materials Chemistry B, 1(2013) 2116-27.

[41] H. Li, Z. Kang, Y. Liu, S.-T. Lee, Carbon nanodots: synthesis, properties and applications, Journal of Materials Chemistry, 22(2012) 24230-53.

[42] S.Y. Lim, W. Shen, Z. Gao, Carbon quantum dots and their applications, Chemical Society Reviews, 44(2015) 362-81.

[43] B. Garg, T. Bisht, Carbon Nanodots as Peroxidase Nanozymes for Biosensing, Molecules, 21(2016) 1653.

[44] H. Liu, T. Ye, C. Mao, Fluorescent Carbon Nanoparticles Derived from Candle Soot, Angewandte Chemie International Edition, 46(2007) 6473-5.

[45] S.N. Baker, G.A. Baker, Luminescent Carbon Nanodots: Emergent Nanolights, Angewandte Chemie International Edition, 49(2010) 6726-44.

[46] J. Shangguan, J. Huang, D. He, X. He, K. Wang, R. Ye, et al., Highly Fe^{3+}-Selective Fluorescent Nanoprobe Based on Ultrabright N/P Codoped Carbon Dots and Its Application in Biological Samples, Analytical Chemistry, 89(2017) 7477-84.

Chapter 2

Overview of Luminescent Carbon Dots: "Bottom-up" Synthesis Methods, Properties and Sensing Applications

2.1 Introduction

This chapter presents literature review on the CDs as the newest member in the carbon nanostructures family that are emerging as an excellent alternative to traditional semiconductor quantum dots in various applications especially in chemical sensor and environmental related fields. CDs have attracted great attentions from the research community because they exhibit excellent biocompatibility, low toxicity, high chemical stability and photostability. The synthetic approaches, especially the bottom-up synthetic routes, and also the physical, chemical, and optical properties of CDs will be described in details. Moreover, the applications of these CDs in the field of chemical sensors will also be reviewed.

2.2 Synthesis of carbon dots via "bottom-up" methods

The fluorescent carbon dots were first discovered by Xu et al. when they were purifying single-walled carbon nanotubes (SWCNTs) from arc-discharged soot [1]. From that time on, various synthetic approaches have been developed for the preparation of CDs. Most of previous reports are focusing on approaches that are green, facile, cost-effective, size-controllable and large scale methods to obtain CDs of advanced functions with various compositions and structures. Depending on the direction of size development of the starting materials, the synthesis of CDs can be generally divided into two kinds of approaches that are "top-down" and "bottom-up". The "top-down" approach, on one hand, fabricate CDs form bulk structures of carbon such as graphite, activated carbon, and carbon nanotubes by treatments such as arcdischarge [1], laser ablation [2], electrochemical oxidation [3], chemical oxidation [4], and ultrasonic method [5]. On the other hand, bottom-up approaches synthesize CDs from molecular precursors for example citric acid, glucose, and other carbohydrates using thermal decomposition [6], hydrothermal or solvothermal treatment [7, 8], microwave synthesis [9], and ultrasonic method [10] and so on.

Comparing to the “top-down” approaches, the bottom-up approaches have obvious advantages in turning the composition and photo properties (such as high yields and quantum yields) by careful selection of precursors and carbonization conditions. In this chapter some representative “bottom-up” methods for preparation of CDs will be described in details.

2.2.1 Thermal heating method

Previously, thermal decomposition has been employed for fabricating different semiconductor and magnetic nanomaterials. Recently, numerous studies have reported that external heat can contribute to the dehydration and carbonization of organic molecules and turn them into CDs. This method has advantages of facile, solvent free, wide precursor tolerance, economical and scalable production. For instant Chen et al. reported green synthesis of water-soluble CNDs with multicolor photoluminescence from polyethylene glycol by a simple one-pot thermal treatment [11]. In the formation of such CNDs, PEG played two essential roles that are the carbon source and surface passivating agent. The as-prepared CNDs shown to be soluble in water and common organic solvents, and emitted bright multicolor fluorescence with excitation and pH dependent emission properties (Scheme 2.1).

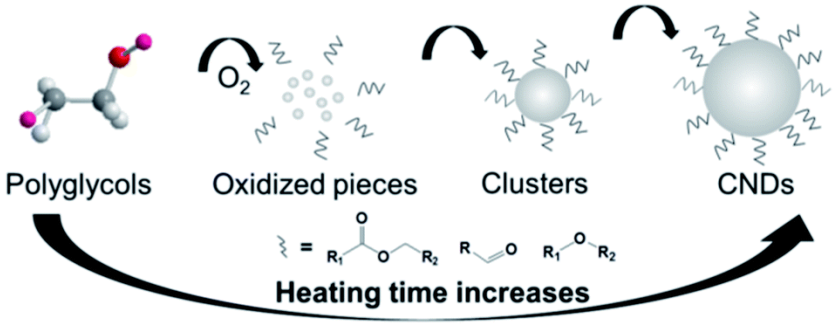

Scheme 2.1 Formation of NCDs via thermal decomposition method [11]

2.2.2 Hydrothermal or solvothermal method

Hydrothermal carbonization is a facile, economical, and environmentally friendly route to produce novel carbon-based materials from saccharides, carbohydrates, organic acids, and natural materials. In general, a solution of organic precursor is sealed and reacted in a stainless steel autoclave reactor which is then heated to a designed temperature and kept for an intentional period of time.

Yuan et al. [12] reported bright multicolor fluorescent CDs by simply controlling the fusion and carbonization of citric acid and diaminonaphthalene under solvothermal method at 200^{o}C in a various time (Scheme 2.2). The synthesized CDs exhibited multicolor emission of blue, green, yellow, orange, and red with the PLs were centered at 430, 513, 535, 565, and 604 nm, respectively.

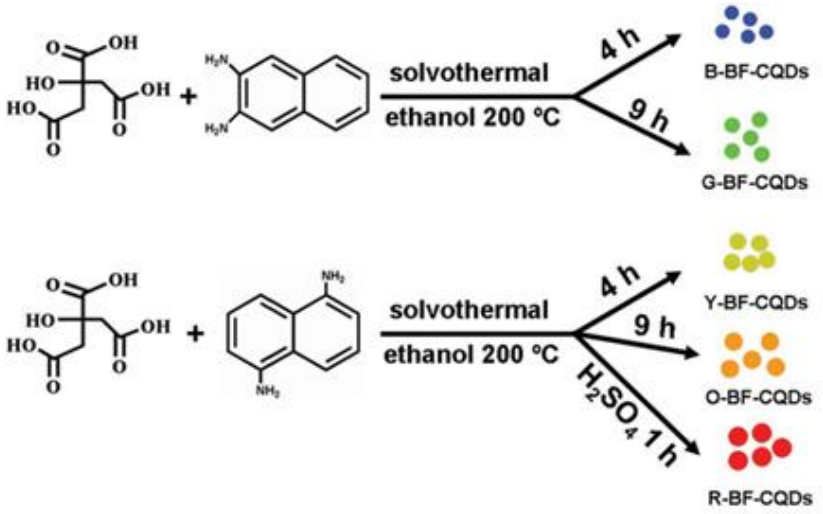

Scheme 2.2 Solvothermal synthetic route of multicolor emission CDs, which are blue, green, yellow, orange, and red from up to down, respectively [12]

2.2.3 Microwave assisted method

Microwave, a type of electromagnetic with a large wavelength range from 1 mm to 1m commonly used in daily life and scientific research, is capable to provide intensive energy break off the chemical bonds of the precursors. Thus, microwave assisted method is considered an energy efficient approach for producing CDs. Moreover, the reaction time for synthesizing CDs by microwave assisted method may be extremely reduced. In general, microwave assisted method including the pyrolysis and functionalization of the reactants.

A fast large-scale synthesis of fluorescent carbon dots (CDs) without high temperature or high pressure has been developed by Wang et al. [13]. Using benzenediols (catechol, resorcinol and hydroquinone) as the carbon precursor and sulfuric acid as the catalyst, three distinct CDs with strong and stable luminescence were prepared via a microwave-assisted method within 2 min (Scheme 2.3).

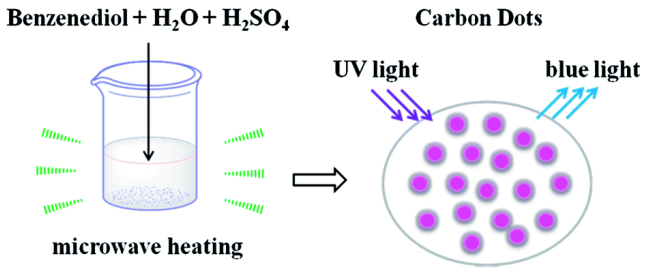

Scheme 2.3 Microwave assisted synthetic route of fluorescent CDs [13]

2.2.4 Ultrasonic method

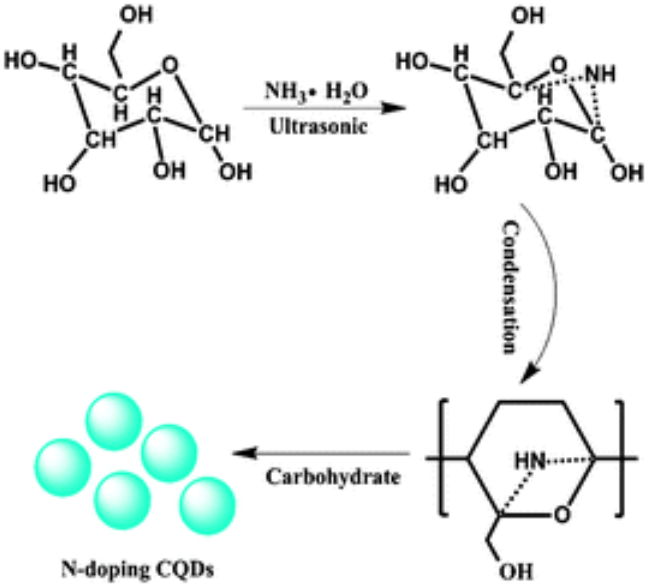

Scheme 2.4 The formation process of the NCDs [14]

Some organic materials under ultrasonic irradiation will go through the process of dehydration, polymerization, and carbonization successively leading to the formation of nucleation. Thus, ultrasonic synthetic methods for preparing CDs are developed. For example water-soluble fluorescent N-doped carbon dots (NCDs) were synthesized via a facile one-pot ultrasonic reaction between glucose and ammonium hydroxide was reported by Ma et al. [14]. In this process, a suitable amount (2.0 g) of glucose was added to aqua ammonia (30%, 40 mL) and deionized water (100 mL) to form an achromatic suspension which is then ultrasonic treated for 24 h at room temperature.

2.2.5 Other “bottom-up” methods

Li et al. reported a facile and versatile molten salt method to prepare hydrosoluble carbon dots from various precursors with high yield and large scale [15]. Citric acid and other precursors such as sodium lignosulphonate, sucrose, glucose, and *p*-phenylenediamine were used as a precursor in the eutectic mixture of $NaNO_3/KNO_3/NaNO_2$ (7:53:40 mass ratio) with a melting point of 140°C.

Chen et al. developed a process to synthesize carbon quantum dots (CQDs) on a large scale by using hydroquinone and ethylenediamine (EDA) as the precursors and the EDA-catalyzed decomposition of hydrogen peroxide at room temperature (Scheme 2.5) [16].

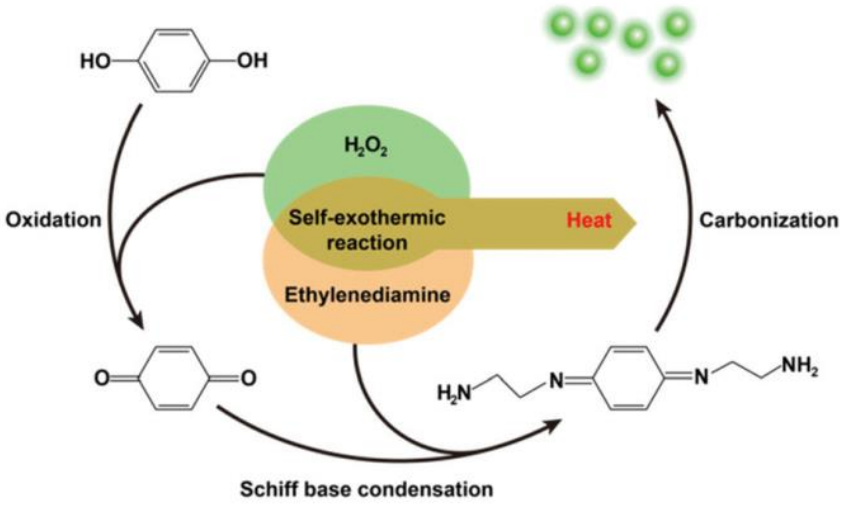

Scheme 2.5 Reaction process of core–shell structural CQDs at room temperature

Li et al. reported a simple, fast, energy and labor efficient for synthesizing CDs which involving only the mixing of a saccharide and base [17]. This process produced uniform and green luminescent carbon dots with an average size of 3.5 nm without the need for additional energy input or external heating.

The electrochemical synthesis was also used for producing CDs. In this method, the electrochemical carbonization of low-molecular-weight compounds (alcohols under basic conditions) and the size of the resultant CDs could be adjustable by changing the synthesis potential [18].

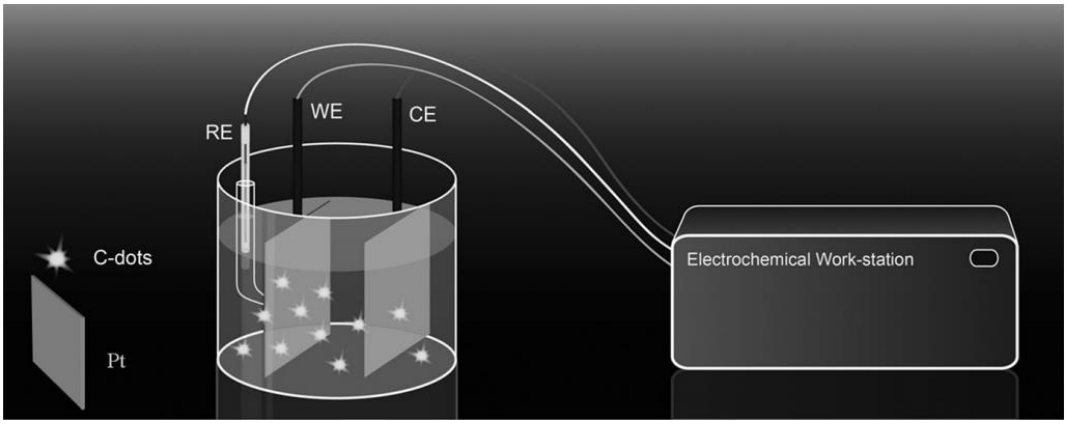

Scheme 2.6 Electrochemical synthesis of C-dots [18]

2.3 Physical and chemical properties of carbon dots

2.3.1 Morphology and structure of carbon dots

Although different synthetic methods have been developed, it is still challenged for controlling the shape and size of CDs. All the synthesized CDs are either spherical (quasi-spherical) of flat disk in shape and the typical size of CDs is usually less than 10 nm. In addition, it was also reported that the size of the as-prepared CDs could be as large as 800 nm [19].

It is noticeable that the particles size of CDs is mostly independent on the synthesis method as well as precursors. For instant, the synthesis of CDs by laser ablation method using either graphite with size less than 2 μm or nanocarbon with size less than 50 nm as precursors created the same size of CDs [20, 21].

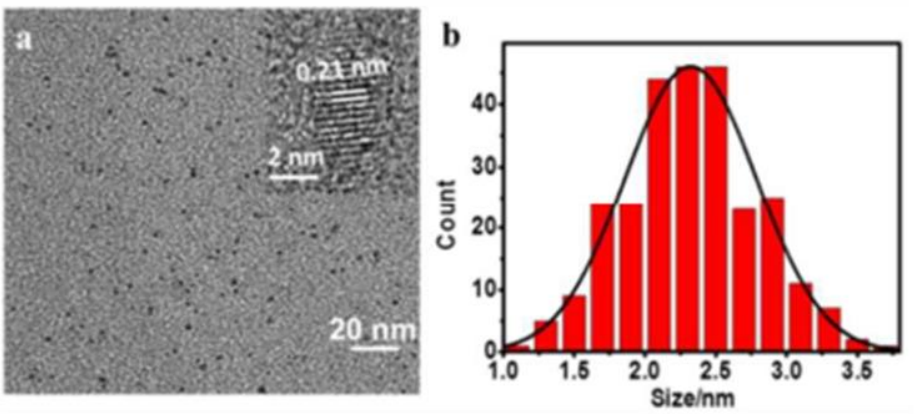

Fig. 2.1 (a) TEM image of the CDs (insert is the HRTEM image of one nanoparticle); and (b) the size distribution of CDs [15]

Transmission electron microscopy (TEM) has been a primary technique for visualization of CDs, providing important information upon particle morphology, size distribution, and crystalline organization. High-resolution TEM (HRTEM) experiments have been applied to confirm the periodicity of the graphitic core, reflecting its crystalline nature. For carbon dots, the corresponding structure could be crystalline, amorphous or crystalline with partly amorphous. Fig. 2.1 presents a TEM and HRTEM image of an example CDs. The TEM demonstrated that CDs are well-dispersed and have a narrow size distribution with an average size of ~2.4 nm. The HRTEM shown that the lattice spacing of CDs is 0.21 nm, which corresponds to the (100) facet of graphitic carbon [15].

2.3.2 Composition of carbon dot

Generally, luminescent CDs are composed of a carbon core and surface functional groups binding to the surface of the CDs. The basic elements of luminescent CDs are C, H, and O in the form of carbon core, carboxyl groups and hydroxyl groups which attached on the surface of the CDs. In addition, there are some doping element such as B [22], P [23], S [24], and especially N [12, 14], the most popular doping element in CDs that introduced N atom to carbon lattice or functional groups such as NH_2, CONH, or NO_x to the surface of the CDs. There are also publications on synthesis of co-doping CDs, for instant N, S co-doped CDs [7]. Recently, doping CDs with metal elements such as Cu [25], Zn [26] or Se [27] are also reported. Previous reports have shown that the emission properties of the CDs could be modulated by functionalization of the CDs with various types of organic molecules or solvents.

Elucidating the functional groups upon CDs' surfaces is accomplished through application of several widely used analytical methods. X-ray photoelectron spectroscopy (XPS) provides information upon specific atomic units present upon CDs' surface. An example of an XPS analysis is provided in Fig. 2.2 [28]. The spectral analysis reveals the distinct nitrogen-, oxygen-, and carbon-bonded units displayed upon the CDs' surface. Fourier transform infrared (FTIR) spectroscopy usually complements XPS, illuminating distinct functional units through recording of typical vibration bands (Fig. 2.3) [29].

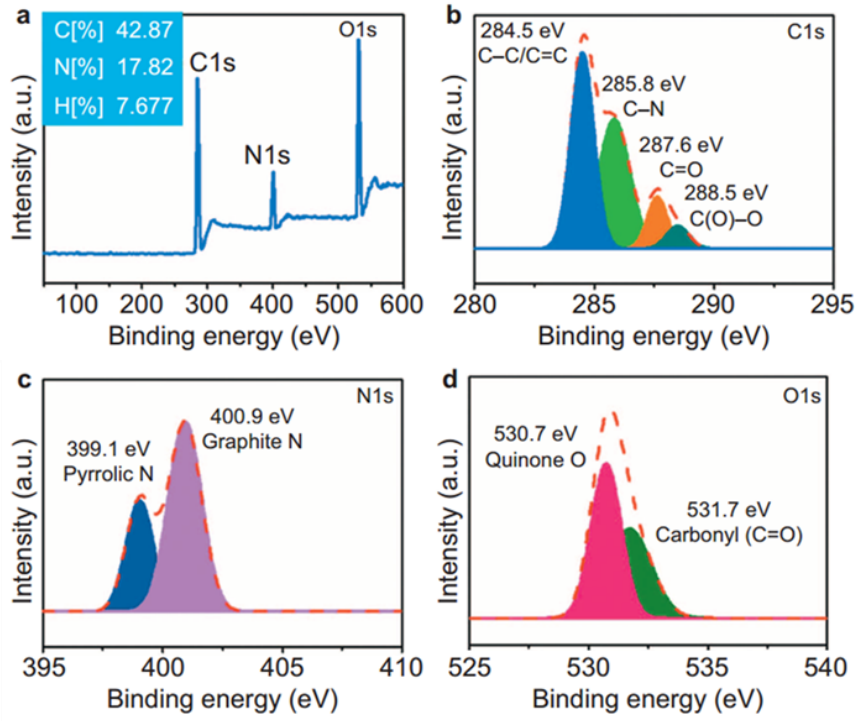

Fig. 2.2 (a-d) XPS (full survey, C_{1s}, N_{1s}, and O_{1s}, respectively) of N-GQDs (insets of (a) is the element amount from element analysis) [28]

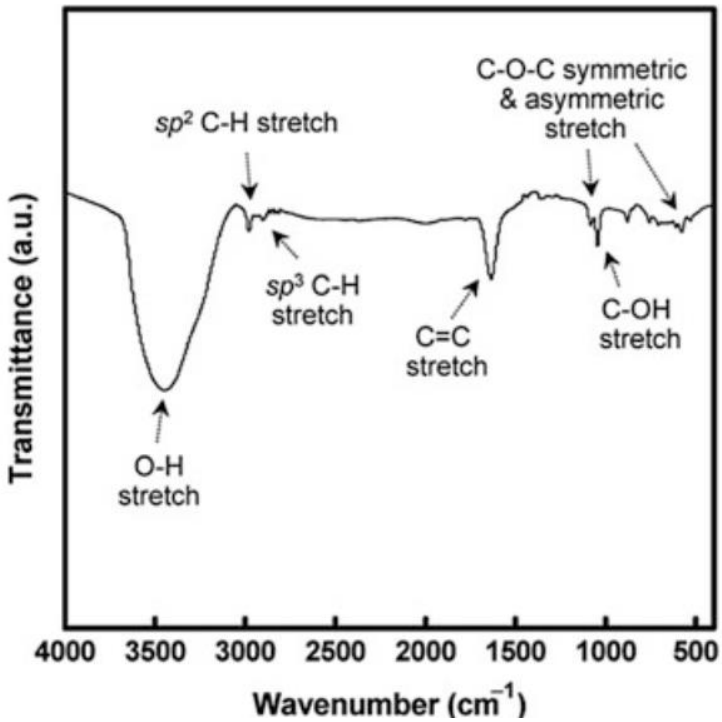

Fig. 2.3 FTIR spectrum of a CD sample (distinct vibration bands corresponding to CDs' surface units are indicated) [29]

2.3.3 Optical properties of carbon dots

2.3.3.1 Absorbance

According to previous reports, CDs are effective in photon-harvesting in short-wavelength region because of π-π* transition of C=C bonds, thus they typically show strong optical absorption in the UV region (260–320 nm), with a tail extending into the visible range [30, 31]. The positions of the UV absorption peaks of CDs prepared by different methods are quite different. In the case of longer wavelength color emission or multicolor emission CDs, the absorption profiles of them may demonstrate multiple electronic absorption transitions and could be assigned to π-π* transition of C=C bonds from the aromatic sp^2 domains and (n-π*) transition of functional groups C-O/C=O and the transition of conjugated C-N/C=N [28].

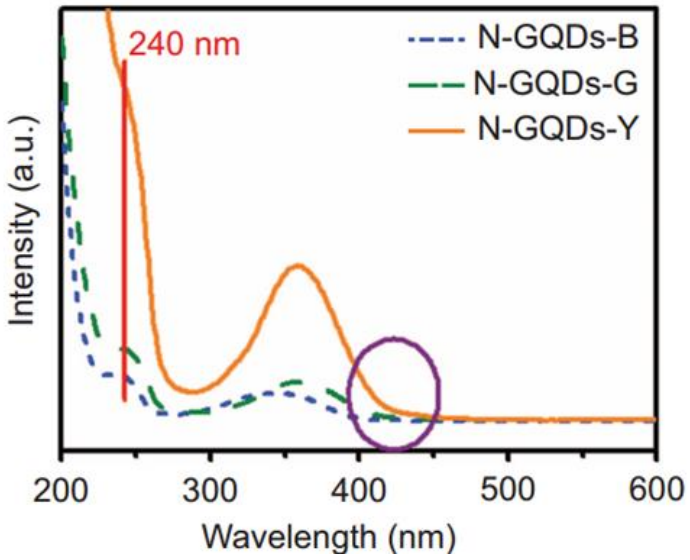

Fig. 2.4 UV-vis spectra of CDs sample [28]

2.3.3.2 Photoluminescence (PL)

CDs with different color from blue to red have been synthesized and most common are blue and green, which in many cases show wide emission spectra due to the hetetogeneity in chemical composition and size. Frequently, the PL intensity maximum of CDs red-shifts as the excitation wavelength increases exhibiting excitation dependent emission wavelength and intensity [32]. As shown in Fig. 2.5, the PL spectra of nitrogen-doped CDs show excitation shifts by changing the

excitation wavelength from 290 to 460 nm, along with a notable change of the PL intensities [33]. CDs have only one maximum emission which is excited by the only maximum excitation. The excitation-independent fluorescence behavior has also emerged, which may be attributed to their uniform size and surface chemistry [34], and the intensity of fluorescence increased to the maximum and then decreased (Fig. 2.5) [33]. In general, the PL emission spectra of CDs are symmetrical in the main, with large Stokes shifts as compared with that of organic dyes [35]. In addition, previous reports have shown that by adjusting the synthetic routes, CDs which exhibited PL in the visible-to-near infrared (NIR) spectral range can also be achieved [14]. The NIR PL emission is particularly useful that makes CDs suitable for the imaging of biological samples with deeper depths in the NIR window. Moreover, PL from CDs can also be quenched by electron acceptors or donors. The photo-induced electron transfer properties of CDs made them being promising materials for applications in energy conversion.

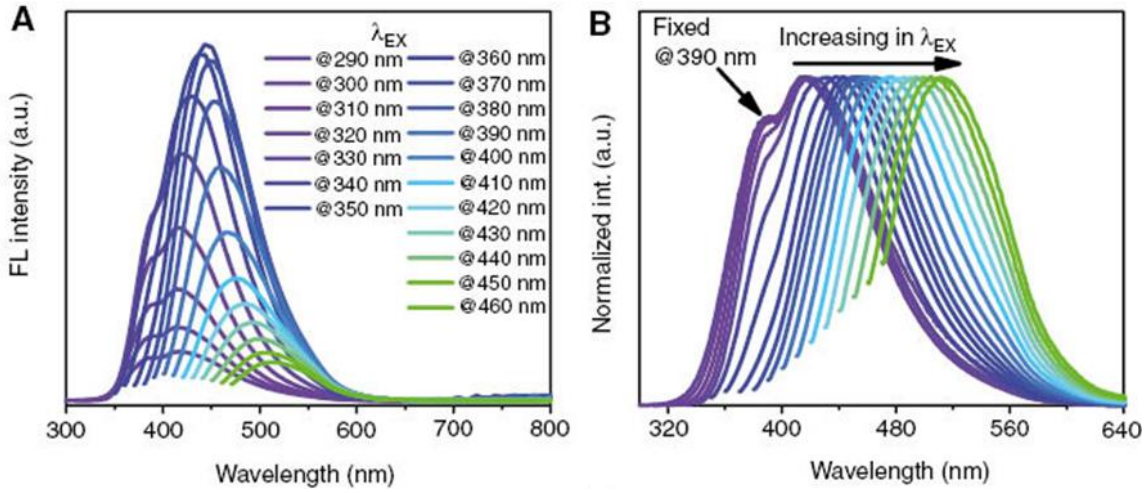

Fig. 2.5 (a, b) PL and normalized PL spectra of a CDs sample [33]

2.3.3.3 Quantum yields (QY)

Quantum yield (QY) is a significant parameter to characterize PL. The PL quantum yield (QY) of bare CDs is usually very low (typically <10%) due to the emissive traps on the surface. To increase the QY, a number of methods have been developed, such as passivation [36], doping with other elements [37], and purification processes. For example, Sun et al. functionalized CDs with diamine-terminated

oligomeric PEG (PEG_{1500N}) or poly (propionylethyleneimine-co-ethyleneimine) (PPEI-EI) to obtain the products which yielded bright emissions (4–10%) [2]. Another route that proposed by Zheng is a reductive pathway to promote the QY from 2% to 24% via treating the CDs with $NaBH_4$ [38]. In addition, Qu et al. fabricated N doped CDs exhibiting almost the highest QY of 94% [39].

2.3.3.4 Fluorescent mechanisms

Up to now, many groups have proposed various mechanisms to uncover the fluorescent origin of CDs, which may guide tuning the performance of the CDs. In Pan's opinion, the fluorescence is assigned to the free zigzag sites with a carbine-like triplet ground stage [40]. Afterwards, Zhu et al. hypothesized that the coexistence of defect state emission and intrinsic state emission and their competitive emission centers lead to green and blue emission, explaining most of the fluorescent features [41]. Another hypothesis made by Liu et al. assumed that the π-π electron transition contributes to the fluorescence and strong electron donating effect of functional groups can boost the charge transfer efficiency [42]. Moreover, the size of CDs is also thought to be the possible reasons for the excitation-dependent phenomenon that fluorescent emissions can red-shift as the increase of the excitation wavelength [43]. Hu et al. synthesized a series of CDs by changing the reagents and reaction conditions and proposed that the surface epoxides or hydroxyls were predominantly responsible for the resulting PL red shift [44]. More recently, Ding et al. also hypothesized that red shift of the emission peaks of CDs, changing from 440 to 625 nm, was attributed to a gradual reduction of band-gap with increasing incorporation of oxygen species into the surface functional groups [45]. However, after years of intensive researches, the exact mechanism for the PL of carbon dots is still under debate.

2.4 Applications of carbon dots in sensing

The most essential property of CDs is that they exhibited excellent optical performance compared with that of other carbon nanomaterials. Extensive studies have been devoted to developing the optical applications of CDs, especially fluorescence-based applications. As novel fluorescent probes, CDs are providing great potential for sensing applications because of highly sensitive to analytes in a very short time. In addition, the ultras mall size, high photostability, low toxicity, good

biocompatibility and excellent dispersion of CDs result in improved detection sensitivity, stability, selectivity and security compared with traditional organic dyes and semiconductor quantum dots. Up to now, the detection of analytes include inorganic ions [34, 46-48], small organic molecules [49-53], and large biomaterials [54, 55] based on either fluorescence turn-on or turn-off mechanisms. The following of this chapter will focus on recent fluorescence sensing applications of CDs.

2.4.1 Detection of inorganic ions

CDs have been widely used as fluorescence sensing probes for detection of inorganic ions including metal cations [34, 46-48] and non-metallic anions [56-58].

Though metal cations play important roles in environmental, biological and chemical systems, they are also posed toxicity to human being because of the possible leading to serious damage of the kidneys, liver and brain. Therefore, highly sensitive and selective probes for metal cations are highly desired. Since CDs display strong PL and possess rich organic functional groups on their surfaces, they are considered suitable for fluorescence sensing probes for metal ions detection. To these days, numerous metal cations including Fe^{3+} [34], Ag^{+} [46], Au^{3+} [47], Hg^{2+} [48], Cu^{2+} [59], Cr^{6+} [60], Cd^{2+} [61], Pb^{2+} [62], and Ni^{2+} [63], have been detected using different CD-based fluorescent sensors. Most studies mainly focused on the detection of Fe^{3+}, Hg^{2+} and Cu^{2+}, probably because of their prominent role or high toxicity in biological systems.

Recently, CDs have also been employed as fluorescent probes to detect non-metallic ions including pyrophosphate (PPi) ions [57], and sulphite [58] via “on–off–on” fluorescence responses.

2.4.2 Detection of small organic molecules

Similar to the selective and sensitive detection of inorganic ions, monitoring small organic molecules with fluorescent CDs has also become an attractive topic in recent years. Organic materials such as glucose [22], ascorbic acid [49], bisphenol A [50], dihydroxybenzene [51], hydroquinone [52], 2,4,6-trinitrotoluene [53], and 2,4,6-trinitrophenol (TNP) [64] have been optically detected using fluorescent CDs probes based on a turn-on or turn-off fluorescence response. The fluorescence of CDs can be

quenched directly by the detected organic molecules with the aid of metal ions or oxidation agents. Another mechanism is that the fluorescence of CDs, as an indirect sensing probe, can first be quenched by metal ions and then recovered by specific organic molecules.

2.4.3 Detection of biomaterials

The flexibility of CD-based fluorescent sensors is also demonstrated by their ability to detect a wide range of biotargets including DNA [54], protein kinase [55] alkaline phosphatase [65], phosphate-containing metabolites [66], chondroitin sulfate and heparin [67], and human immunoglobulin G [68]. The most frequently used methods for detection of biomaterials are based on specific fluorescence resonance energy transfer (FRET) between functional CDs and a quencher.

2.4.4 Fluorescence sensing mechanism

The above mentioned has shown that CDs could be effectively applied as fluorescent probes for selective and sensitive detections of inorganic ions, small organic molecules and large biomaterials. Although there are various targets, the constructed fluorescence sensing platform was primarily based on turn-off (fluorescence quenching) and turn-on (fluorescence recovering) fluorescence responses. On one hand, the turn-off response based on the fluorescence quenching of CDs or functionalized CDs by targets appears to be static quenching (complexation) [59], dynamic quenching (collisional deactivation) [66] or sometimes involving both static and dynamic quenching mechanisms, which frequently can be analyzed using the evaluation of fluorescence lifetime. On the other hand, the turn-on fluorescence response based on the mechanism that is usually contained two steps [49, 69]. Firstly, the fluorescence quenching of CDs or functionalized CDs occurs because of the strong interaction between CDs (or functionalized CDs) and quencher. Secondly, the pre-formed composite structure of CDs and quencher is broken down with the addition of targets, leading to the freedom of fluorescent CDs into solution; therefore, the corresponding fluorescence is recovered. Nevertheless, the fluorescence recovering process is still ambiguous when CDs, quencher and target are in coexistence.

2.5 Summary

To sum up, recent developments of luminescent CDs including different "bottom-up" synthetic routes, physical and chemical properties, and sensing applications are reviewed. It can be observed that by carefully select starting materials and producing methods, various color emission CDs could be obtained. However, the fabrication of longer wavelength emission CDs, particularly multicolor emission CDs is still a challenge. In addition, there are some proposed hypotheses nevertheless, reasonable explanation on the emission mechanism for photoluminescence properties of CDs is still unclear to these days. Therefore, to explore environmentally friendly, economical and facile processes for synthesis of highly PL emission CDs, especially longer wavelength color emission CDs and multicolor emission CDs as well as its photoluminescence mechanism is still highly desired.

2.6 References

[1] X. Xu, R. Ray, Y. Gu, H.J. Ploehn, L. Gearheart, K. Raker, et al., Electrophoretic Analysis and Purification of Fluorescent Single-Walled Carbon Nanotube Fragments, Journal of the American Chemical Society, 126(2004) 12736-7.

[2] Y.-P. Sun, B. Zhou, Y. Lin, W. Wang, K.A.S. Fernando, P. Pathak, et al., Quantum-Sized Carbon Dots for Bright and Colorful Photoluminescence, Journal of the American Chemical Society, 128(2006) 7756-7.

[3] J. Lu, J.-x. Yang, J. Wang, A. Lim, S. Wang, K.P. Loh, One-Pot Synthesis of Fluorescent Carbon Nanoribbons, Nanoparticles, and Graphene by the Exfoliation of Graphite in Ionic Liquids, ACS Nano, 3(2009) 2367-75.

[4] Z.-A. Qiao, Y. Wang, Y. Gao, H. Li, T. Dai, Y. Liu, et al., Commercially activated carbon as the source for producing multicolor photoluminescent carbon dots by chemical oxidation, Chemical Communications, 46(2010) 8812-4.

[5] S.Y. Park, H.U. Lee, E.S. Park, S.C. Lee, J.-W. Lee, S.W. Jeong, et al., Photoluminescent Green Carbon Nanodots from Food-Waste-Derived Sources: Large-Scale Synthesis, Properties, and Biomedical Applications, ACS Applied Materials & Interfaces, 6(2014) 3365-70.

[6] B.C.M. Martindale, G.A.M. Hutton, C.A. Caputo, E. Reisner, Solar Hydrogen Production Using Carbon Quantum Dots and a Molecular Nickel Catalyst, Journal of the American Chemical Society, 137(2015) 6018-25.

[7] D. Qu, M. Zheng, P. Du, Y. Zhou, L. Zhang, D. Li, et al., Highly luminescent S, N co-doped graphene quantum dots with broad visible absorption bands for visible light photocatalysts, Nanoscale, 5(2013) 12272-7.

[8] K. Jiang, S. Sun, L. Zhang, Y. Lu, A. Wu, C. Cai, et al., Red, Green, and Blue Luminescence by Carbon Dots: Full-Color Emission Tuning and Multicolor Cellular Imaging, Angewandte Chemie International Edition, 54(2015) 5360-3.

[9] L. Tang, R. Ji, X. Cao, J. Lin, H. Jiang, X. Li, et al., Deep Ultraviolet Photoluminescence of Water-Soluble Self-Passivated Graphene Quantum Dots, ACS Nano, 6(2012) 5102-10.

[10] H. Li, X. He, Y. Liu, H. Huang, S. Lian, S.-T. Lee, et al., One-step ultrasonic synthesis of water-soluble carbon nanoparticles with excellent photoluminescent properties, Carbon, 49(2011) 605-9.

[11] M. Chen, W. Wang, X. Wu, One-pot green synthesis of water-soluble carbon nanodots with multicolor photoluminescence from polyethylene glycol, Journal of Materials Chemistry B, 2(2014) 3937-45.

[12] F. Yuan, Z. Wang, X. Li, Y. Li, Z.a. Tan, L. Fan, et al., Bright Multicolor Bandgap Fluorescent Carbon Quantum Dots for Electroluminescent Light-Emitting Diodes, Advanced Materials, 29(2017) 1604436-n/a.

[13] J. Wang, C. Cheng, Y. Huang, B. Zheng, H. Yuan, L. Bo, et al., A facile large-scale microwave synthesis of highly fluorescent carbon dots from benzenediol isomers, Journal of Materials Chemistry C, 2(2014) 5028-35.

[14] Z. Ma, H. Ming, H. Huang, Y. Liu, Z. Kang, One-step ultrasonic synthesis of fluorescent N-doped carbon dots from glucose and their visible-light sensitive photocatalytic ability, New Journal of Chemistry, 36(2012) 861-4.

[15] L. Li, C. Lu, S. Li, S. Liu, L. Wang, W. Cai, et al., A high-yield and versatile method for the synthesis of carbon dots for bioimaging applications, Journal of Materials Chemistry B, 5(2017) 1935-42.

[16] B.B. Chen, Z.X. Liu, W.C. Deng, L. Zhan, M.L. Liu, C.Z. Huang, A large-scale synthesis of photoluminescent carbon quantum dots: a self-exothermic reaction driving the formation of the nanocrystalline core at room temperature, Green Chemistry, 18(2016) 5127-32.

[17] Y. Li, X. Zhong, A.E. Rider, S.A. Furman, K. Ostrikov, Fast, energy-efficient synthesis of luminescent carbon quantum dots, Green Chemistry, 16(2014) 2566-70.

[18] J. Deng, Q. Lu, N. Mi, H. Li, M. Liu, M. Xu, et al., Electrochemical Synthesis of Carbon Nanodots Directly from Alcohols, Chemistry – A European Journal, 20(2014) 4993-9.

[19] S. Yang, H. Zeng, H. Zhao, H. Zhang, W. Cai, Luminescent hollow carbon shells and fullerene-like carbon spheres produced by laser ablation with toluene, Journal of Materials Chemistry, 21(2011) 4432-6.

[20] S. Hu, Y. Guo, W. Liu, P. Bai, J. Sun, S. Cao, Controllable synthesis and Photoluminescence (PL) of amorphous and crystalline carbon nanoparticles, Journal of Physics and Chemistry of Solids, 72(2011) 749-54.

[21] X. Li, H. Wang, Y. Shimizu, A. Pyatenko, K. Kawaguchi, N. Koshizaki, Preparation of carbon quantum dots with tunable photoluminescence by rapid laser passivation in ordinary organic solvents, Chemical Communications, 47(2011) 932-4.

[22] X. Shan, L. Chai, J. Ma, Z. Qian, J. Chen, H. Feng, B-doped carbon quantum dots as a sensitive fluorescence probe for hydrogen peroxide and glucose detection, Analyst, 139(2014) 2322-5.

[23] S. Sarkar, K. Das, M. Ghosh, P.K. Das, Amino acid functionalized blue and phosphorous-doped green fluorescent carbon dots as bioimaging probe, RSC Advances, 5(2015) 65913-21.

[24] S. Chandra, P. Patra, S.H. Pathan, S. Roy, S. Mitra, A. Layek, et al., Luminescent S-doped carbon dots: an emergent architecture for multimodal applications, Journal of Materials Chemistry B, 1(2013) 2375-82.

[25] J. Du, Y. Zhao, J. Chen, P. Zhang, L. Gao, M. Wang, et al., Difunctional Cu-doped carbon dots: catalytic activity and fluorescence indication for the reduction reaction of p-nitrophenol, RSC Advances, 7(2017) 33929-36.

[26] J. Cheng, C.-F. Wang, Y. Zhang, S. Yang, S. Chen, Zinc ion-doped carbon dots with strong yellow photoluminescence, RSC Advances, 6(2016) 37189-94.

[27] S. Yang, J. Sun, P. He, X. Deng, Z. Wang, C. Hu, et al., Selenium Doped Graphene Quantum Dots as an Ultrasensitive Redox Fluorescent Switch, Chemistry of Materials, 27(2015) 2004-11.

[28] D. Qu, M. Zheng, J. Li, Z. Xie, Z. Sun, Tailoring color emissions from N-doped graphene quantum dots for bioimaging applications, Light Sci Appl, 4(2015) e364.

[29] R. Jelinek, Characterization and Physical Properties of Carbon-Dots, Carbon Quantum Dots: Synthesis, Properties and Applications, Springer International Publishing, Cham, 2017, 29-46.

[30] S.N. Baker, G.A. Baker, Luminescent Carbon Nanodots: Emergent Nanolights, Angewandte Chemie International Edition, 49(2010) 6726-44.

[31] L. Li, G. Wu, G. Yang, J. Peng, J. Zhao, J.-J. Zhu, Focusing on luminescent graphene quantum dots: current status and future perspectives, Nanoscale, 5(2013) 4015-39.

[32] X.T. Zheng, A. Ananthanarayanan, K.Q. Luo, P. Chen, Glowing Graphene Quantum Dots and Carbon Dots: Properties, Syntheses, and Biological Applications, Small, 11(2015) 1620-36.

[33] B. Zheng, Y. Chen, P. Li, Z. Wang, B. Cao, F. Qi, et al., Ultrafast ammonia-driven, microwave-assisted synthesis of nitrogen-doped graphene quantum dots and their optical properties, Nanophotonics2017, 259-67.

[34] S. Li, Y. Li, J. Cao, J. Zhu, L. Fan, X. Li, Sulfur-Doped Graphene Quantum Dots as a Novel Fluorescent Probe for Highly Selective and Sensitive Detection of Fe3+, Analytical Chemistry, 86(2014) 10201-7.

[35] H. Nie, M. Li, Q. Li, S. Liang, Y. Tan, L. Sheng, et al., Carbon Dots with Continuously Tunable Full-Color Emission and Their Application in Ratiometric pH Sensing, Chemistry of Materials, 26(2014) 3104-12.

[36] S.-T. Yang, X. Wang, H. Wang, F. Lu, P.G. Luo, L. Cao, et al., Carbon Dots as Nontoxic and High-Performance Fluorescence Imaging Agents, The Journal of Physical Chemistry C, 113(2009) 18110-4.

[37] X. Zhai, P. Zhang, C. Liu, T. Bai, W. Li, L. Dai, et al., Highly luminescent carbon nanodots by microwave-assisted pyrolysis, Chemical Communications, 48(2012) 7955-7.

[38] H. Zheng, Q. Wang, Y. Long, H. Zhang, X. Huang, R. Zhu, Enhancing the luminescence of carbon dots with a reduction pathway, Chemical Communications, 47(2011) 10650-2.

[39] D. Qu, M. Zheng, L. Zhang, H. Zhao, Z. Xie, X. Jing, et al., Formation mechanism and optimization of highly luminescent N-doped graphene quantum dots, 4(2014) 5294.

[40] D. Pan, J. Zhang, Z. Li, M. Wu, Hydrothermal Route for Cutting Graphene Sheets into Blue-Luminescent Graphene Quantum Dots, Advanced Materials, 22(2010) 734-8.

[41] S. Zhu, J. Zhang, S. Tang, C. Qiao, L. Wang, H. Wang, et al., Surface Chemistry Routes to Modulate the Photoluminescence of Graphene Quantum Dots: From Fluorescence Mechanism to Up-Conversion Bioimaging Applications, Advanced Functional Materials, 22(2012) 4732-40.

[42] Q. Liu, B. Guo, Z. Rao, B. Zhang, J.R. Gong, Strong Two-Photon-Induced Fluorescence from Photostable, Biocompatible Nitrogen-Doped Graphene Quantum Dots for Cellular and Deep-Tissue Imaging, Nano Letters, 13(2013) 2436-41.

[43] Z. Wang, H. Zeng, L. Sun, Graphene quantum dots: versatile photoluminescence for energy, biomedical, and environmental applications, Journal of Materials Chemistry C, 3(2015) 1157-65.

[44] S. Hu, A. Trinchi, P. Atkin, I. Cole, Tunable Photoluminescence Across the Entire Visible Spectrum from Carbon Dots Excited by White Light, Angewandte Chemie International Edition, 54(2015) 2970-4.

[45] H. Ding, S.-B. Yu, J.-S. Wei, H.-M. Xiong, Full-Color Light-Emitting Carbon Dots with a Surface-State-Controlled Luminescence Mechanism, ACS Nano, 10(2016) 484-91.

[46] A. Suryawanshi, M. Biswal, D. Mhamane, R. Gokhale, S. Patil, D. Guin, et al., Large scale synthesis of graphene quantum dots (GQDs) from waste biomass and their use as an efficient and selective photoluminescence on-off-on probe for Ag^{+} ions, Nanoscale, 6(2014) 11664-70.

[47] T. Yang, F. Cai, X. Zhang, Y. Huang, Nitrogen and sulfur codoped graphene quantum dots as a new fluorescent probe for Au^{3+} ions in aqueous media, RSC Advances, 5(2015) 107340-7.

[48] B. Shi, L. Zhang, C. Lan, J. Zhao, Y. Su, S. Zhao, One-pot green synthesis of oxygen-rich nitrogen-doped graphene quantum dots and their potential application in pH-sensitive photoluminescence and detection of mercury(II) ions, Talanta, 142(2015) 131-9.

[49] J.-J. Liu, Z.-T. Chen, D.-S. Tang, Y.-B. Wang, L.-T. Kang, J.-N. Yao, Graphene quantum dots-based fluorescent probe for turn-on sensing of ascorbic acid, Sensors and Actuators B: Chemical, 212(2015) 214-9.

[50] H. Huang, Z. Feng, Y. Li, Z. Liu, L. Zhang, Y. Ma, et al., Highly sensitive detection of bisphenol A in food packaging based on graphene quantum dots and peroxidase, Analytical Methods, 7(2015) 2928-35.

[51] Y. Li, H. Huang, Y. Ma, J. Tong, Highly sensitive fluorescent detection of dihydroxybenzene based on graphene quantum dots, Sensors and Actuators B: Chemical, 205(2014) 227-33.

[52] Y. He, J. Sun, D. Feng, H. Chen, F. Gao, L. Wang, Graphene quantum dots: Highly active bifunctional nanoprobes for nonenzymatic photoluminescence detection of hydroquinone, Biosensors and Bioelectronics, 74(2015) 418-22.

[53] L. Fan, Y. Hu, X. Wang, L. Zhang, F. Li, D. Han, et al., Fluorescence resonance energy transfer quenching at the surface of graphene quantum dots for ultrasensitive detection of TNT, Talanta, 101(2012) 192-7.

[54] Z.S. Qian, X.Y. Shan, L.J. Chai, J.J. Ma, J.R. Chen, H. Feng, DNA nanosensor based on biocompatible graphene quantum dots and carbon nanotubes, Biosensors and Bioelectronics, 60(2014) 64-70.

[55] Y. Wang, L. Zhang, R.-P. Liang, J.-M. Bai, J.-D. Qiu, Using Graphene Quantum Dots as Photoluminescent Probes for Protein Kinase Sensing, Analytical Chemistry, 85(2013) 9148-55.

[56] N. Yu, H. Peng, H. Xiong, X. Wu, X. Wang, Y. Li, et al., Graphene quantum dots combined with copper(II) ions as a fluorescent probe for turn-on detection of sulfide ions, Microchimica Acta, 182(2015) 2139-46.

[57] L. Lin, X. Song, Y. Chen, M. Rong, T. Zhao, Y. Jiang, et al., One-pot synthesis of highly greenish-yellow fluorescent nitrogen-doped graphene quantum dots for pyrophosphate sensing via competitive coordination with Eu^{3+} ions, Nanoscale, 7(2015) 15427-33.

[58] S. Chen, Y. Song, Y. Li, Y. Liu, X. Su, Q. Ma, A facile photoluminescence modulated nanosensor based on nitrogen-doped graphene quantum dots for sulfite detection, New Journal of Chemistry, 39(2015) 8114-20.

[59] F. Wang, Z. Gu, W. Lei, W. Wang, X. Xia, Q. Hao, Graphene quantum dots as a fluorescent sensing platform for highly efficient detection of copper(II) ions, Sensors and Actuators B: Chemical, 190(2014) 516-22.

[60] S. Huang, H. Qiu, F. Zhu, S. Lu, Q. Xiao, Graphene quantum dots as on-off-on fluorescent probes for chromium(VI) and ascorbic acid, Microchimica Acta, 182(2015) 1723-31.

[61] L. Zhang, D. Peng, R.-P. Liang, J.-D. Qiu, Nitrogen-Doped Graphene Quantum Dots as a New Catalyst Accelerating the Coordination Reaction between Cadmium(II) and 5,10,15,20-Tetrakis(1-methyl-4-pyridinio)porphyrin for Cadmium(II) Sensing, Analytical Chemistry, 87(2015) 10894-901.

[62] Y.-X. Qi, M. Zhang, Q.-Q. Fu, R. Liu, G.-Y. Shi, Highly sensitive and selective fluorescent detection of cerebral lead(II) based on graphene quantum dot conjugates, Chemical Communications, 49(2013) 10599-601.

[63] H. Huang, L. Liao, X. Xu, M. Zou, F. Liu, N. Li, The electron-transfer based interaction between transition metal ions and photoluminescent graphene quantum dots (GQDs): A platform for metal ion sensing, Talanta, 117(2013) 152-7.

[64] L. Lin, M. Rong, S. Lu, X. Song, Y. Zhong, J. Yan, et al., A facile synthesis of highly luminescent nitrogen-doped graphene quantum dots for the detection of 2,4,6-trinitrophenol in aqueous solution, Nanoscale, 7(2015) 1872-8.

[65] Y. Zhu, G. Wang, H. Jiang, L. Chen, X. Zhang, One-step ultrasonic synthesis of graphene quantum dots with high quantum yield and their application in sensing alkaline phosphatase, Chemical Communications, 51(2015) 948-51.

[66] J.-J. Liu, X.-L. Zhang, Z.-X. Cong, Z.-T. Chen, H.-H. Yang, G.-N. Chen, Glutathione-functionalized graphene quantum dots as selective fluorescent probes for phosphate-containing metabolites, Nanoscale, 5(2013) 1810-5.

[67] Y. Li, H. Sun, F. Shi, N. Cai, L. Lu, X. Su, Multi-positively charged dendrimeric nanoparticles induced fluorescence quenching of graphene quantum dots for heparin and chondroitin sulfate detection, Biosensors and Bioelectronics, 74(2015) 284-90.

[68] H. Zhao, Y. Chang, M. Liu, S. Gao, H. Yu, X. Quan, A universal immunosensing strategy based on regulation of the interaction between graphene and graphene quantum dots, Chemical Communications, 49(2013) 234-6.

[69] Z.S. Qian, X.Y. Shan, L.J. Chai, J.J. Ma, J.R. Chen, H. Feng, A universal fluorescence sensing strategy based on biocompatible graphene quantum dots and graphene oxide for the detection of DNA, Nanoscale, 6(2014) 5671-4.

Chapter 3

One Pot Solid-state Synthesis of Highly Fluorescent N and S Co-doped Carbon Dots and Its Use as Fluorescent Probe for Ag^+ Detection in Aqueous Solution

3.1 Introduction

In recent years, the rapid development of industries causing heavy metal ion pollution has become a critical worldwide issue because it is a serious threat to human health [1]. As a type of noble metal, silver (Ag) is very important to humans because it has many applications in daily life, such as electronics, photography, and pharmacy, due to its attractive properties and multi-functions [2]. As a consequence, a large amount of silver is being released into the environment from the industrial wastes. Recent studies have reported serious problems in both human health and the environment due to the antibacterial activity of Ag nanoparticles, which can generate toxic Ag^+ ions [3, 4]. As a result, Ag ions have been classified as one of the most poisonous heavy metal ions [2]. Undoubtedly, the selective and sensitive detection of Ag^+ is very important for maintaining the environment and human health. Recent approaches to detect heavy metal ions include inductively coupled plasma mass spectrometry [5], atomic absorption spectrometry [6], and stripping voltammetry [7], which are rather expensive and complicated procedures that involve time consuming sample pretreatment steps and are also non-portable, which limits their applications, even though they offer excellent sensitivity and multi element analysis [8]. The fluorescent sensor has attracted increasing attention because of its simple operation, cost effectiveness, high sensitivity, and intuitive and rapid response. Up to now, various fluorescent probes have been developed actively, including organic dye molecules, metal nanoparticles, and semiconductor quantum dots. On the other hand, it requires more study to solve the serious drawbacks, such as toxicity, low sensitivity, low selectivity, and hydrophobicity.

Carbon dots have attracted considerable attention in recent years in chemo- and bio-sensing, photo-catalysis, bio-imaging, light emitting diodes, and solar cells [9-12]

because of their good stability, low cytotoxicity, and high biocompatibility compared to those of organic fluorophores and semiconductor quantum dots [13-15]. In addition, heteroatom-doped carbon dots, such as nitrogen-doped and sulfur-doped CDs, have been also synthesized and studied as sensing probes for the detection of metal ions [16, 17]. On the other hand, most of the resulting carbon dots suffer from low quantum yields (always less than 10%), which severely limit their availability for practical applications [18]. The sensitivity for the detection of heavy metal ions was based on fluorescent quenching metal ions [19], and to the best of the authors' knowledge, fluorescent probe-based carbon dots for the detection of Ag^+ ions are still rare [20, 21]. Therefore, the development of green, low cost, and highly sensitive probes based on carbon dots for the detection of Ag^+ are highly desired.

This chapter reports a facile, one pot, solid-state synthesis of N and S co-doped carbon dots (CDs) using a new precursor, caffeine, which is a naturally occurring purine. With its heterocyclic aromatic structure that consists of a pyrimidine ring fused to an imidazole ring, caffeine can be an effective precursor for synthesizing carbon dots. By choosing a suitable additive, ammonium persulfate in this study, CDs emitting deep blue color emission with a quantum yield of 38% were synthesized. Moreover, when combining two additives, ammonium persulfate and urea, the as-prepared CDs exhibited even better optical properties, showing bright blue color emission with an excellent quantum yield of as much as 69%. The quantum yield obtained in this study was higher than those in previous publications and even comparable to those of carbon dots synthesized by the hydrothermal treatment of additives with citric acid, which is a unique molecule for the synthesis of highly fluorescent carbon nanodots [22]. With its excellent quantum yield, the CDs can be applied to the fluorescent detection of heavy metal ions without further chemical modifications or surface functionalization. The efficient and effective quenching of fluorescence emission in the newly fabricated CDs was observed. The CDs can be quenched obviously by adding Ag^+ at fairly low concentrations. Therefore, a selective and sensitive fluorescence platform can be built up for the detection of Ag^+ in aqueous media. This process is a very promising method

for the environmentally friendly, cost-effective and scalable fabrication of highly photo-luminescent carbon dots.

3.2 Experimental

3.2.1 Chemicals

Caffeine, ammonium persulfate, urea, sodium chloride, potassium bromide for FTIR, and sulfuric acid were purchased from Deajung Chemicals and Metals Co. Ltd (Korea). Quinine sulfate dihydrate was kindly provided by Wako Pure Chemical Industries, Ltd (Japan). All reagents were used as received. Metal salts, such as $AgNO_3$, $AlCl_3.6H_2O$, $Cd(CH_3COO)_2.2H_2O$, $Co(NO_3)_2.6H_2O$, $CuSO_4.5H_2O$, $Fe(NO_3)_3.9H_2O$, KCl, LiBr, $MgCl_2.6H_2O$, NaCl, $Ni(SO_4)_2.6H_2O$, $Pb(NO_3)_2$, $SnCl_4.5H_2O$, and $ZnCl_2$ were purchased from Sigma-Aldrich Co. Ltd. (USA). Deionized water with a resistivity of 18.2 $M\Omega\ cm^{-1}$ was used in all experiments.

3.2.2 Characterizations

The UV-visible spectra were recorded on an UV-visible spectrophotometer (UV-vis., SPECORD 210 PLUS-223F1107, Germany) using a quartz cell with a 1 cm optical path. The photoluminescence (PL) emission spectra were taken on a Cary Eclipse fluorescence spectrophotometer (Agilent Technologies, G9800AA, USA).

The Fourier transform infrared (FTIR) spectra were recorded on a FTIR spectrometer (KBr disk method; NEXUS, USA) at wavenumbers of 400-4000 cm^{-1}. Transmission electron microscopy (TEM, JEM-2100, JEOL, Japan) images were taken with an operating voltage of 200 kV. X-ray photoelectron spectroscopy (XPS) was performed on an ESCALB-MKII250 photoelectron spectrometer (VG Co., USA) with Al Kα X-ray radiation as the X-ray source for excitation.

3.2.3 Synthesis of N and S co-doped carbon dots

The N and S co-doped CDs were synthesized in one pot using a green, facile, solid-state method. Typically, a solid mixture containing 1g of caffeine, 2g of ammonium persulfate, and 3g of urea were ground to a fine powder in a ceramic mortar. The mixture was then transferred to an alumina crucible and covered with aluminum

foil. The crucible was placed into a siliconit muffle furnace, heated to 180^{o}C, and kept at this temperature for 3 h. After cooling to ambient temperature, 60 mL of DI water was added to the solid product followed by vigorous stirring for 60 min using a magnetic bar. The mixture was filtered using filter paper first and then through a 0.22 µm membrane to eliminate the large particles. The obtained light yellow solution was purified against DI water using dialysis tubing with pore size 1,000 Da for 3 h to eliminate the impurities and unreacted reactants. Caffeine only, a mixture of caffeine and urea, and mixture of caffeine and ammonium persulfate were also used as reactants to synthesize various CDs.

3.2.4 Detection of heavy metal ions

The fluorescent detection probe was prepared by diluting the as-prepared CDs with DI water to form a solution of 20 µg mL^{-1}. The fluorescence emission intensity at 426 nm of the blank sample excited at 360 nm was measured and marked as F_0. To determine the Ag^+ concentration, 3 µL of Ag^+ with a concentration range of 50 µM to 500 mM was added to 3 mL of the above CDs solution. After 1 min for equilibration, the fluorescent intensity (F) of each sample was measured. The selectivity towards Ag^+ was determined by adding other related analogues, including Al^{3+}, Cd^{2+}, Co^{2+}, Cu^{2+}, Fe^{3+}, K^+, Li^+, Mg^{2+}, Na^+, Ni^{2+}, Pb^{2+}, Sn^{4+}, and Zn^{2+}, in a similar manner. All experiments were performed at room temperature.

3.2.5 Determination of the Quantum Yields.

The quantum yields (QYs) of the CDs were determined using a widely accepted relative method. The QY of a sample was calculated using the following equation with quinine sulfate (QY = 54% in 0.1 M H_2SO_4) as a reference:

$$\emptyset = \emptyset' \times \frac{A'}{I'} \times \frac{I}{A} \times \frac{n^2}{n'^2}$$

where ϕ is the QY of the testing sample, I is the testing sample's integrated emission intensity, n is the refractive index (1.33 for water), and A is the optical density. The prime symbol (′) refers to the reference dye with a known QY. To minimize the re-absorption effects, absorption was always kept below 0.05 at the excitation wavelength.

3.3 Results and discussion

3.3.1 Synthesis and characterization of CDs

As described in Scheme 3.1, the precursor, caffeine, is carbonized and converted to CDs in the presence of ammonium persulfate and urea through a facile solid-state process by thermal heating of their solid mixture at 180^{o}C for 3 hours, followed by further purification to obtain an aqueous solution of CDs. Typically, a CDs aqueous solution with a concentration of 3.6 mg mL^{-1} is obtained when 1 g of caffeine is used as a carbon precursor together with 2 g of ammonium persulfate and 3 g of urea.

As shown in Scheme 3.2, no color emission was observed under UV irradiation when only caffeine or a mixture of caffeine and urea was used, which indicates unsuccessful CD formation. On the other hand, when urea was replaced with ammonium persulfate, a deep blue fluorescence was obtained, which indicates the successful formation of CDs. Moreover, when caffeine, ammonium persulfate, and urea were used together as precursors, the as-prepared product exhibited highly bright blue color emission with a red-shift around 26 nm compared to that of the CDs synthesized using the ammonium persulfate. This shows that ammonium persulfate may have a pivotal role. Moreover, urea, despite not being converted to CDs, also plays an important part in the formation of CDs. For convenience, the CDs synthesized without and with urea are called o-CDs and u-CDs, respectively.

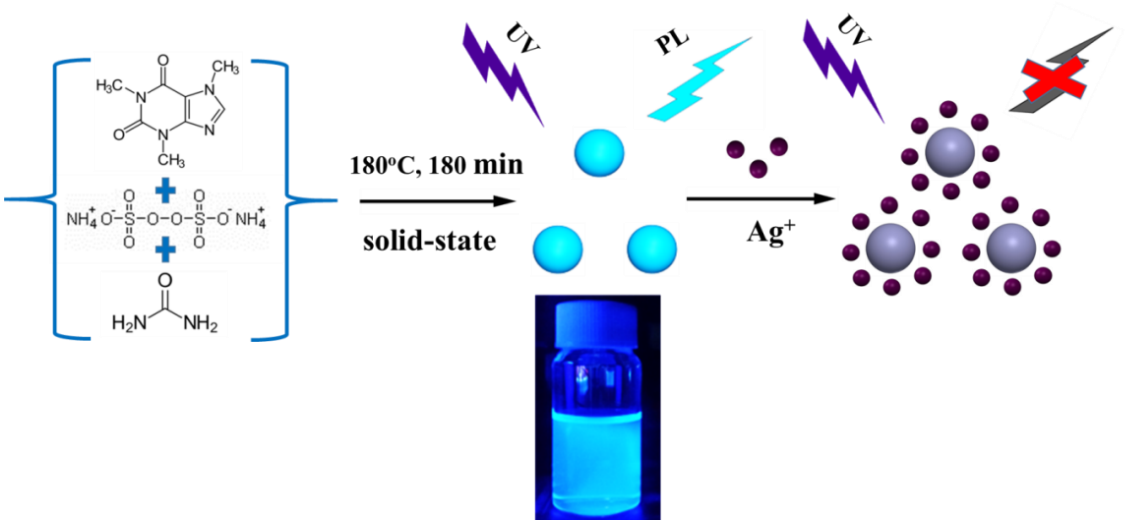

Scheme 3.1 Schematic diagram of the synthesis of CDs and their application in the label-free detection of Ag^{+}

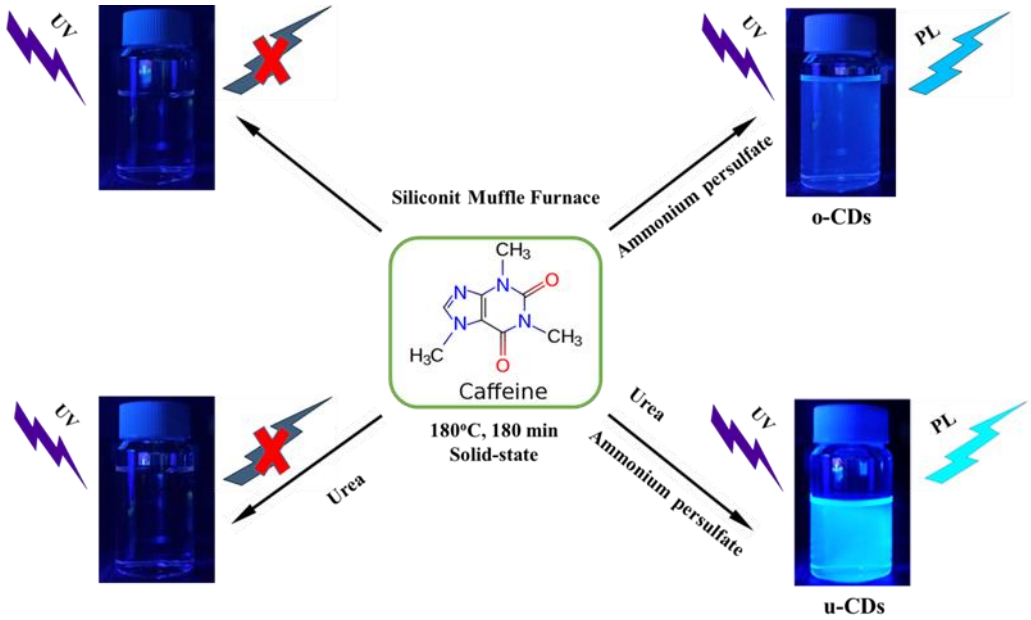

Scheme 3.2 Schematic diagram of the thermal treatment of caffeine, a solid mixture of caffeine with urea, with ammonium persulfate and with both urea and ammonium persulfate, respectively

3.3.2 Instrumental analysis of CDs

3.3.2.1 TEM analysis

The morphology and structure of the CDs were analyzed by TEM. All samples were prepared by drop-casting a diluted aqueous solution of CDs on a carbon-coated copper grid. Fig. 3.1 presents a TEM image of u-CDs with a size distribution between 6 and 26 nm (mean size ~ 13 nm) as shown in the particle size distribution histogram (inset of Fig. 1a), which is larger than that of o-CDs with a size distribution between 4 and 9 nm (average size is ~ 6 nm), as shown in Fig.3.3. High resolution TEM (HRTEM, Fig. 3.2) revealed the high crystallinity of the u-CDs with lattice spacings of 0.25 nm and 0.32 nm, which show good agreement with the in-plane lattice spacing of graphene (102 facet) and the spacing between the graphene layers (002 facet), respectively [23-25].

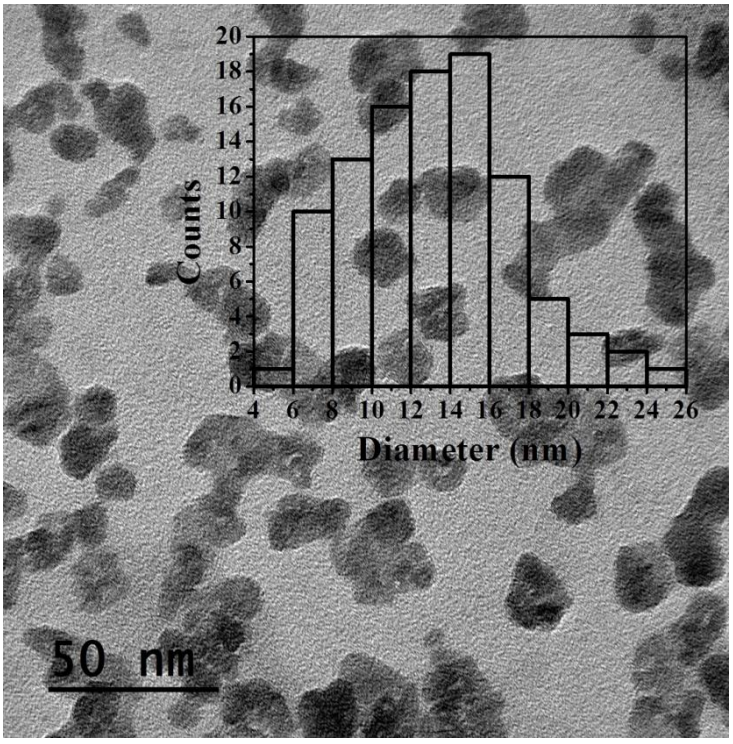

Fig. 3.1 TEM image of u-CDs. Inset is the particle size distribution histogram of u-CDs

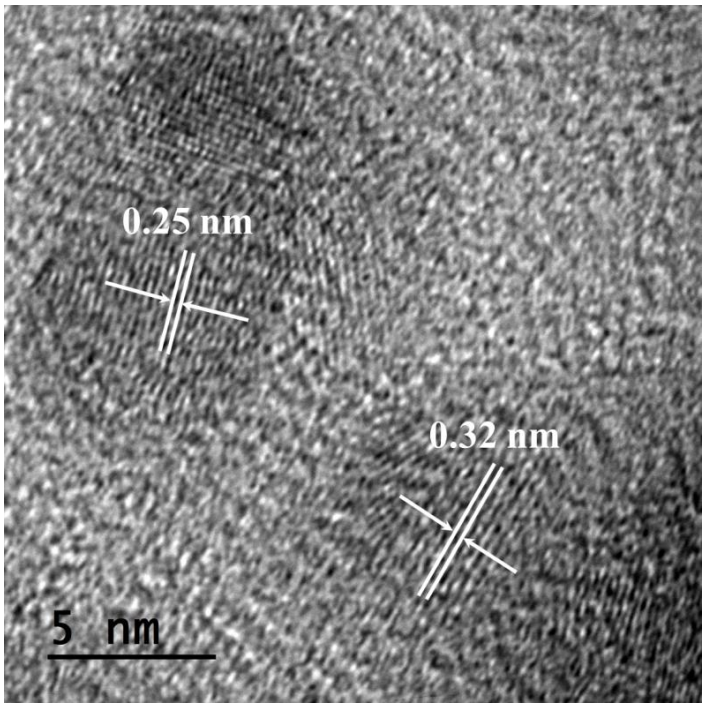

Fig. 3.2 HRTEM image of u-CDs

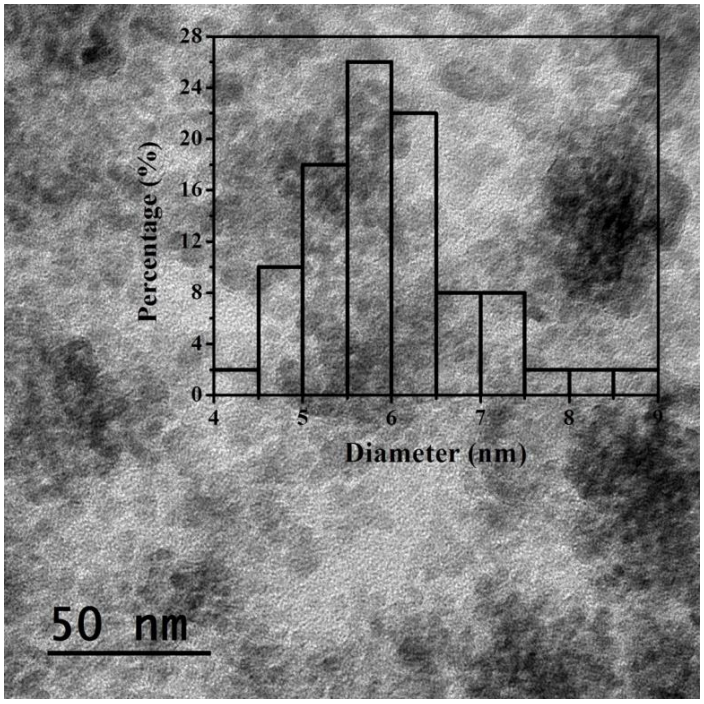

Fig. 3.3 TEM image of o-CDs. Inset is the particle size distribution histogram of o-CDs

3.3.2.2 XPS analysis

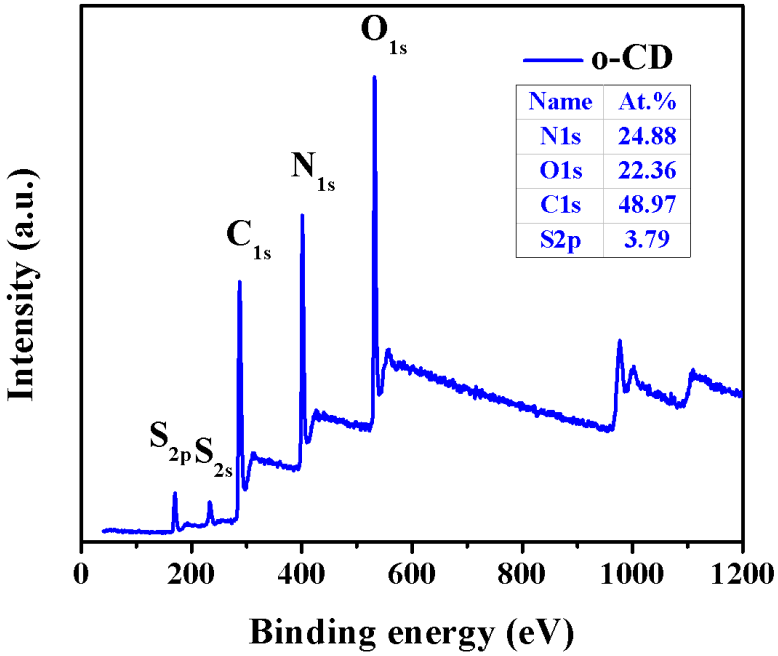

Fig. 3.4 XPS survey spectra of o-CDs

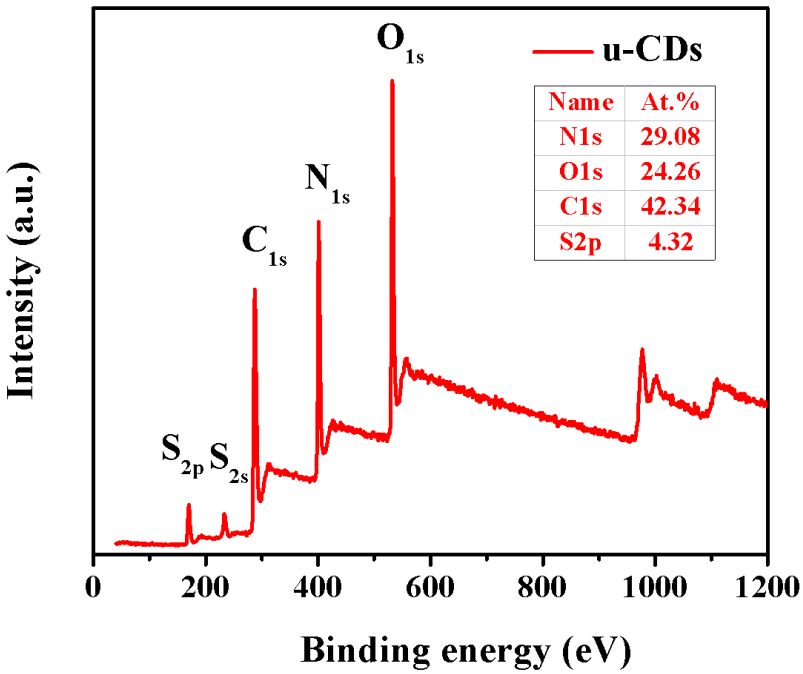

Fig. 3.5 XPS survey spectra of u-CDs

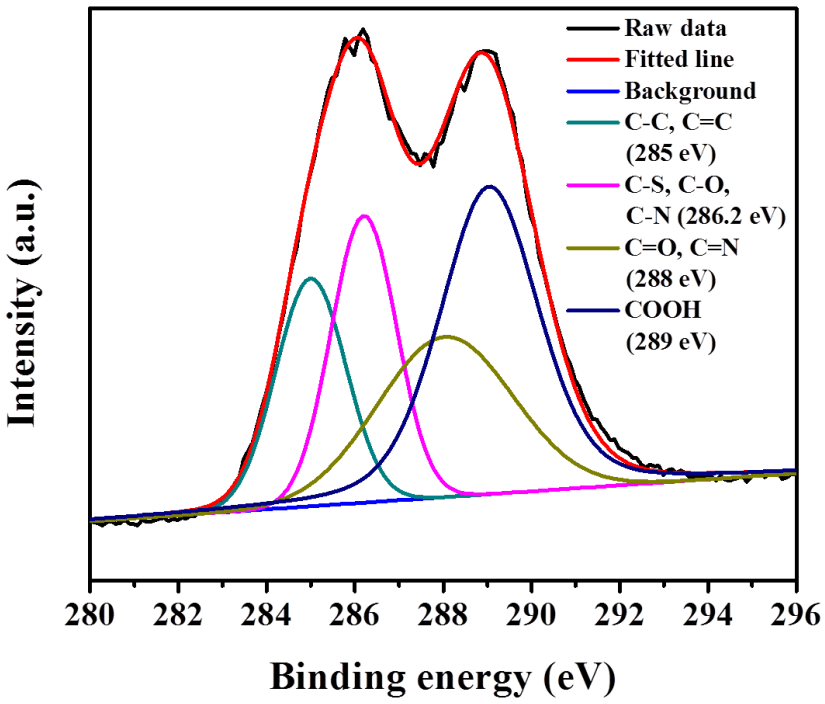

Fig. 3.6 High-resolution XPS spectra of C_{1s} of u-CDs

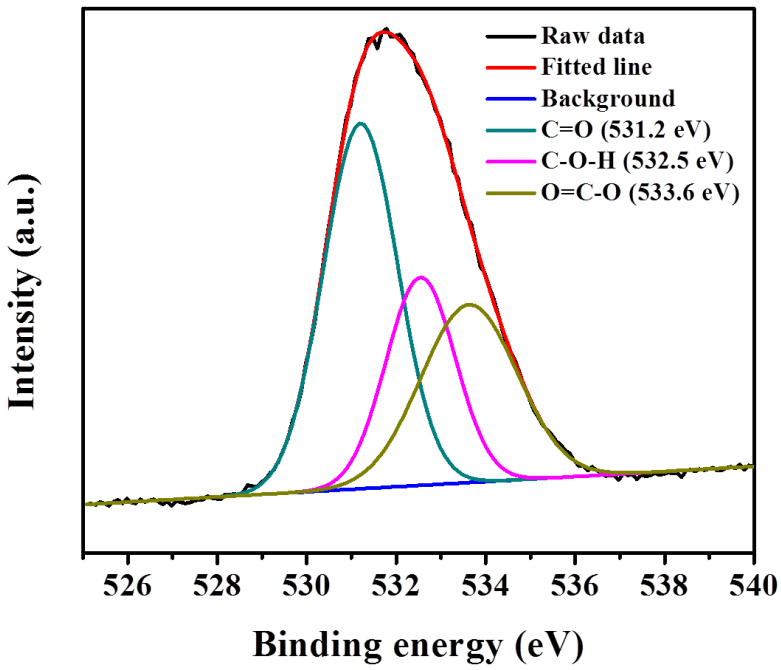

Fig. 3.7 High-resolution XPS spectra of O_{1s} of u-CDs

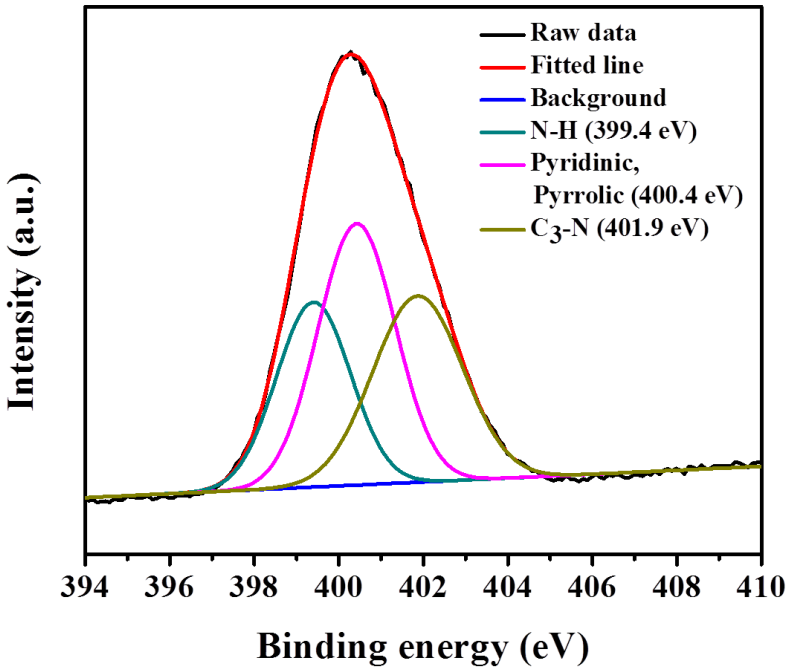

Fig. 3.8 High-resolution XPS spectra of N_{1s} of u-CDs

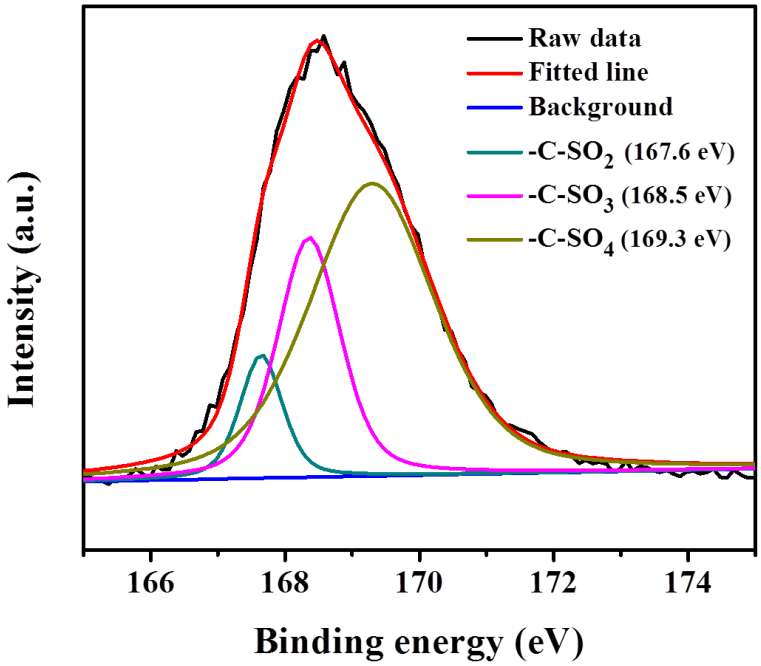

Fig. 3.9 High-resolution XPS spectra of S_{2p} of u-CDs

XPS was used to characterize the elemental composition of the CDs. As shown in Fig. 3.4 and Fig. 3.5, three dominant peaks at 532.1 (O_{1s}), 401.1 (N_{1s}), and 287.1 eV (C_{1s}) were observed for both o-CDs and u-CDs and two weak peaks centered at 233.1 and 170.1 eV were assigned to S_{2s} and S_{2p}, respectively [26], which indicates the incorporation of N and S atoms to the CDs fabricated in this study. The existence of a S_{2p} peak at approximately 170 eV and the absence of a peak at 162 eV indicate that the doped S atoms exist as the sulfate/sulfite form in the CDs rather than the sulfide form [24]. The higher atomic percentage of N, O, and S in u-CDs than those in o-CDs suggests that more functional groups exist on the surface of u-CDs, which can result in enhanced optical properties. Fig. 3.6 to Fig 3.9 present the high-resolution C_{1s}, O_{1s}, N_{1s}, and S_{2p} XPS spectra of the u-CDs. The C_{1s} peak (Fig. 3.6) could be deconvoluted into four peaks centered at 285, 286.2, 288, and 289 eV, which were assigned to C–C/C=C, C–S/C–N/C–O, C=O/C=N, and COOH species, respectively. The C=O, C–O–H, and O=C–O groups were observed in the O_{1s} deconvoluted spectra (Fig. 3.7) at 531.2 eV, 532.5 eV and 533.6 eV, respectively [27]. The N_{1s} spectrum (Fig. 3.8) revealed the presence of N–H (399.4 eV), C–N–C (pyridinic-like and pyrrolic-like, 400.4 eV) and C_3–N (graphite like, 401.9 eV) groups [28]. The high resolution spectrum of S_{2p} (Fig. 3.9) displayed three peaks at 167.6, 168.5, and 169.3 eV, which were assigned to the oxidized sulfur groups, i.e., –C–S(O)x–C–bonds (x=2, 3, 4) rather from the –C–S– bond [23, 26, 29].

3.3.2.3 FTIR analysis

The surface functional groups of the N and S co-doped CDs was analyzed by FTIR spectroscopy. The FTIR spectra of both o-CDs and u-CDs revealed the presence of almost the same functional groups (Fig. 3.10). The O-H and N-H stretching vibrations in the region of 2800-3440 cm^{-1} indicated the presence of hydroxyl and amino groups, which contribute to the highly hydrophilic nature of CDs [30-33]. The weak band observed at 2340 cm^{-1} was assigned to C-N and S-H bond, and the strong bands at 1700 and 1300 cm^{-1} are ascribed to the C=O and C-O stretching vibrations of the carbonyl and carbonyl groups, respectively [34, 35]. The other band related to the C-S and C-N stretching vibrations is also shown in 1235 cm^{-1} [29, 36, 37].

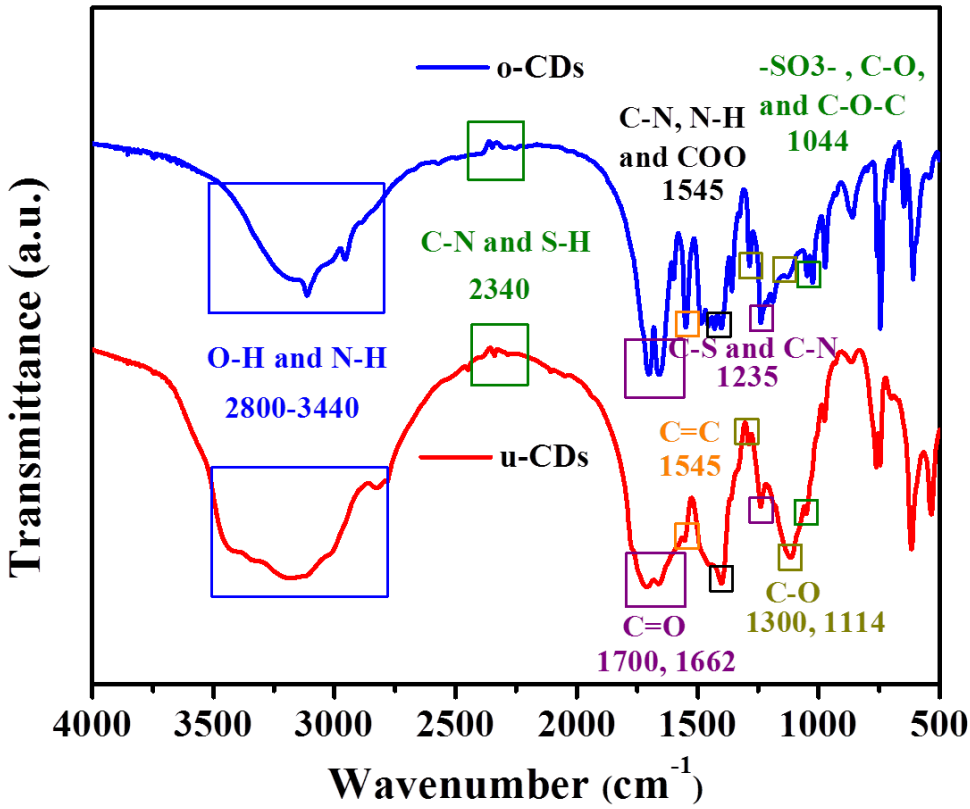

Fig. 3.10 FTIR spectra of the o-CDs and u-CDs

3.3.2.4 Optical analysis

The PL and UV-vis. properties were analyzed to explore the optical properties of the CDs. Fig. 3.11 presents the PL emission spectra of the aqueous solutions of o-CDs and u-CDs under an excitation wavelength of 340 nm and 360 nm, respectively, where the PL intensities of each CD were highest. Comparing to o-CDs, u-CDs shown stronger PL emission and their highest PL intensity was about 6 times higher than that of the former. Also, the highest PL peak position of the latter is located at about 426 nm, which is a red-shifted about 26 nm from that of the former (400 nm) (Fig. 3.11). The inset image of Fig. 3.11 presents a photograph of the aqueous solutions of o-CDs and u-CDs taken under 365 nm UV-lamp irradiation at 20W power, which clearly shows that both solutions exhibit a blue fluorescence color, but the u-CDs emit stronger PL. Fig. 3.12 shows the PL emission of u-CDs at various excitation wavelengths. As the excitation wavelength was increased from 290 nm to 400 nm, the PL emission peak

increased from 386 nm to 440 nm and the maximum fluorescence intensity of the u-CDs was observed at 426 nm with a full width at half maximum of 70 nm when excited at 360 nm. The o-CDs showed similar results except that the maximum fluorescence intensity was observed at 400 nm with a full width at half maximum of 70 nm when excited at 340 nm (Fig. 3.13). Moreover, the PLE spectra of o-CDs and u-CDs exhibited a strongest excitation peak at 340 nm and 360 nm, which are in accordance with their strongest PL peak at 400 nm and 420 nm, respectively (Fig. 3.14 and 3.15).

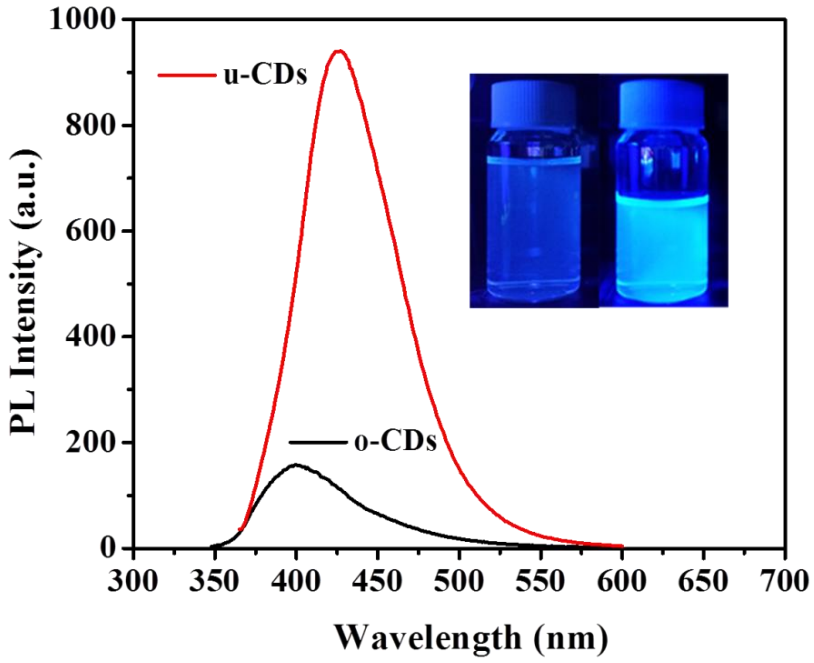

Fig. 3.11 PL spectra of o-CDs and u-CDs with a concentration of 20 µg mL^{-1}. The o-CDs and u-CDs were excited at 340 nm and 360 nm, respectively. Inset is a photograph image of o-CDs (left) and u-CDs (right) in water under 20 W and 365 nm UV lamp irradiation

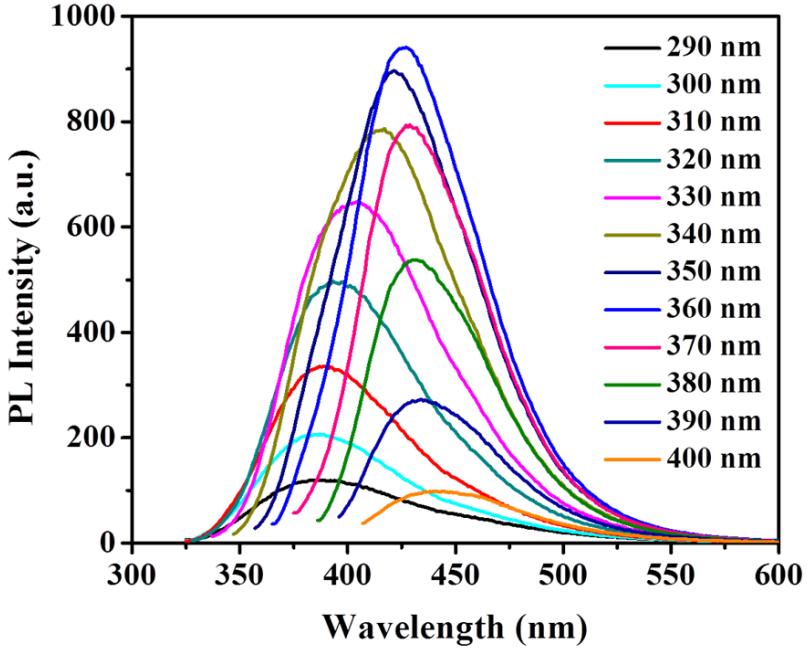

Fig. 3.12 PL emission spectra of the u-CDs at various excitation wavelengths

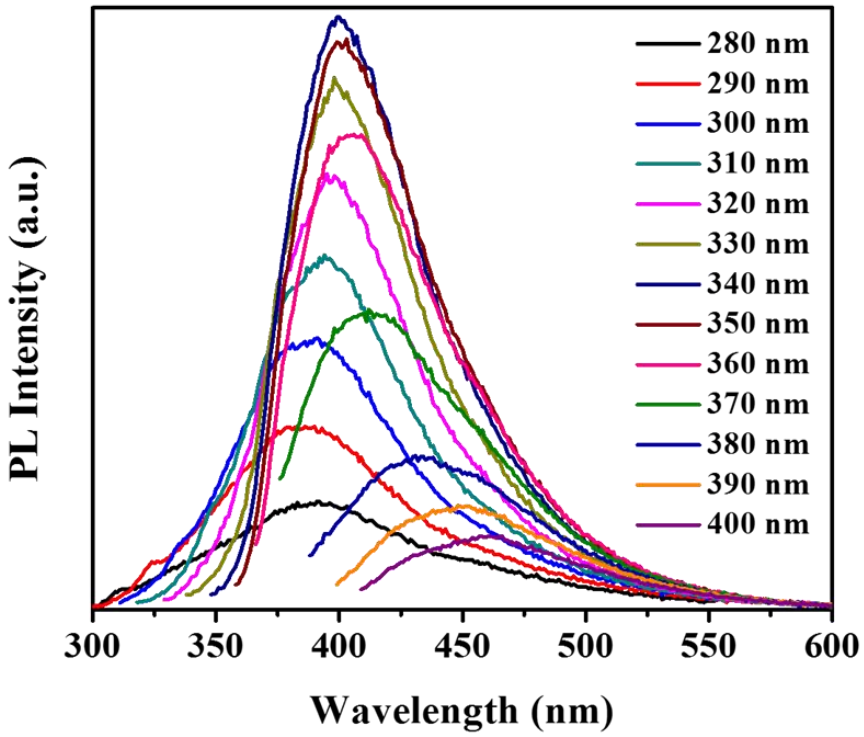

Fig. 3.13 PL emission spectra of the o-CDs at various excitation wavelengths

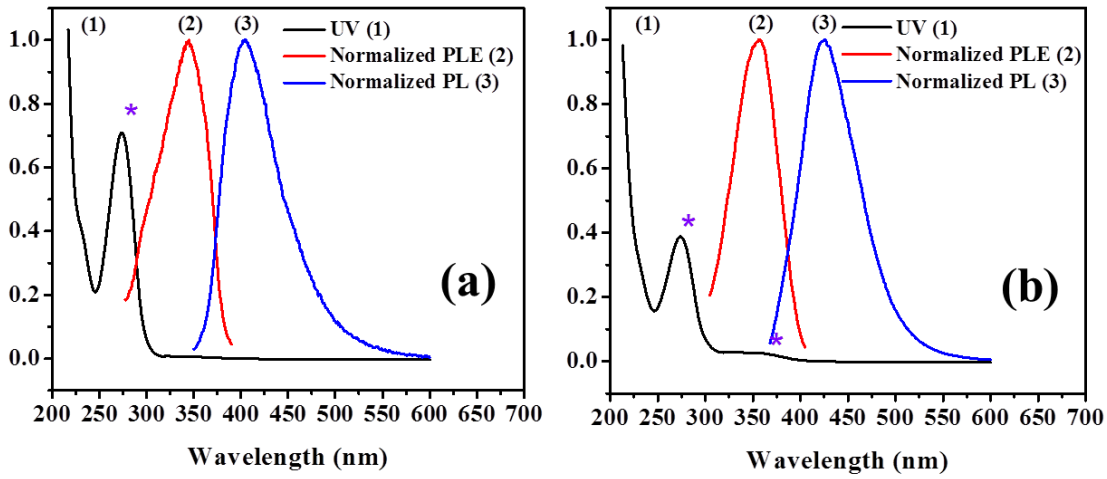

Fig. 3.14 UV-vis absorption (left), normalized PL excitation (middle), and normalized PL emission (right) spectra of the aqueous dispersion of o-CDs (a) and u-CDs (b)

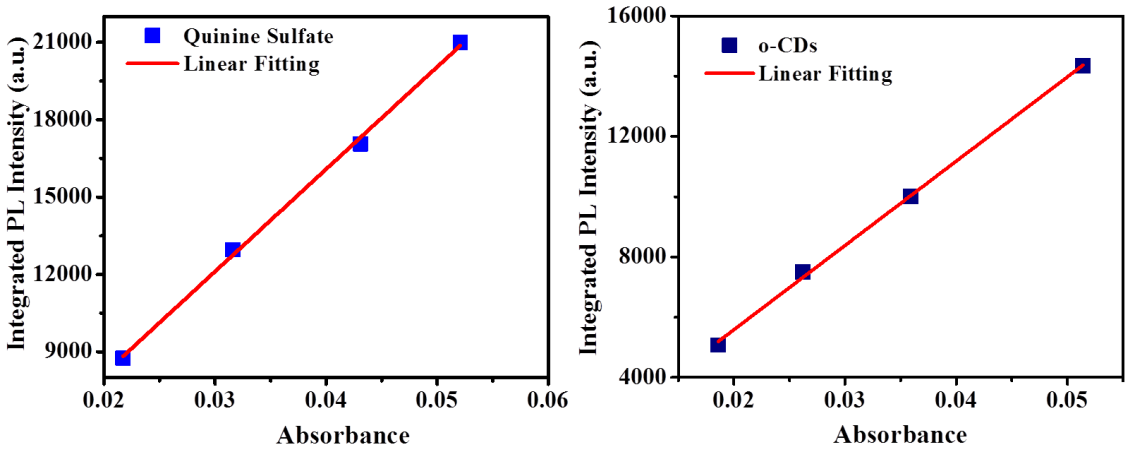

	Quinine sulfate				o-CDs			
Abs	0.0217	0.0316	0.0431	0.0521	0.0186	0.0262	0.0359	0.0514
Integrated PL	8757	12956	17062	20992	5075	7500	10001	14345
Slope	**396743**				**279649**			
QY	**54**				**38**			

Fig. 3.15 Plots of integrated PL intensity of o-CDs and quinine sulfate (referenced dye) as a function of optical absorbance at 360 nm and relevant data in water

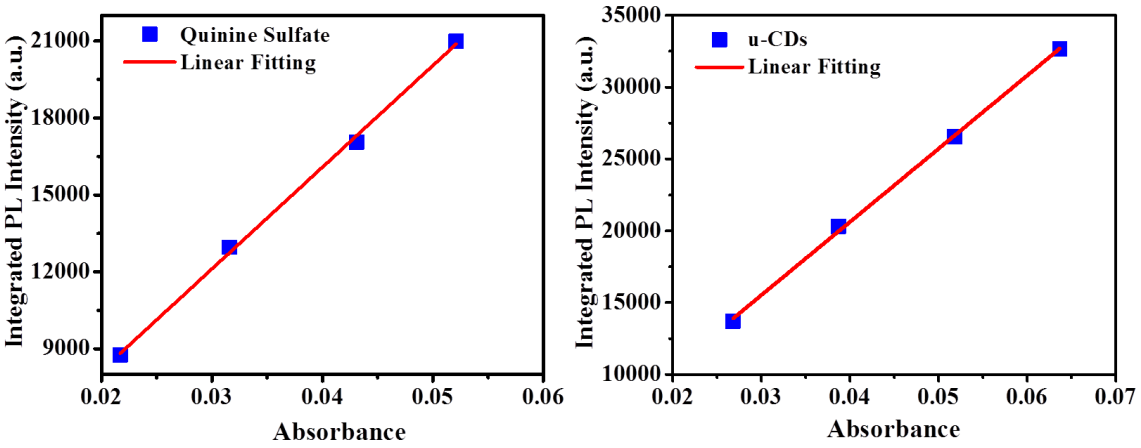

	Quinine sulfate				u-CDs			
Abs	0.0217	0.0316	0.0431	0.0521	0.0268	0.0387	0.0518	0.0637
Integrated PL	8757	12956	17062	20992	13694	20310	26539	32655
Slope	**396743**				**509556**			
QY	**54**				**69**			

Fig. 3.16 Plots of integrated PL intensity of u-CDs and quinine sulfate (referenced dye) as a function of optical absorbance at 360 nm and relevant data in water

As shown in Figs. 3.14 and 3.15, the UV-vis spectra of both the o-CDs and u-CDs solution showed a strong absorption peak at 270 nm, which was assigned to the π–π* transition of aromatic sp^2 domains from the carbon core. On the other hand, only the UV-vis spectra of u-CDs exhibited a broad absorption shoulder at approximately 360 nm, which was attributed to the transition of n–π* and the contribution of surface moieties. This also corresponds well with the maximum PLE at 360 nm and PL at 426 nm of the u-CDs.

To obtain the fluorescence QYs of the CDs, the integrated emission intensities of the CDs were compared with that of quinine sulfate as the standard under excitation of 360 nm [38]. As shown in Figs. 3.16 and 3.17, the QYs of the u-CDs were determined to be 69%, which is much higher than that of o-CDs (38%). The QY obtained in this study was higher than those of previously reported N, S co-doped carbon dots, and even comparable to that of the excellent QYs of N, S co-doped carbon dots synthesized by the hydrothermal treatment of citric acid, which is a unique molecule for the synthesis of highly fluorescent carbon nanodots with nitrogen and sulfur sources (Table 3.1).

The superior optical characterization of the u-CDs can be attributed to the presence of both ammonium persulfate and urea in the precursors. Although it itself could not react with caffeine to produce CDs, urea combined with ammonium persulfate can facilitate the polymerization and carbonization of caffeine, producing larger as-synthesized CDs with more functional groups on their surface, as shown in TEM and XPS analysis. As a result, the u-CDs exhibited a red-shift in PL emission and a much higher quantum yields compared to that of the o-CDs.

	Precursors	Method	QY (%)	Reference
1	L-cysteine, citric acid	Hydrothermal	73	[23]
2	Sulfamide, sodium citrate	Hydrothermal	55	[24]
3	Gentamycin	Thermal treatment	27.2	[26]
4	Methionine, acrylic acid	Hydrothermal	10.55	[30]
5	Thiourea, citric acid	Hydrothermal	78	[33]
6	L-cysteine, citric acid	Microwave	25	[39]
7	NaOH, α-lipoic acid	Hydrothermal	54.4	[40]
8	Glutathione	Thermal treatment	39.9	[41]
9	APS, glucose, and EDA	Thermal treatment	21.6	[42]
10	Heparin sodium	Thermal treatment	7.41	[43]
11	**Caffeine, APS**	**Thermal treatment**	**38**	**This work**
12	**Caffeine, APS, and urea**	**Thermal treatment**	**69**	**This work**

Table 3.1 Reference papers with precursor, synthesis method, and quantum yields (QYs) of N and S co-doped carbon dots

3.3.3 Effect of pH and ionic strength on the PL of CDs

The stable PL emission over a wide range of pH and ionic strengths is very important for practical applications as metal ion sensors. As shown in Fig. 3.19, as the pH was increased from 1.0 to 6.0, a gradual increase in the PL intensity was observed, and from 6.0 to 10.0, it showed only a marginal change. The PL intensity of u-CDs began to decrease rapidly and the PL showed a red-shift from 10.0 (Fig. 3.18). Even

under extreme pH conditions, the PL intensity of the u-CDs maintains approximately 30% of its highest value, which indicates the wide operation range of the u-CDs fabricated in this study. The decrease in PL intensity in strongly basic media and the red-shift phenomenon when the pH increased from 10.0 to 13.0 may be due to the aggregation of the as-synthesized u-CDs.[28, 44-46] Protonation–deprotonation of the amide groups on the u-CDs surfaces is another reason for the pH dependent PL changes [28, 47].

To examine the stability of the u-CDs under high ionic strength environments, the fluorescence intensity of the u-CDs was measured in a solution containing different concentrations of NaCl. As shown in Fig. 2.20, only a negligible change in the PL intensity was observed even when the NaCl concentration was as high as 1 M, showing that u-CDs are stable even under high ionic strength conditions. The reason is that there were almost no ionized functional groups located on the surfaces of the u-CDs [16]. The stability of the u-CDs even in a severe environment suggests that they could potentially be applied in many practical applications.

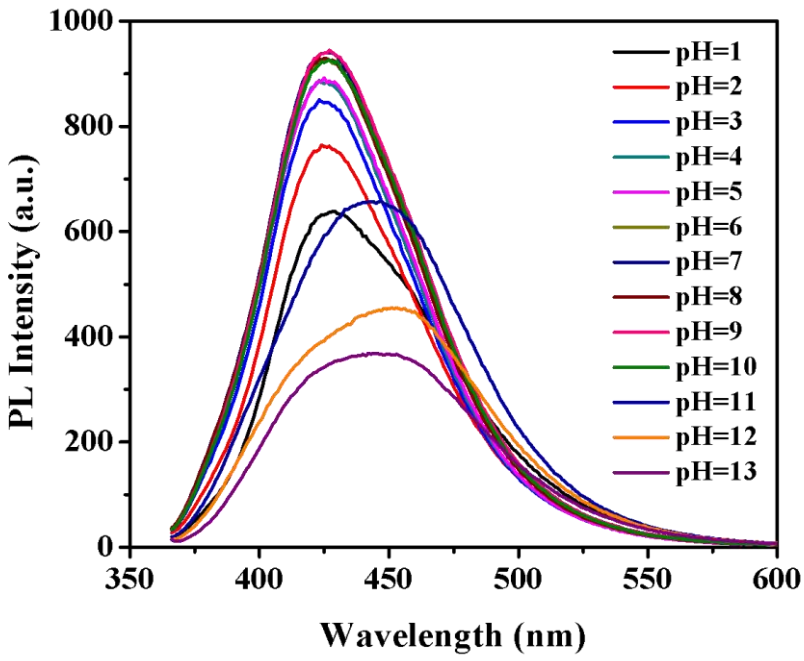

Fig. 3.17 PL emissions of u-CDs at various pH values. The concentration of u-CDs was 20 μg mL^{-1}

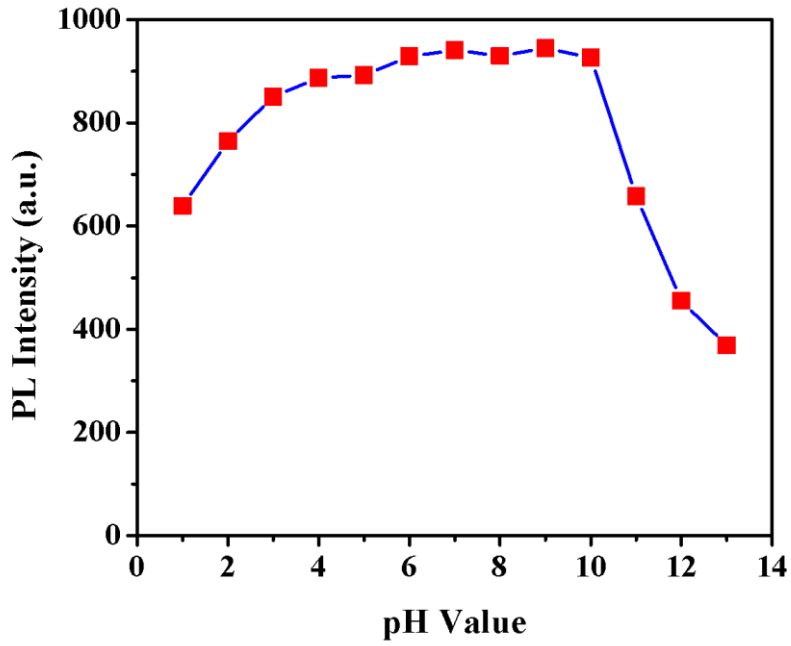

Fig. 3.18 PL intensity of the u-CDs at the excitation of 360 nm as the pH values was changed. The concentration of u-CDs was 20 μg mL^{-1}

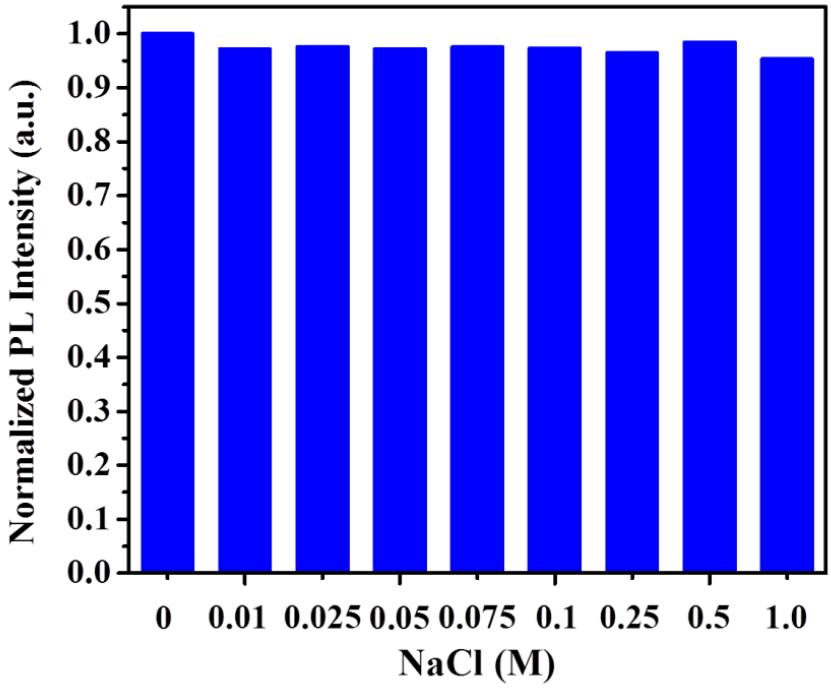

Fig. 3.19 Normalized PL intensity of u-CDs (20 μg mL^{-1}) at various ionic strength of NaCl

3.3.4 Selectivity

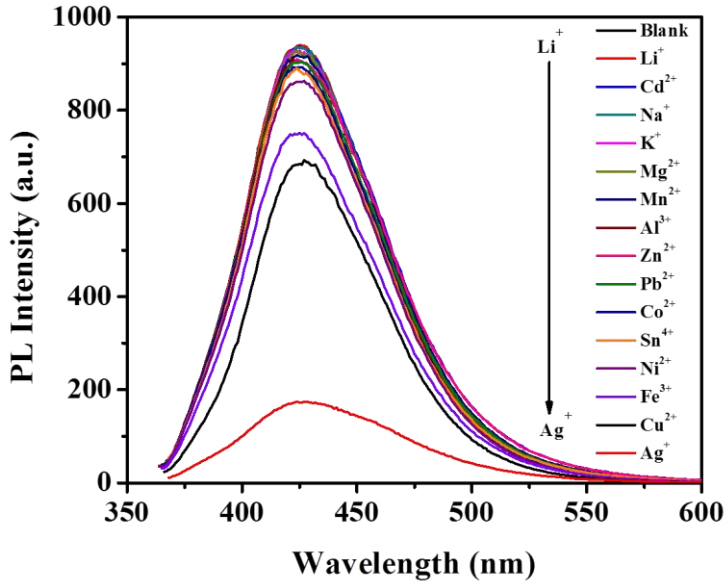

Fig. 3.20 PL emission spectra of solutions of u-CDs in the presence of various metal ions. The concentration of u-CDs and metal ions were 20μg mL^{-1} and 100 μM, respectively

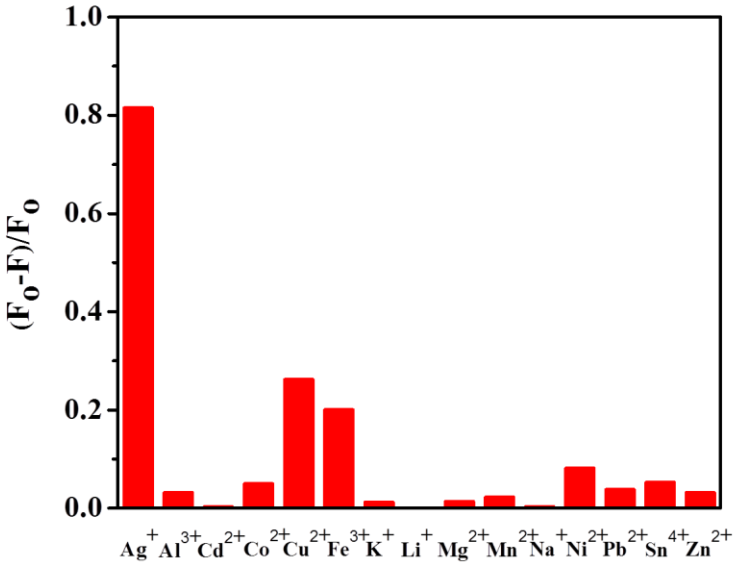

Fig. 3.21 Fluorescence enhancement factors [$(F_0 - F)/F_0$] of u-CDs solutions in the presence of various metal ions. The concentration of u-CDs and metal ions were 20μg mL^{-1} and 100 μM, respectively

To explore the fluorescence sensing of the u-CDs, the fluorescence response of the u-CDs were studied in the presence of various metal ions, such as Ag^{+}, Al^{3+}, Cd^{2+}, Co^{2+}, Fe^{3+}, K^{+}, Li^{+}, Mn^{2+}, Na^{+}, Ni^{2+}, Pb^{2+}, Sn^{4+}, and Zn^{2+} at concentrations of 100 µM, as shown in Fig. 3.21 and 3.22. The PL intensity of the u-CDs was quenched the strongest in the presence of Ag^{+} ions; a lower PL quenching effect was found in the presence of other ions. A serious decrease in the fluorescence intensity of the u-CDs occurred in the presence of Ag^{+} within 1 min, suggesting that u-CDs can be used effectively to monitor Ag^{+} ions in an aqueous solution. The high selectivity of the u-CDs towards Ag^{+} may be because the interaction between ions and the carboxylate or hydroxyl groups made the u-CDs close to each other, which accelerated the non-radiative recombination of the excitons through an effective electron-transfer process, leading to a substantial decrease in the fluorescence of u-CDs [46]. In turn, the Ag^{+} ions may have strong binding affinity and rapid chelating kinetics with the functional groups (amino, carboxyl, and hydroxyl groups) on the surface of the u-CDs, allowing a change in the electronic structure of the u-CDs, which can also affect the distribution of excitons. Therefore, the non-radiative recombination of the excitons can be facilitated through an effective electron transfer process [48, 49].

3.3.5 Sensitivity

The sensitivity of u-CDs toward Ag^{+} ions was examined in detail. The concentration dependent fluorescence measurements of u-CDs at various concentrations of Ag^{+} ions were monitored to prove the feasibility of Ag^{+} ion detection. As shown in Fig. 3.23 and 3.24, as the concentration of Ag^{+} ions increased from 50 nM to 500 µM, and there was a notable and linear decrease in the PL intensity, which means high sensitivity of u-CDs towards Ag^{+} ions. Even at higher concentrations, there was a gradual increase in the fluorescence enhancement factors $[(F_0-F)/F_0]$, to as high as 0.5 mM.

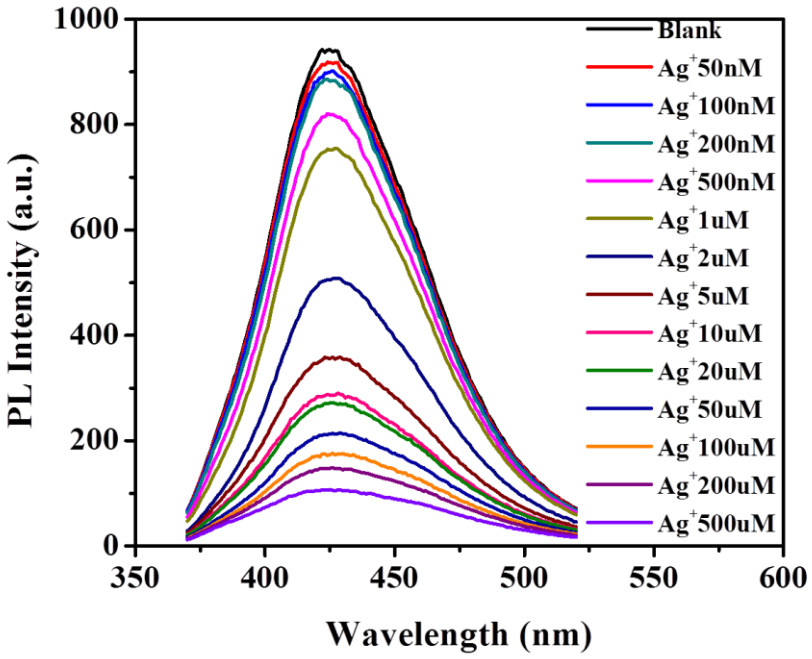

Fig. 3.22 PL emission spectra of u-CDs at various concentrations of Ag^+ ions

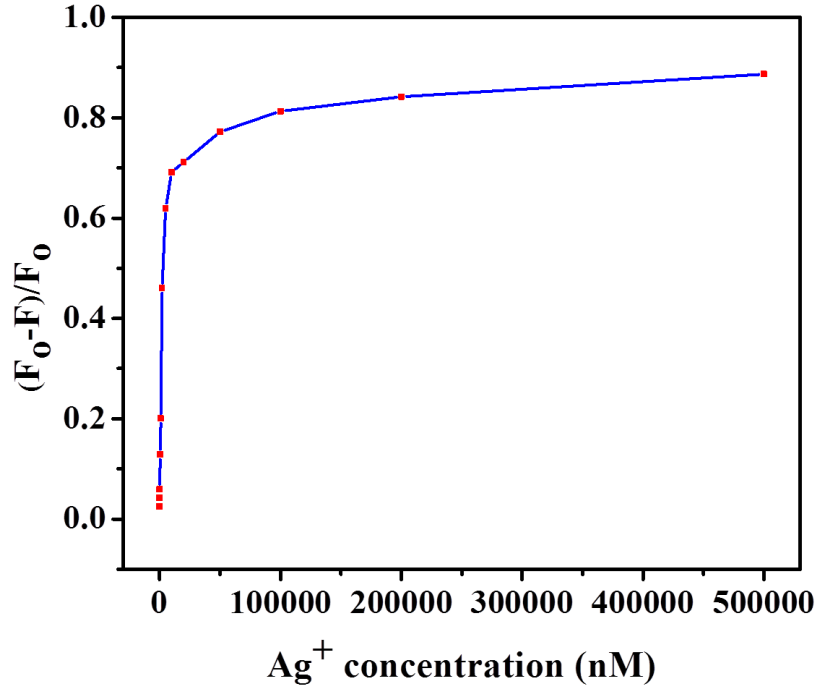

Fig. 3.23 Correlation between the fluorescence enhancement factors $[(F_0-F)/F_0]$ and the concentration of Ag^+ ions

3.4 Conclusion

In this research, a facile one-step process for the synthesis of highly fluorescent N and S co-doped carbon dots (CDs) by thermal heating a solid mixture of caffeine, ammonium persulfate, and urea was reported. CDs could not be produced with caffeine alone, whereas the addition of urea enhanced the formation of CDs of caffeine in the presence of ammonium persulfate. The CDs fabricated in this study exhibited bright blue photo-luminescence with an excellent quantum yield as high as 69%. This approach presents an environmentally friendly, cost-effective and convenient method for the scalable fabrication of highly photo-luminescent carbon dots. Furthermore, the as-prepared CDs can be used as a sensing probe for the label-free, sensitive detection of Ag^{+} ions with high sensitivity and selectivity. This strategy may offer a new approach for the development of inexpensive and sensitive sensors in biological and environmental applications.

3.5 References

[1] W. de Vries, P.F.A.M. Römkens, G. Schütze, Critical Soil Concentrations of Cadmium, Lead, and Mercury in View of Health Effects on Humans and Animals, Reviews of Environmental Contamination and Toxicology, Springer New York, New York, NY, 2007, 91-130.

[2] H.T. Ratte, Bioaccumulation and toxicity of silver compounds: A review, Environmental Toxicology and Chemistry, 18(1999) 89-108.

[3] Z.-m. Xiu, Q.-b. Zhang, H.L. Puppala, V.L. Colvin, P.J.J. Alvarez, Negligible Particle-Specific Antibacterial Activity of Silver Nanoparticles, Nano Letters, 12(2012) 4271-5.

[4] Y. Yin, M. Shen, X. Zhou, S. Yu, J. Chao, J. Liu, et al., Photoreduction and Stabilization Capability of Molecular Weight Fractionated Natural Organic Matter in Transformation of Silver Ion to Metallic Nanoparticle, Environmental Science & Technology, 48(2014) 9366-73.

[5] J.L. Barriada, A.D. Tappin, E.H. Evans, E.P. Achterberg, Dissolved silver measurements in seawater, TrAC Trends in Analytical Chemistry, 26(2007) 809-17.

[6] M. Chamsaz, M. Hossein Arbab-Zavar, J. Akhondzadeh, Triple-phase Single-drop Microextraction of Silver and Its Determination Using Graphite-Furnace Atomic-Absorption Spectrometry, Analytical Sciences, 24(2008) 799-801.

[7] R. Mikelova, J. Baloun, J. Petrlova, V. Adam, L. Havel, J. Petrek, et al., Electrochemical determination of Ag-ions in environment waters and their action on plant embryos, Bioelectrochemistry, 70(2007) 508-18.

[8] C.-Y. Lin, C.-J. Yu, Y.-H. Lin, W.-L. Tseng, Colorimetric Sensing of Silver(I) and Mercury(II) Ions Based on an Assembly of Tween 20-Stabilized Gold Nanoparticles, Analytical Chemistry, 82(2010) 6830-7.

[9] S.Y. Lim, W. Shen, Z. Gao, Carbon quantum dots and their applications, Chemical Society Reviews, 44(2015) 362-81.

[10] S. Qu, D. Zhou, D. Li, W. Ji, P. Jing, D. Han, et al., Toward Efficient Orange Emissive Carbon Nanodots through Conjugated sp^2-Domain Controlling and Surface Charges Engineering, Advanced Materials, 28(2016) 3516-21.

[11] L. Wang, B. Li, F. Xu, X. Shi, D. Feng, D. Wei, et al., High-yield synthesis of strong photoluminescent N-doped carbon nanodots derived from hydrosoluble chitosan for mercury ion sensing via smartphone APP, Biosensors and Bioelectronics, 79(2016) 1-8.

[12] I.P.-J. Lai, S.G. Harroun, S.-Y. Chen, B. Unnikrishnan, Y.-J. Li, C.-C. Huang, Solid-state synthesis of self-functional carbon quantum dots for detection of bacteria and tumor cells, Sensors and Actuators B: Chemical, 228(2016) 465-70.

[13] A. Jaiswal, S.S. Ghosh, A. Chattopadhyay, One step synthesis of C-dots by microwave mediated caramelization of poly(ethylene glycol), Chemical Communications, 48(2012) 407-9.

[14] C. Ding, A. Zhu, Y. Tian, Functional Surface Engineering of C-Dots for Fluorescent Biosensing and in Vivo Bioimaging, Accounts of Chemical Research, 47(2014) 20-30.

[15] M. Zheng, Z. Xie, D. Qu, D. Li, P. Du, X. Jing, et al., On–Off–On Fluorescent Carbon Dot Nanosensor for Recognition of Chromium(VI) and Ascorbic Acid Based on the Inner Filter Effect, ACS Applied Materials & Interfaces, 5(2013) 13242-7.

[16] H. Zhang, Y. Chen, M. Liang, L. Xu, S. Qi, H. Chen, et al., Solid-Phase Synthesis of Highly Fluorescent Nitrogen-Doped Carbon Dots for Sensitive and Selective Probing Ferric Ions in Living Cells, Analytical Chemistry, 86(2014) 9846-52.

[17] S. Bian, C. Shen, Y. Qian, J. Liu, F. Xi, X. Dong, Facile synthesis of sulfur-doped graphene quantum dots as fluorescent sensing probes for Ag^+ ions detection, Sensors and Actuators B: Chemical, 242(2017) 231-7.

[18] C. Xiong, W. Liang, H. Wang, Y. Zheng, Y. Zhuo, Y. Chai, et al., In situ electro-polymerization of nitrogen doped carbon dots and their application in an

electrochemiluminescence biosensor for the detection of intracellular lead ions, Chemical Communications, 52(2016) 5589-92.

[19] M. Algarra, B.B. Campos, K. Radotic, D. Mutavdzic, T. Bandosz, J. Jimenez-Jimenez, et al., Luminescent carbon nanoparticles: effects of chemical functionalization, and evaluation of Ag^+ sensing properties, Journal of Materials Chemistry A, 2(2014) 8342-51.

[20] X. Gao, Y. Lu, R. Zhang, S. He, J. Ju, M. Liu, et al., One-pot synthesis of carbon nanodots for fluorescence turn-on detection of Ag^+ based on the Ag^+-induced enhancement of fluorescence, Journal of Materials Chemistry C, 3(2015) 2302-9.

[21] D. Qu, M. Zheng, L. Zhang, H. Zhao, Z. Xie, X. Jing, et al., Formation mechanism and optimization of highly luminescent N-doped graphene quantum dots, Scientific Reports, 4(2014) 5294.

[22] S. Zhu, Q. Meng, L. Wang, J. Zhang, Y. Song, H. Jin, et al., Highly Photoluminescent Carbon Dots for Multicolor Patterning, Sensors, and Bioimaging, Angewandte Chemie International Edition, 52(2013) 3953-7.

[23] Y. Dong, H. Pang, H.B. Yang, C. Guo, J. Shao, Y. Chi, et al., Carbon-Based Dots Co-doped with Nitrogen and Sulfur for High Quantum Yield and Excitation-Independent Emission, Angewandte Chemie International Edition, 52(2013) 7800-4.

[24] Q. Xu, Y. Liu, C. Gao, J. Wei, H. Zhou, Y. Chen, et al., Synthesis, mechanistic investigation, and application of photoluminescent sulfur and nitrogen co-doped carbon dots, Journal of Materials Chemistry C, 3(2015) 9885-93.

[25] S. Zhu, J. Zhang, S. Tang, C. Qiao, L. Wang, H. Wang, et al., Surface Chemistry Routes to Modulate the Photoluminescence of Graphene Quantum Dots: From Fluorescence Mechanism to Up-Conversion Bioimaging Applications, Advanced Functional Materials, 22(2012) 4732-40.

[26] H. Huang, Y.-C. Lu, A.-J. Wang, J.-H. Liu, J.-R. Chen, J.-J. Feng, A facile, green, and solvent-free route to nitrogen-sulfur-codoped fluorescent carbon nanoparticles for cellular imaging, RSC Advances, 4(2014) 11872-5.

[27] Y. Wang, S.-H. Kim, L. Feng, Highly luminescent N, S- Co-doped carbon dots and their direct use as mercury(II) sensor, Analytica Chimica Acta, 890(2015) 134-42.

[28] X. Sun, J. He, Y. Meng, L. Zhang, S. Zhang, X. Ma, et al., Microwave-assisted ultrafast and facile synthesis of fluorescent carbon nanoparticles from a single precursor: preparation, characterization and their application for the highly selective detection of explosive picric acid, Journal of Materials Chemistry A, 4(2016) 4161-71.

[29] D. Sun, R. Ban, P.-H. Zhang, G.-H. Wu, J.-R. Zhang, J.-J. Zhu, Hair fiber as a precursor for synthesizing of sulfur- and nitrogen-co-doped carbon dots with tunable luminescence properties, Carbon, 64(2013) 424-34.

[30] X. Cui, Y. Wang, J. Liu, Q. Yang, B. Zhang, Y. Gao, et al., Dual functional N- and S-co-doped carbon dots as the sensor for temperature and Fe^{3+} ions, Sensors and Actuators B: Chemical, 242(2017) 1272-80.

[31] Y. Chen, Y. Wu, B. Weng, B. Wang, C. Li, Facile synthesis of nitrogen and sulfur co-doped carbon dots and application for Fe(III) ions detection and cell imaging, Sensors and Actuators B: Chemical, 223(2016) 689-96.

[32] J. Jiang, Y. He, S. Li, H. Cui, Amino acids as the source for producing carbon nanodots: microwave assisted one-step synthesis, intrinsic photoluminescence property and intense chemiluminescence enhancement, Chemical Communications, 48(2012) 9634-6.

[33] D. Qu, M. Zheng, P. Du, Y. Zhou, L. Zhang, D. Li, et al., Highly luminescent S, N co-doped graphene quantum dots with broad visible absorption bands for visible light photocatalysts, Nanoscale, 5(2013) 12272-7.

[34] Y. Zheng, D. Yang, X. Wu, H. Yan, Y. Zhao, B. Feng, et al., A facile approach for the synthesis of highly luminescent carbon dots using vitamin-based small organic molecules with benzene ring structure as precursors, RSC Advances, 5(2015) 90245-54.

[35] C. Zhu, J. Zhai, S. Dong, Bifunctional fluorescent carbon nanodots: green synthesis via soy milk and application as metal-free electrocatalysts for oxygen reduction, Chemical Communications, 48(2012) 9367-9.

[36] J. Zhang, L. Yang, Y. Yuan, J. Jiang, S.-H. Yu, One-Pot Gram-Scale Synthesis of Nitrogen and Sulfur Embedded Organic Dots with Distinctive Fluorescence Behaviors in Free and Aggregated States, Chemistry of Materials, 28(2016) 4367-74.

[37] H. Peng, J. Travas-Sejdic, Simple Aqueous Solution Route to Luminescent Carbogenic Dots from Carbohydrates, Chemistry of Materials, 21(2009) 5563-5.

[38] M. Grabolle, M. Spieles, V. Lesnyak, N. Gaponik, A. Eychmüller, U. Resch-Genger, Determination of the Fluorescence Quantum Yield of Quantum Dots: Suitable Procedures and Achievable Uncertainties, Analytical Chemistry, 81(2009) 6285-94.

[39] L. Li, B. Yu, T. You, Nitrogen and sulfur co-doped carbon dots for highly selective and sensitive detection of Hg(Ⅱ) ions, Biosensors and Bioelectronics, 74(2015) 263-9.

[40] H. Ding, J.-S. Wei, H.-M. Xiong, Nitrogen and sulfur co-doped carbon dots with strong blue luminescence, Nanoscale, 6(2014) 13817-23.

[41] W. Wang, Y.-C. Lu, H. Huang, A.-J. Wang, J.-R. Chen, J.-J. Feng, Solvent-free synthesis of sulfur- and nitrogen-co-doped fluorescent carbon nanoparticles from glutathione for highly selective and sensitive detection of mercury(II) ions, Sensors and Actuators B: Chemical, 202(2014) 741-7.

[42] W. Wang, Y.-C. Lu, H. Huang, A.-J. Wang, J.-R. Chen, J.-J. Feng, Facile synthesis of N, S-codoped fluorescent carbon nanodots for fluorescent resonance energy transfer recognition of methotrexate with high sensitivity and selectivity, Biosensors and Bioelectronics, 64(2015) 517-22.

[43] Y. Sun, C. Shen, J. Wang, Y. Lu, Facile synthesis of biocompatible N, S-doped carbon dots for cell imaging and ion detecting, RSC Advances, 5(2015) 16368-75.

[44] D. Pan, J. Zhang, Z. Li, C. Wu, X. Yan, M. Wu, Observation of pH-, solvent-, spin-, and excitation-dependent blue photoluminescence from carbon nanoparticles, Chemical Communications, 46(2010) 3681-3.

[45] Z. Yang, M. Xu, Y. Liu, F. He, F. Gao, Y. Su, et al., Nitrogen-doped, carbon-rich, highly photoluminescent carbon dots from ammonium citrate, Nanoscale, 6(2014) 1890-5.

[46] Y. Guo, Z. Wang, H. Shao, X. Jiang, Hydrothermal synthesis of highly fluorescent carbon nanoparticles from sodium citrate and their use for the detection of mercury ions, Carbon 2013, pp. 583-9.

[47] M.J. Krysmann, A. Kelarakis, P. Dallas, E.P. Giannelis, Formation Mechanism of Carbogenic Nanoparticles with Dual Photoluminescence Emission, Journal of the American Chemical Society, 134(2012) 747-50.

[48] Y. Zhang, P. Cui, F. Zhang, X. Feng, Y. Wang, Y. Yang, et al., Fluorescent probes for "off–on" highly sensitive detection of Hg^{2+} and L-cysteine based on nitrogen-doped carbon dots, Talanta, 152(2016) 288-300.

[49] J. Ju, W. Chen, Synthesis of highly fluorescent nitrogen-doped graphene quantum dots for sensitive, label-free detection of Fe(III) in aqueous media, Biosensors and Bioelectronics, 58(2014) 219-25.

Chapter 4

Pyromellitic Acid Derived Highly Fluorescent N-doped Carbon Dots for Sensitive and Selective Determination of 4-Nitrophenol

4.1 Introduction

The precise analysis of aromatic nitrocompounds, such as nitrobenzene, nitrotoluenes, and nitrophenols, in natural water and effluent is very important in environmental regulation because of its large impact on the ecological system [1]. These compounds have severe toxicity not only to human beings but also to animals, plants, and aquatic life. Various aromatic nitrocompounds have been documented in environmental regulations [1, 2]. In particular, 4-nitrophenol (4-NP) is one of the nitrophenols in the List of Priority Pollutants of the U.S.A Environmental Protection Agency because of its high toxicity but low degradability and high solubility in water. The inhalation or ingestion of 4-NP, even within a short period of time, can cause headaches, drowsiness, nausea, and cyanosis [3]. Therefore, it is strongly recommended that the use of 4-NP be strictly controlled and supervised due to its potential carcinogenicity, teratogenicity, and mutagenicity [4]. In addition, it has been identified as a dangerous food chain pollutant that can remain in agriculture crops, vegetables, fruits, and water resources when used as an ingredient in fertilizers or pesticides. On the other hand, 4-NP is still used extensively as an intermediate chemical in many chemical processes, including pharmaceuticals, dyestuffs, pesticides, insecticides, herbicides, leather fungicides, and acid-base indicators [5]. As a result, 4-NP can inevitably be discharged into the environment during its production and use in agriculture and industry [2]. Based on the above description, it is crucial to establish a simple and reliable method for the determination of trace amounts of 4-NP in many applications. A range of techniques have been developed to determine the concentration of 4-NP, such as spectrophotometry [6], capillary zone electrophoresis [4], electrochemical methods [7], and chemiluminescence [8]. Most of the above methods have many drawbacks, such as long processing time, requirement of expensive instrument, and/or long and

tedious procedures. Therefore, the development of effective detection methods for 4-NP that is cost effective, uses inexpensive instrumentation, simple operation, rapid response, as well as high sensitivity and selectivity are in strong demand.

Carbon dots (CDs) have attracted increasing attention due to their outstanding performance, abundant and inexpensive precursors, efficiently synthesis methods, and immense potential for extensive applications [9]. Up to now, various synthetic routes, such as physical and chemical approaches, have been reported for the production of CDs using various organic compounds and natural sources as precursors. In addition, numerous heteroatom-doped CDs and CD-based composites have also been studied to enhance the electrical, electrochemical, and optical properties of pristine CDs [10]. Doping is a common method that involves the incorporation of hetero atoms of appropriate elements, such as B, Si, N, P, S, and Se into the host carbon lattice to tune the electrical and chemical properties of CDs [11-16]. Among them, N doping is the most investigated procedure for improving the photo-emission of CDs. This is because nitrogen bonding to carbon can enhance the photoluminescence (PL) emission of CDs significantly by inducing an upward shift in the Fermi level and electrons in the conduction band [17], which can be used in many applications, including sensing [18], bioimaging [13], and catalysis [19]. Two approaches, “top-down” and “bottom-up”, are generally employed to synthesize N-doped CDs. The top-down method takes advantage of green and economic precursors from biomass materials, such as milk and silk, but the CDs prepared from this approach mostly show low quantum yields (QYs) [13, 20, 21]. Instead, the latter approach has been used widely to produce high quantum yield CDs through various methods, including hydrothermal or solvothermal treatment [22, 23], solid-phase treatment [24, 25], and microwave-assisted treatment [26, 27], in the presence of high nitrogen containing reactants. These methods produce NCDs with a high QYs but usually exhibit blue color emission [18, 24, 28]. Blue color emission is close to autofluorescence and is induced by ultraviolet (UV) excitation [29, 30], which could cause low tissue penetration and high photo-damaging side effects, limiting applications, particularly in bio-related fields. The development of facile and cost effective approaches for the synthesis of long-wavelength PL excitation-emission CDs is still a challenge [31].

In this study, uniform and high QY CDs were synthesized by the facile, one pot hydrothermal treatment of a novel precursor, called pyromellitic acid (PA), and ethylenediamine (EDA). The as-prepared CDs exhibited excellent water solubility, pure bright cyan color emission (484 nm) with visible light excitation (415 nm), and a quantum yield as high as 75%, which is one of the highest values reported thus far. Owing to its highly cyan fluorescence, the newly synthesized CDs were applied effectively as a fluorescence platform for the sensitive and selective determination of 4-NP without further chemical modification or surface functionalization. This strategy offers a very promising approach for the determination of 4-NP in terms of simple operation, high selectivity, high sensitivity, and low detection limit.

4.2 Experimental

4.2.1 Chemicals

Ethylenediamine (EDA), sodium chloride, sodium hydroxide, potassium chloride, boric acid, potassium bromide for Fourier transform infrared (FTIR) spectroscopy, hydrochloric acid, and sulfuric acid were purchased from Deajung Chemicals and Metals Co. Ltd (Korea). Quinine sulfate dihydrate was obtained from Wako Pure Chemical Co. Ltd (Japan). Pyromellytic acid (PA), ascorbic acid, caffeine, catechol, cysteine, ethylenediaminetetraacetic acid (EDTA), glucose, glycine, hydroquinone, 3-nitrophenol, 2-nitroaniline, 2-nitrophenol, 4-nitrophenol, phenylboronic acid, and taurine were supplied by Sigma-Aldrich Co. Ltd. (USA) and used as received. Deionized (DI) water with a resistivity of 18.2 MΩ cm^{-1} was used in all experiments.

4.2.2 Characterizations

The UV-vis spectra were recorded with an UV-vis spectrophotometer (Analytik Jena, SPECORD 210 PLUS, Germany) using a quartz cell with a 1 cm optical path. The photoluminescence (PL) emission spectra were taken using a Cary Eclipse fluorescence spectrophotometer (Agilent Technologies, G9800AA, USA). The FTIR (Thermo Fisher Scientific, NEXUS, USA) spectra were recorded at 400-4000 cm^{-1}. Transmission electron microscopy (TEM, JEM-2100, JEOL, Japan) was conducted at an operating

voltage of 200 kV. X-ray photoelectron spectroscopy (XPS, ESCALB-MKII250, VG Co., USA) was performed using Al Kα X-ray radiation.

4.2.3 Synthesis of N-doped CDs (NCDs)

The NCDs were synthesized via a green, facile, and one pot hydrothermal synthesis. Typically, 1 mmol of PA and 4 mmol of EDA were added to 5 mL of DI water and stirred until a clear solution formed. The solution was then transferred to a Teflon-lined stainless-steel autoclave, sealed, and placed into a siliconit muffle furnace. The furnace was heated to 200^{o}C and kept at this temperature for 6 h. After cooling to ambient temperature, the bright yellowish green solution was washed with ethanol and centrifuged at 9,000 rpm for 15 min. The as-synthesized NCDs in this study were collected and re-dispersed easily into DI water.

4.2.4 Sensitivity and selectivity measurement of 4-NP

The fluorescent detection probe was prepared by diluting the as-prepared NCDs with a 0.05 M alkaline borate buffer (at pH 9.0) to form a 20 μg mL^{-1} solution. The fluorescence emission intensity at 484 nm of the blank sample excited at 415 nm was measured and marked as F_0. To determine the 4-NP concentration, 30 μL of 4-NP with a concentration range of 10 μM to 20 mM was added to 2.97 mL of the above NCDs solution. After 3 min equilibration, the fluorescent intensity (F) of each sample was measured. The selectivity towards 4-NP was determined by adding other related analogues, including ascorbic acid, caffeine, EDTA, catechol, cysteine, glucose, glycine, hydroquinone, 3-nitrophenol, 2-nitroaniline, 2-nitrophenol, phenylboronic acid, and taurine in a similar manner. All experiments were conducted at room temperature.

4.2.5 Determination of QYs of NCDs.

The QY of the NCDs was determined by a widely used relative method [32]. In particular, quinine sulfate (QY = 54% in 0.1 M H_2SO_4) was selected as the reference. The QY of a sample can be calculated using the following equation:

$$\emptyset = \emptyset' \times \frac{A'}{I'} \times \frac{I}{A} \times \frac{n^2}{n'^2}$$

where ϕ is the QY of the testing sample; I is the testing sample's integrated emission intensity; n is the refractive index (1.33 for water); and A is the optical density. The prime symbol (′) refers to the referenced dye with a known QY, quinine sulfate. To obtain more reliable results, a series of solutions of NCDs and referenced dyes with a known QY were prepared at concentrations adjusted so that the optical absorbance would be between 0-0.1 at 415 nm. The QYs were determined by a comparison of the integrated PL intensity versus the absorbance curves, as shown in Fig. 4.10.

4.3 Results and discussion

4.3.1 TEM, XPS and FT-IR analysis

TEM was used to examine the morphology and structures of the NCDs. The samples were prepared by drop-casting a diluted aqueous solution of NCDs onto a carbon-coated copper grid. As shown in Fig. 4.1, the as-prepared NCDs are almost spherical with a uniform dispersion and a narrow size distribution between 2.8 nm to 6.4 nm. The high magnification image of a single NCD (HR-TEM, inset of Fig. 4.2) revealed a d-spacing of 0.24 nm, which indicates the presence of the (1002) lattice planes of sp^2 graphitic carbon, as reported previously [16, 31, 33-35].

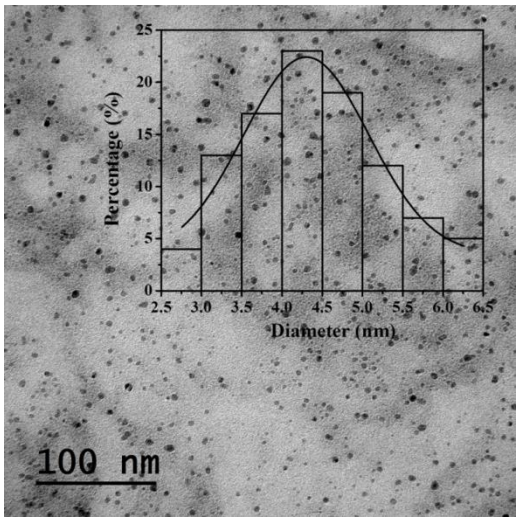

Fig. 4.1 TEM image of NCDs. Inset is the histogram of the particle size distribution of NCDs

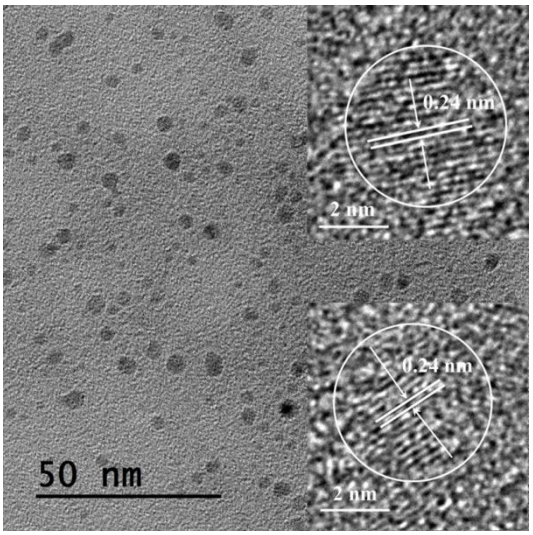

Fig. 4.2 TEM image of NCDs. Inset are HRTEM images of NCDs

The elemental composition of the NCDs was characterized by XPS. The three dominant peaks were observed at 285.1 eV, 399.5 eV, and 530.4 eV, which were assigned to C_{1s}, N_{1s}, and O_{1s}, respectively (Fig. 4.3). The strong N_{1s} peak indicated a reaction between PA and EDA, leading to the successful formation of nitrogen-doped CDs. Fig. 4.4-4.6 shows the high resolution C_{1s}, O_{1s}, and N_{1s} XP spectra, respectively. The C_{1s} peak in Fig. 4.4 was deconvoluted into three sub-peaks centered at 284.4, 285.6, and 287.4 eV, which were assigned to C–C/C=C, C–N/C–O, and C=O related carbon peaks, respectively [36, 37]. In addition, the C=O and C–O–H/C–O–C groups were observed in the O_{1s} deconvoluted XP spectra (Fig. 4.5) at 530.4 eV and 531.6 eV [22, 36, 38]. In addition, the N_{1s} spectrum in Fig. 4.6 could be deconvoluted into two peaks centered at 399.0 eV and 400.7 eV, which were ascribed to pyridinic N (C_2–N–H)/amidic N (O=C–NH) and pyrrolic N (C_2–N–H)/graphitic N (C_3–N–H) [36, 38, 39]. The XP spectra clearly indicated the incorporation of N into graphitic carbon (pyridine-like N, pyrrole-like N, and graphitic-like N) and amide N on the surface of the NCDs, which can contribute greatly to the PL enhancement of CDs.

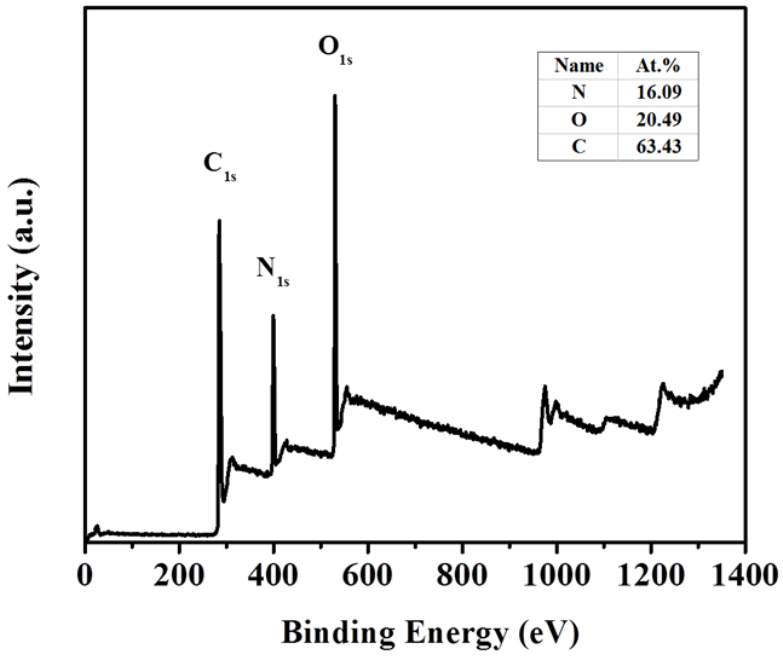

Fig. 4.3 XPS survey spectra of NCDs

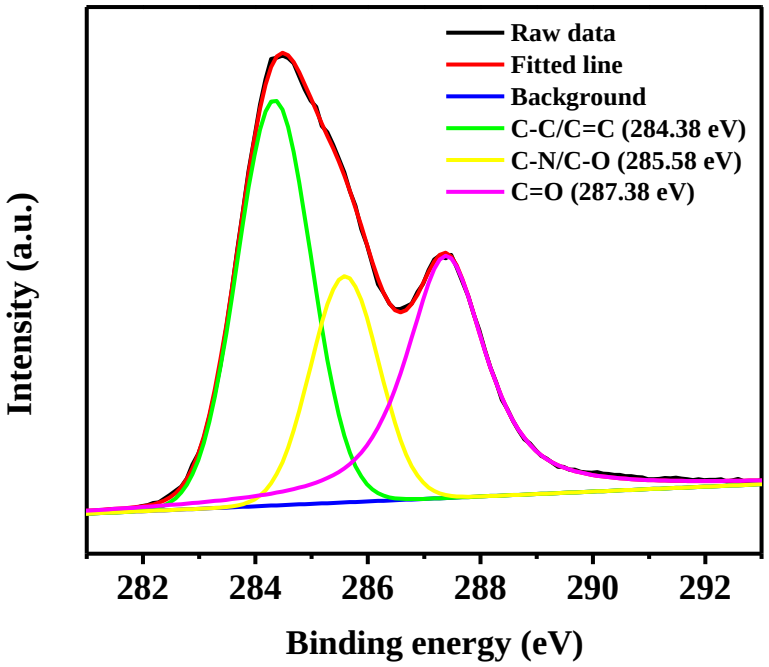

Fig. 4.4 High-resolution XPS spectra of C_{1s}

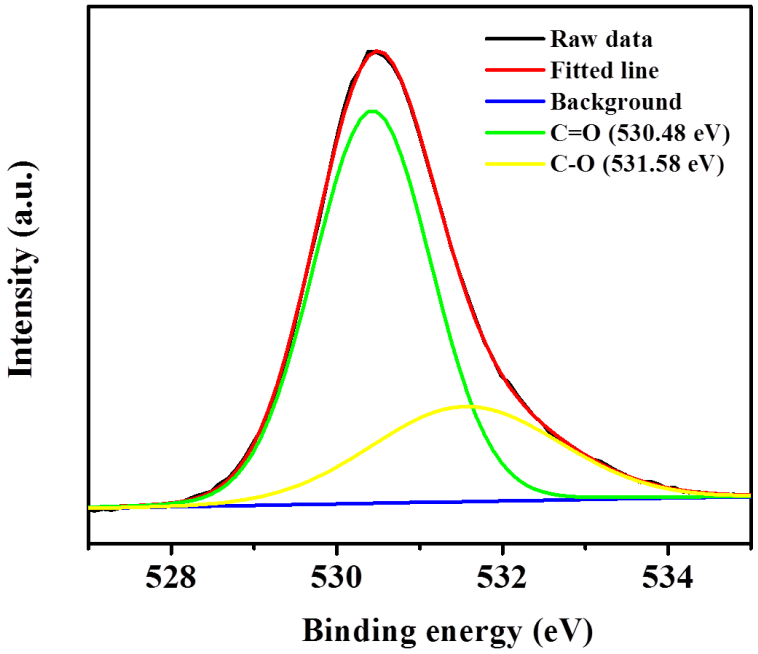

Fig. 4.5 High-resolution XPS spectra of O_{1s}

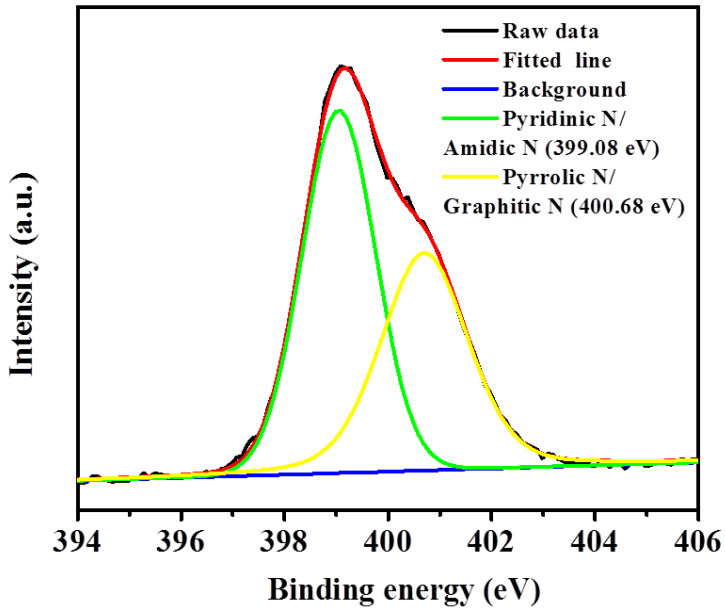

Fig. 4.6 High-resolution XPS spectra of N_{1s}

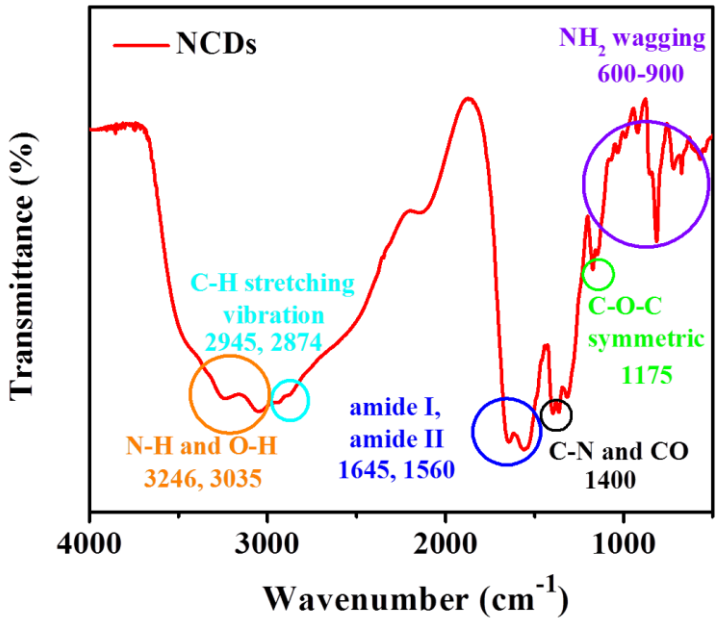

Fig. 4.7 FTIR spectra of NCDs

The incorporation of N atoms in CDs was evaluated by FTIR spectroscopy. The absorption peaks at 3035 and 3246 cm^{-1} were assigned to the stretching vibration of O-H and N-H, respectively, indicating the presence of hydroxyl and amino groups on the NCDs fabricated in this study (Fig. 4.7) [25]. In addition, the peaks at 1570 cm^{-1} (amide II) and 1658 cm^{-1} (amide I) were attributed to the bending vibrations of the amide group, which strongly confirms the formation of amide bonds by the reaction between the carboxylic acids of PA and the diamines of EDA [40]. The peaks at 2945 and 2874 cm^{-1} were assigned to the C–H stretching vibration [18, 22, 41] and the peak at 1400 cm^{-1} could be identified as C-N and C-O groups [18, 22, 25]. Pronounced signals at 1175 cm^{-1} could be assigned to the symmetric band of C–O–C and the bands from 600 to 900 cm^{-1} could be ascribed to the NH_2 wagging bands [42].

XPS and FT-IR spectroscopy confirmed the successful incorporation of a nitrogen atom into the carbon structures. In addition, the large amount of carboxyl and hydroxyl groups on the surface of the NCDs suggests that the NCDs are functionalized with abundant hydrophilic groups, which might contribute to the superior hydrophilicity of NCDs.

4.3.2 PL properties of NCDs

From fundamental and application viewpoints, strong PL emission is one of the most useful features of NCDs. Fig. 4.8 shows the photoluminescence excitation (PLE) spectra of the NCDs. The two peaks at 415 and 430 nm correspond to those observed in the UV-vis absorption spectrum. As shown in Fig. 4.9, the PL emission intensity of the NCDs was highest when it is exited at 415 nm. The fluorescence emission peak position at 484 nm remained unchanged when the excitation wavelength was increased from 350 to 450 nm, indicating that the NCDs obtained have good purity [43]. Moreover, it was reported that the excitation independent behavior of the NCDs could be attributed to the uniform size and surface state of the sp^2 clusters in the NCDs [22, 28, 39, 41], which is consistent with the TEM observations of the NCDs fabricated in this study. The excitation wavelength in visible light and the emission with a pure cyan color of the obtained NCDs are important advantages over those obtained from previous processes, which mostly resulted in blue color emission, as shown in Table 4.1. In addition, the blue color emission of the CDs in previous papers was induced by ultraviolet (UV) excitation, which is likely to be accompanied by low tissue penetration and high photo-damaging side effects [31]. On the other hand, the cyan color emission of the NCDs prepared in this study under visible light excitation could be used effectively in biosensing and bioimaging applications.

The QY of the NCDs fabricated in this study was measured to be as high as 75% (Fig. 4.10). This was is higher than those of previously reported N-doped CDs, which used citric acid, a unique molecule for the synthesis of CDs, and its related compounds Table 4.1. More importantly, the QY of the as-prepared NCDs was even comparable to the QYs of the excellent CDs synthesized from citric acid and EDA in a previous report under the same conditions (76% of QYs) [41, 44, 45], suggesting that PA could be a very promising candidate for the fabrication of high QY CDs.

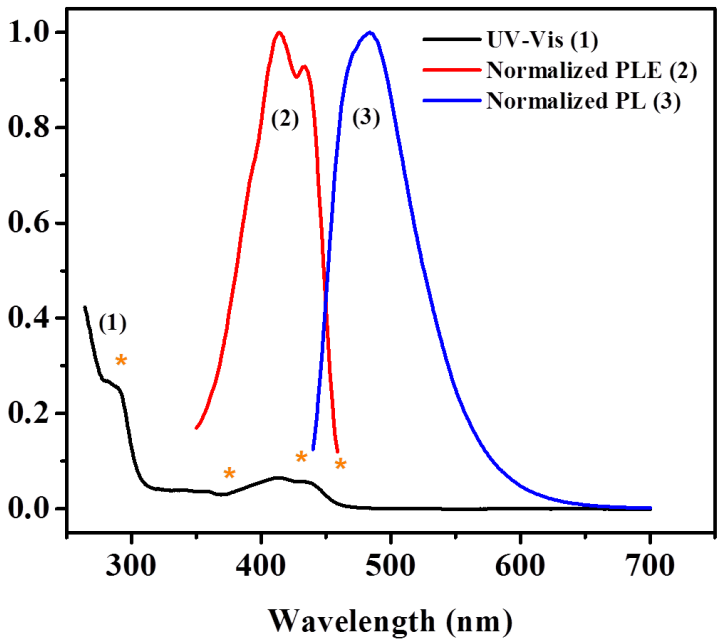

Fig. 4.8 UV-vis absorption, normalized PL excitation, and normalized PL emission spectra of the aqueous dispersion of NCDs

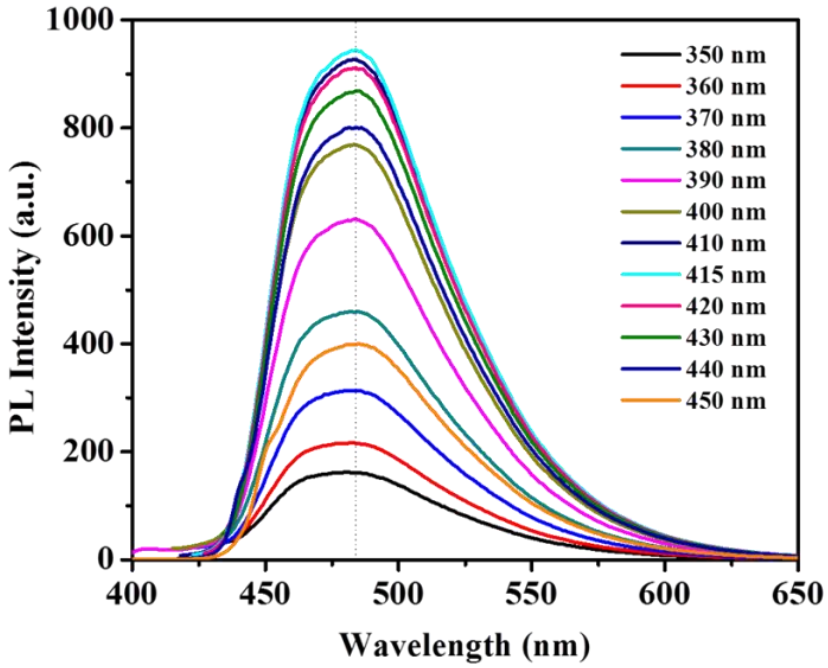

Fig. 4.9 PL emission spectra of the u-CDs at various excitation wavelengths

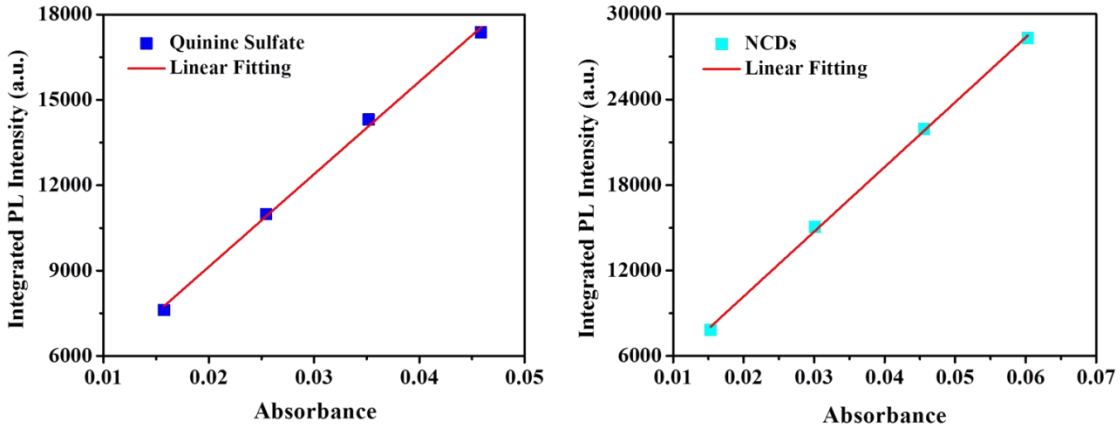

	Quinine sulfate				NCDs			
Abs	0.01574	0.02545	0.03519	0.04587	0.01531	0.03012	0.04561	0.06030
Integrated PL	7616	10985	14311	17377	7814	15065	21933	28317
Slope	**325300**				**454457**			
QY	**54**				**75.44**			

Fig. 4.10 Plots of integrated PL intensity of NCDs and quinine sulfate (referenced dye) as a function of optical absorbance at 415 nm and relevant data in water

The basic formation mechanism might be similar to that between citric acid and diamine because the PA also has multi-carboxylic acid groups. First, the amide bond can be formed by a reaction between amines of EDA and carboxylic acids of PA [45]. The remaining carboxylic acids and amines in the intermediate structure can react further with other molecules to form polymeric networked structures [46] followed by carbonization and aromatization [36], as shown in Scheme 4.1. Four carboxylic acid groups and the aromatic backbone of PA can result in a more conjugated and networked structure than those when citric acid is used as a precursor.

	Precursors	Method	Color emission	Ex (nm)	Em (nm)	QY (%)	References
1	Ammonium citrate, EDA	Hydrothermal	Blue	360	445	66.8	[18]
2	Ammonium citrate	Hydrothermal	Blue	365	437	13.5	[22]
3	Citric acid, PEG-diamine	Thermal treatment	Blue	360	435	31	[25]
4	Ammonium citrate dibasic	Microwave assisted	Blue	340	435	19.8	[27]
5	Citric acid, Tris-HMA	Thermal treatment	Blue	335	425	59.2	[28]
6	Calcium citrate, urea	Microwave assisted	Yellowish-green	390	520	10.1	[41]
7	Citric acid, EDA (Optimum)	Hydrothermal	Blue	360	450	94	[45]
	Citric acid, EDA (200°C)	Hydrothermal	Blue	360	450	76	
8	Sodium citrate, NH_4CO_3	Hydrothermal	Blue	340	435	68.22	[48]
9	Citric acid, ethanolamine	Pyrolysis	Blue	375	455	50	[49]
10	**Pyromellitic acid, EDA**	**Hydrothermal**	**Cyan**	**415**	**484**	**75**	**This work**

Table 4.1 Reference papers reported N-doped carbon dots using citric acid and its relatives as precursors

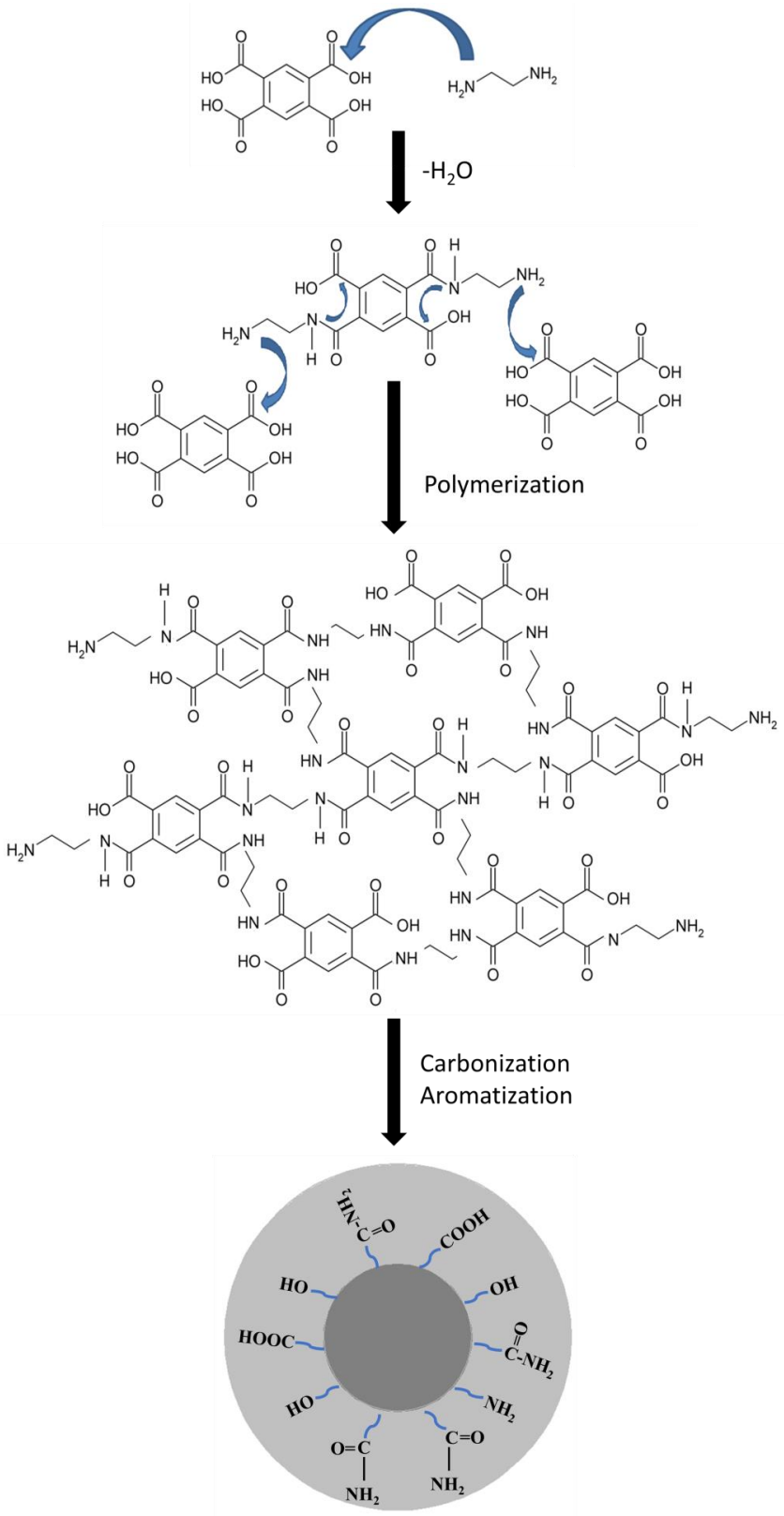

Scheme 4.1 Schematic diagram of mechanism of formation of NCDs

4.3.3 Effect of pH and ionic strength on the PL of NCDs

For practical applications of CDs as photoluminescent sensors, it is very important that the PL emission of the synthesized CDs be stable under extreme environmental conditions, such as pH and ionic strength. To investigate the effect of the solution pH on the sensing characteristics of NCDs, the PL intensity of the NCDs was measured at pH ranging from 1 to 13. As shown in Fig. 4.11-12, when the pH was increased from 4 to 11, the NCDs exhibited a negligible change in PL intensity, suggesting that the fabricated NCDs are stable in wide range of environments from medium acidic to medium basic media. The decrease in PL intensity of the NCDs in strongly acidic (pH 1-3) and basic (pH 12-13) media and the red-shift phenomenon of PL when the pH was increased from 1 to 3 can be attributed to the aggregation of NCDs [22, 27, 47, 48] and the protonation-deprotonation of the amide groups on the surfaces of the NCDs [27, 49], which are common behaviors of CDs.

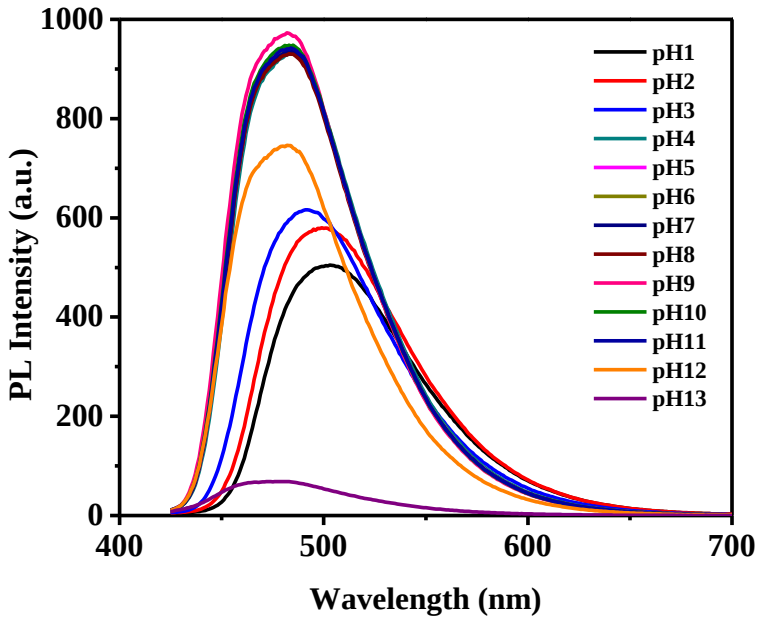

Fig. 4.11 PL emissions of NCDs at various pH values

The PL intensity of NCDs was measured in a solution containing different concentrations of NaCl to determine the stability of NCDs in a high ionic strength environment. Fig. 4.13 shows only a marginal change in the PL intensity of NCDs when the NaCl concentration was as high as 2 M, indicating that the NCDs are stable even

under extreme ionic strength conditions. The stability of NCDs at extreme ionic strengths can be explained by the near absence of ionized functional groups on the surfaces of the NCDs [25]. The excellent stability of the NCDs, even under severe environmental conditions, suggests that they have potential luminescent-based sensing applications.

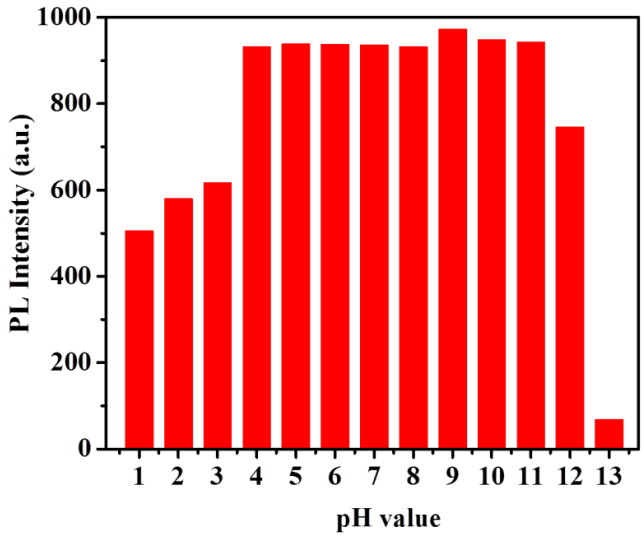

Fig. 4.12 PL intensity of the NCDs at the excitation of 415 nm as the pH values was changed. The concentration of NCDs was 20 µg mL^{-1}

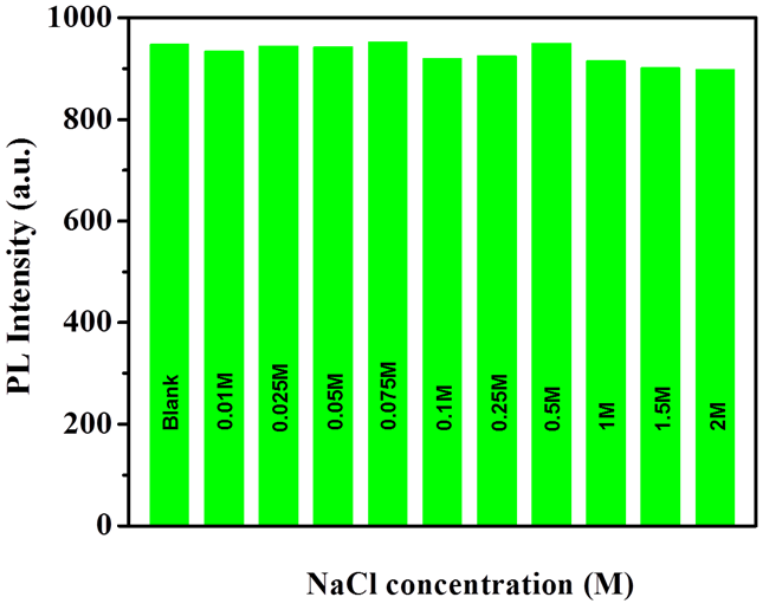

Fig. 4.13 PL intensity of NCDs (20 µg mL^{-1}) at various ionic strength of NaCl

4.3.4 Sensitivity and Selectivity of NCDs

The sensitivity of NCDs toward 4-NP, the most toxic compound compared to other mononitrophenols that are difficult to remove from groundwater and surface water due to their solubility and stability, was investigated in detail. In addition, the linear response range and the limit of detection (LOD) were determined. As shown in Fig. 4.14, the PL intensity decreased with increasing 4-NP concentration due to the quenching of PL.

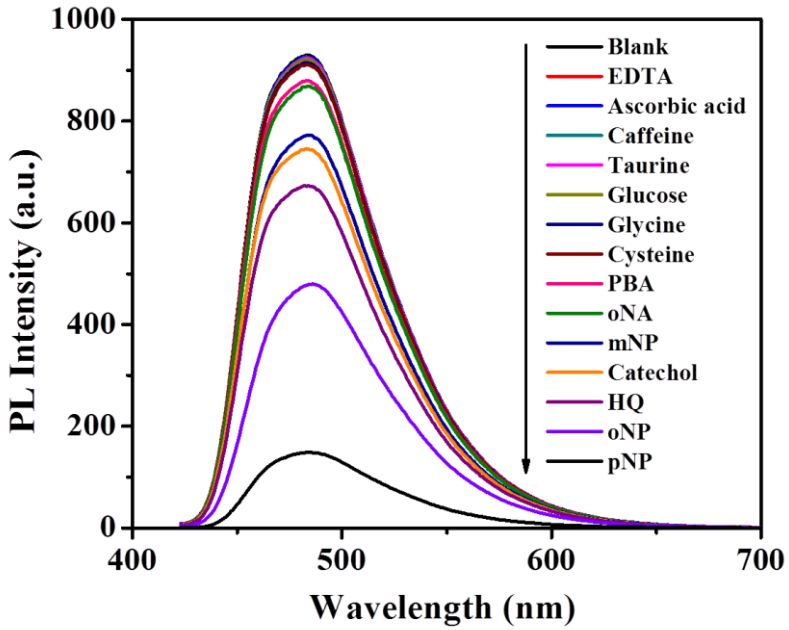

Fig. 4.14 PL emission spectra of solutions of NCDs in the presence of various metal ions

PL quenching can be induced by energy transfer between CDs and 4-NP [50]. As shown in Scheme 4.2, energy transfer can be facilitated by the formation of a zwitterionic spirocyclic Meisenheimer complex via the combination of NCDs and 4-NP. As a result of the formation of a Meisenheimer complex, the negative charge may be delocalized over the cyclohexadienine ring and the nitro group, whereas a positive charge may be distributed over the iminium group. The energy transfer process caused by the localization of positive and negative charges may result in substantial PL quenching of the NCDs after 4-NP addition.

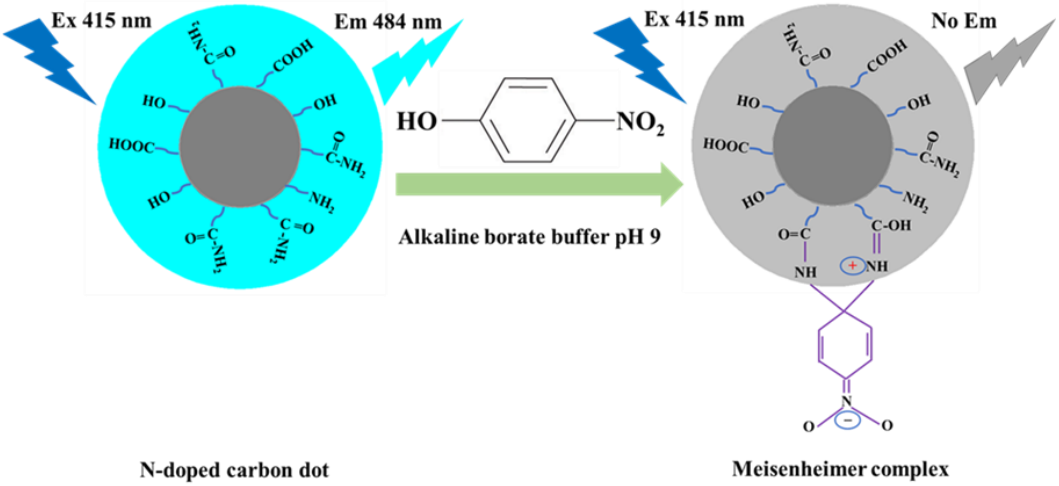

Scheme 4.2 Schematic diagram of mechanism of the quenching effect of NCDs with the presence of 4-NP

Based on the Stern-Volmer semilog plot, the obtained calibration curve was linear within the range of 0.1 to 100 µM 4-NP with a notable linear regression equation of $\log(F_0/F) = 0.0081C\ [\mu M] + 0.0043$, where F_0 and F are the PL intensity of the NCDs in the absence and presence of 4-NP, and C is the concentration of 4-NP in µM. The correlation coefficient was as high as 0.9993 (Fig 4.15 -16). The limit of detection calculated based on the IUPAC criterion (3.3σ) was as low as 17 nM of 4-NP (n=10), which is lower or comparable to the values reported elsewhere, as listed in Table 4.2.

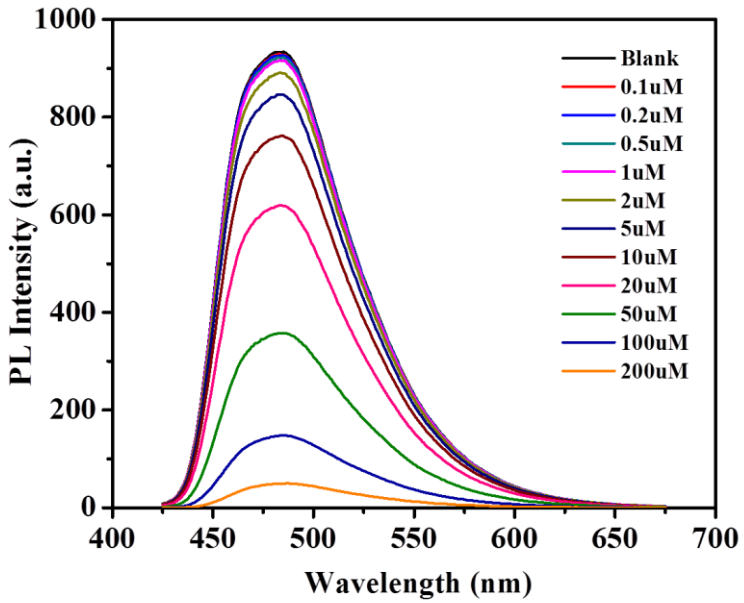

Fig. 4.15 PL emission spectra of NCDs at various concentrations of 4-NP

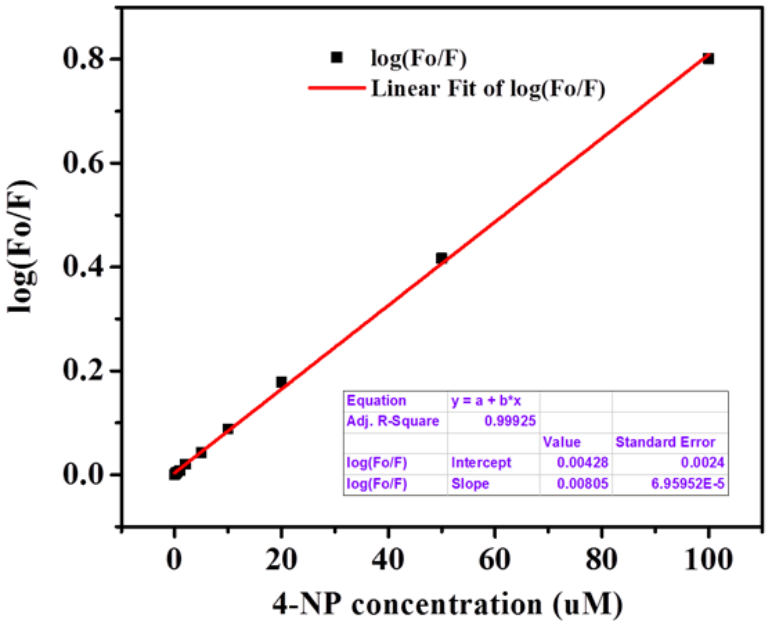

Fig. 4.16 The Stern-Volmer semilog plots for NCDs with different concentrations of 4-NP in test solutions

To examine the selective sensing of NCDs towards 4-NP, the fluorescence response of the NCDs were studied in the presence of various organic compounds, including ascorbic acid, caffeine, catechol, cysteine, ethylenediaminetetraacetic acid

(EDTA), glucose, glycine, hydroquinone, 3-nitrophenol, 2-nitroaniline, 2-nitrophenol, phenylboronic acid, 4-nitrophenol, and taurine at concentrations of 100 µM in a 0.05 M alkaline borate buffer (pH 9.0). As shown in Fig. 4.17, the PL quenching of the NCDs by the 4-NP was 3 to 6 times higher than those by the other organic materials. To visualize the selectivity, photographs of NCDs (left), NCDs in the presence of 4-NP (middle) and glucose (right) are shown in the inset figure of Fig. 4.17; 4-NP quenched more strongly than glucose. The NCDs exhibited excellent selectivity towards other NPs, such as 2-NP and 3-NP, which indicates that the NCDs fabricated in this study can be used effectively for monitoring the 4-NP, which is the most toxic material among all NPs.

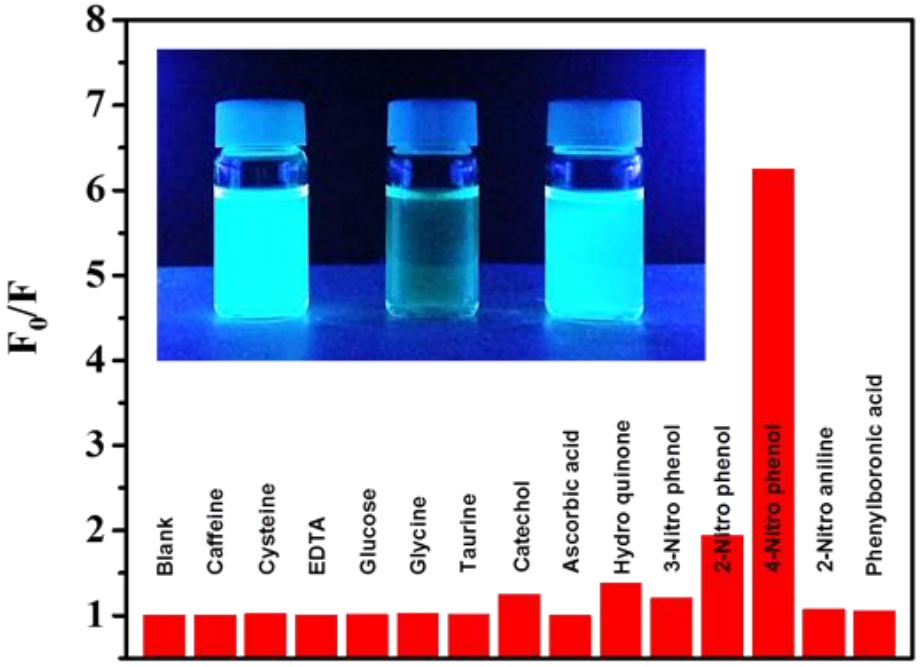

Fig. 4.17 Fluorescence factors (F_0/F) of NCDs solutions in the presence of various organic compounds. In set is a photograph image of NCDs (left) and NCDs with a presence of 4-NP (middle) and glucose (right) in alkaline borate buffer pH 9 under 20 W and 365 nm UV lamp irradiation. The concentration of NCDs and organic compounds were 20µg mL^{-1} and 100 µM, respectively

	Analytical methods	Analytical ranges (μM)	LODs (nM)	References
1	Electrochemical reduction	0.1-120	20	[2]
2	Electrochemical oxidation	1-300	600	[5]
3	Chemiluminescence	0.1-40	76	[8]
4	Fluorescent carbon dots	0.1-50	28	[50]
5	Carbon nanotube film electrode	1.0-35	120	[51]
6	Adsorptive stripping voltammetry	0.1-10	40	[52]
7	MIP-C-dots fluorescent material	0.2-50	60	[53]
8	**N-doped carbon dots**	**0.1-100**	**17**	**This work**

Table 4.2 Different methods for determination of 4-NP

4.4 Conclusion

N-doped carbon dots (NCDs) were fabricated from pyromellitic acid and ethylenediamine as a novel precursors using a green and facile one-pot hydrothermal process. The newly synthesized NCDs exhibited highly pure cyan color emission with a quantum yield as high as 75%. Owing to their excellent optical properties, the NCDs were employed as nanoprobes for the sensitive and selective determination of 4-nitrophenol, a highly toxic compound and one of the most important mononitrophenols in view of environmental contamination. The NCDs exhibited a wide linear range of 0.1 - 100 μM with a high R^2 of 0.9993, excellent selectivity, and a low limit of detection, as low as 17 nM. This approach may provide a new process for inexpensive and sensitive sensors in environmental and biological applications.

References

[1] P. Mulchandani, C.M. Hangarter, Y. Lei, W. Chen, A. Mulchandani, Amperometric microbial biosensor for p-nitrophenol using Moraxella sp.-modified carbon paste electrode, Biosensors and Bioelectronics, 21(2005) 523-7.

[2] J. Li, D. Kuang, Y. Feng, F. Zhang, Z. Xu, M. Liu, A graphene oxide-based electrochemical sensor for sensitive determination of 4-nitrophenol, Journal of Hazardous Materials, 201(2012) 250-9.

[3] Y. Zeng, Y. Zhou, T. Zhou, G. Shi, A novel composite of reduced graphene oxide and molecularly imprinted polymer for electrochemical sensing 4-nitrophenol, Electrochimica Acta, 130(2014) 504-11.

[4] X. Guo, Z. Wang, S. Zhou, The separation and determination of nitrophenol isomers by high-performance capillary zone electrophoresis, Talanta, 64(2004) 135-9.

[5] H. Yin, Y. Zhou, S. Ai, X. Liu, L. Zhu, L. Lu, Electrochemical oxidative determination of 4-nitrophenol based on a glassy carbon electrode modified with a hydroxyapatite nanopowder, Microchimica Acta, 169(2010) 87-92.

[6] A. Niazi, A. Yazdanipour, Spectrophotometric simultaneous determination of nitrophenol isomers by orthogonal signal correction and partial least squares, Journal of Hazardous Materials, 146(2007) 421-7.

[7] Z. Liu, J. Du, C. Qiu, L. Huang, H. Ma, D. Shen, et al., Electrochemical sensor for detection of p-nitrophenol based on nanoporous gold, Electrochemistry Communications, 11(2009) 1365-8.

[8] J. Liu, H. Chen, Z. Lin, J.-M. Lin, Preparation of Surface Imprinting Polymer Capped Mn-Doped ZnS Quantum Dots and Their Application for Chemiluminescence Detection of 4-Nitrophenol in Tap Water, Analytical Chemistry, 82(2010) 7380-6.

[9] W. Liu, C. Li, Y. Ren, X. Sun, W. Pan, Y. Li, et al., Carbon dots: surface engineering and applications, Journal of Materials Chemistry B, 4(2016) 5772-88.

[10] X. Gao, C. Du, Z. Zhuang, W. Chen, Carbon quantum dot-based nanoprobes for metal ion detection, Journal of Materials Chemistry C, 4(2016) 6927-45.

[11] A.B. Bourlinos, G. Trivizas, M.A. Karakassides, M. Baikousi, A. Kouloumpis, D. Gournis, et al., Green and simple route toward boron doped carbon dots with significantly enhanced non-linear optical properties, Carbon, 83(2015) 173-9.

[12] Z. Qian, X. Shan, L. Chai, J. Ma, J. Chen, H. Feng, Si-Doped Carbon Quantum Dots: A Facile and General Preparation Strategy, Bioimaging Application, and Multifunctional Sensor, ACS Applied Materials & Interfaces, 6(2014) 6797-805.

[13] W. Li, Z. Zhang, B. Kong, S. Feng, J. Wang, L. Wang, et al., Simple and Green Synthesis of Nitrogen-Doped Photoluminescent Carbonaceous Nanospheres for Bioimaging, Angewandte Chemie International Edition, 52(2013) 8151-5.

[14] J. Li, Y. Jiao, L. Feng, Y. Zhong, G. Zuo, A. Xie, et al., Highly N,P-doped carbon dots: Rational design, photoluminescence and cellular imaging, Microchimica Acta, 184(2017) 2933-40.

[15] Q. Xu, P. Pu, J. Zhao, C. Dong, C. Gao, Y. Chen, et al., Preparation of highly photoluminescent sulfur-doped carbon dots for Fe(iii) detection, Journal of Materials Chemistry A, 3(2015) 542-6.

[16] S. Yang, J. Sun, P. He, X. Deng, Z. Wang, C. Hu, et al., Selenium Doped Graphene Quantum Dots as an Ultrasensitive Redox Fluorescent Switch, Chemistry of Materials, 27(2015) 2004-11.

[17] Y. Wang, A. Hu, Carbon quantum dots: synthesis, properties and applications, Journal of Materials Chemistry C, 2(2014) 6921-39.

[18] Z. Li, H. Yu, T. Bian, Y. Zhao, C. Zhou, L. Shang, et al., Highly luminescent nitrogen-doped carbon quantum dots as effective fluorescent probes for mercuric and iodide ions, Journal of Materials Chemistry C, 3(2015) 1922-8.

[19] C. Hu, C. Yu, M. Li, X. Wang, Q. Dong, G. Wang, et al., Nitrogen-doped carbon dots decorated on graphene: a novel all-carbon hybrid electrocatalyst for enhanced oxygen reduction reaction, Chemical Communications, 51(2015) 3419-22.

[20] Z.L. Wu, P. Zhang, M.X. Gao, C.F. Liu, W. Wang, F. Leng, et al., One-pot hydrothermal synthesis of highly luminescent nitrogen-doped amphoteric carbon dots

for bioimaging from Bombyx mori silk - natural proteins, Journal of Materials Chemistry B, 1(2013) 2868-73.

[21] L. Wang, H.S. Zhou, Green Synthesis of Luminescent Nitrogen-Doped Carbon Dots from Milk and Its Imaging Application, Analytical Chemistry, 86(2014) 8902-5.

[22] Z. Yang, M. Xu, Y. Liu, F. He, F. Gao, Y. Su, et al., Nitrogen-doped, carbon-rich, highly photoluminescent carbon dots from ammonium citrate, Nanoscale, 6(2014) 1890-5.

[23] M. Li, C. Yu, C. Hu, W. Yang, C. Zhao, S. Wang, et al., Solvothermal conversion of coal into nitrogen-doped carbon dots with singlet oxygen generation and high quantum yield, Chemical Engineering Journal, 320(2017) 570-5.

[24] D.K. Dang, C. Sundaram, Y.-L.T. Ngo, J.S. Chung, E.J. Kim, S.H. Hur, One pot solid-state synthesis of highly fluorescent N and S co-doped carbon dots and its use as fluorescent probe for Ag+ detection in aqueous solution, Sensors and Actuators B: Chemical, (2017).

[25] H. Zhang, Y. Chen, M. Liang, L. Xu, S. Qi, H. Chen, et al., Solid-Phase Synthesis of Highly Fluorescent Nitrogen-Doped Carbon Dots for Sensitive and Selective Probing Ferric Ions in Living Cells, Analytical Chemistry, 86(2014) 9846-52.

[26] X. Qin, W. Lu, A.M. Asiri, A.O. Al-Youbi, X. Sun, Microwave-assisted rapid green synthesis of photoluminescent carbon nanodots from flour and their applications for sensitive and selective detection of mercury(II) ions, Sensors and Actuators B: Chemical, 184(2013) 156-62.

[27] X. Sun, J. He, Y. Meng, L. Zhang, S. Zhang, X. Ma, et al., Microwave-assisted ultrafast and facile synthesis of fluorescent carbon nanoparticles from a single precursor: preparation, characterization and their application for the highly selective detection of explosive picric acid, Journal of Materials Chemistry A, 4(2016) 4161-71.

[28] L. Lin, M. Rong, S. Lu, X. Song, Y. Zhong, J. Yan, et al., A facile synthesis of highly luminescent nitrogen-doped graphene quantum dots for the detection of 2,4,6-trinitrophenol in aqueous solution, Nanoscale, 7(2015) 1872-8.

[29] H. Li, Z. Kang, Y. Liu, S.-T. Lee, Carbon nanodots: synthesis, properties and applications, Journal of Materials Chemistry, 22(2012) 24230-53.

[30] S.Y. Lim, W. Shen, Z. Gao, Carbon quantum dots and their applications, Chemical Society Reviews, 44(2015) 362-81.

[31] D. Qu, M. Zheng, J. Li, Z. Xie, Z. Sun, Tailoring color emissions from N-doped graphene quantum dots for bioimaging applications, Light Sci Appl, 4(2015) e364.

[32] K. Jiang, S. Sun, L. Zhang, Y. Wang, C. Cai, H. Lin, Bright-Yellow-Emissive N-Doped Carbon Dots: Preparation, Cellular Imaging, and Bifunctional Sensing, ACS Applied Materials & Interfaces, 7(2015) 23231-8.

[33] R. Li, Y. Liu, Z. Li, J. Shen, Y. Yang, X. Cui, et al., Bottom-Up Fabrication of Single-Layered Nitrogen-Doped Graphene Quantum Dots through Intermolecular Carbonization Arrayed in a 2D Plane, Chemistry – A European Journal, 22(2016) 272-8.

[34] J. Liu, D. Tang, Z. Chen, X. Yan, Z. Zhong, L. Kang, et al., Chemical redox modulated fluorescence of nitrogen-doped graphene quantum dots for probing the activity of alkaline phosphatase, Biosensors and Bioelectronics, 94(2017) 271-7.

[35] Z. Wang, J. Yu, X. Zhang, N. Li, B. Liu, Y. Li, et al., Large-Scale and Controllable Synthesis of Graphene Quantum Dots from Rice Husk Biomass: A Comprehensive Utilization Strategy, ACS Applied Materials & Interfaces, 8(2016) 1434-9.

[36] Y. Wang, Q. Zhuang, Y. Ni, Facile Microwave-Assisted Solid-Phase Synthesis of Highly Fluorescent Nitrogen–Sulfur-Codoped Carbon Quantum Dots for Cellular Imaging Applications, Chemistry – A European Journal, 21(2015) 13004-11.

[37] X. Pei, D. Xiong, J. Fan, Z. Li, H. Wang, J. Wang, Highly efficient fluorescence switching of carbon nanodots by CO2, Carbon, 117(2017) 147-53.

[38] M. Xu, S. Xu, Z. Yang, M. Shu, G. He, D. Huang, et al., Hydrophilic and blue fluorescent N-doped carbon dots from tartaric acid and various alkylol amines under microwave irradiation, Nanoscale, 7(2015) 15915-23.

[39] F. Zhang, X. Feng, Y. Zhang, L. Yan, Y. Yang, X. Liu, Photoluminescent carbon quantum dots as a directly film-forming phosphor towards white LEDs, Nanoscale, 8(2016) 8618-32.

[40] J. Jiang, Y. He, S. Li, H. Cui, Amino acids as the source for producing carbon nanodots: microwave assisted one-step synthesis, intrinsic photoluminescence property and intense chemiluminescence enhancement, Chemical Communications, 48(2012) 9634-6.

[41] M. Xu, G. He, Z. Li, F. He, F. Gao, Y. Su, et al., A green heterogeneous synthesis of N-doped carbon dots and their photoluminescence applications in solid and aqueous states, Nanoscale, 6(2014) 10307-15.

[42] S. Srivastava, N.S. Gajbhiye, Carbogenic Nanodots: Photoluminescence and Room-Temperature Ferromagnetism, ChemPhysChem, 12(2011) 2624-32.

[43] Y. Ma, Z. Zhang, Y. Xu, M. Ma, B. Chen, L. Wei, et al., A bright carbon-dot-based fluorescent probe for selective and sensitive detection of mercury ions, Talanta, 161(2016) 476-81.

[44] S. Zhu, J. Zhang, S. Tang, C. Qiao, L. Wang, H. Wang, et al., Surface Chemistry Routes to Modulate the Photoluminescence of Graphene Quantum Dots: From Fluorescence Mechanism to Up-Conversion Bioimaging Applications, Advanced Functional Materials, 22(2012) 4732-40.

[45] D. Qu, M. Zheng, L. Zhang, H. Zhao, Z. Xie, X. Jing, et al., Formation mechanism and optimization of highly luminescent N-doped graphene quantum dots, 4(2014) 5294.

[46] S. Zhu, X. Zhao, Y. Song, S. Lu, B. Yang, Beyond bottom-up carbon nanodots: Citric-acid derived organic molecules, Nano Today, 11(2016) 128-32.

[47] D. Pan, J. Zhang, Z. Li, C. Wu, X. Yan, M. Wu, Observation of pH-, solvent-, spin-, and excitation-dependent blue photoluminescence from carbon nanoparticles, Chemical Communications, 46(2010) 3681-3.

[48] Y. Guo, Z. Wang, H. Shao, X. Jiang, Hydrothermal synthesis of highly fluorescent carbon nanoparticles from sodium citrate and their use for the detection of mercury ions, Carbon, 52(2013) 583-9.

[49] M.J. Krysmann, A. Kelarakis, P. Dallas, E.P. Giannelis, Formation Mechanism of Carbogenic Nanoparticles with Dual Photoluminescence Emission, Journal of the American Chemical Society, 134(2012) 747-50.

[50] G.H.G. Ahmed, R.B. Laíño, J.A.G. Calzón, M.E.D. García, Highly fluorescent carbon dots as nanoprobes for sensitive and selective determination of 4-nitrophenol in surface waters, Microchimica Acta, 182(2015) 51-9.

[51] F.C. Moraes, S.T. Tanimoto, G.R. Salazar-Banda, S.A.S. Machado, L.H. Mascaro, A New Indirect Electroanalytical Method to Monitor the Contamination of Natural Waters with 4-Nitrophenol Using Multiwall Carbon Nanotubes, Electroanalysis, 21(2009) 1091-8.

[52] W. Huang, C. Yang, S. Zhang, Simultaneous determination of 2-nitrophenol and 4-nitrophenol based on the multi-wall carbon nanotubes Nafion-modified electrode, Analytical and Bioanalytical Chemistry, 375(2003) 703-7.

[53] T. Hao, X. Wei, Y. Nie, Y. Xu, Y. Yan, Z. Zhou, An eco-friendly molecularly imprinted fluorescence composite material based on carbon dots for fluorescent detection of 4-nitrophenol, Microchimica Acta, 183(2016) 2197-203.

Chapter 5

Multicolor Emission Carbon Dots Derived from Pyromellitic Acid and Diamines via Solvothermal Method

5.1 Introduction

Multicolor photoluminescent nanomaterials which can be excited by a single wavelength have attracted much attention of research community because they have potential applications in sensing, bioimaging, light-emitting diodes, full-color display, and optoelectronic devices [1-5]. Previously, numerous multicolor emission nanomaterials have been reported including semiconductor quantum dots [6-8], rare-earth based nanoparticles [9-11], polymer dots [12, 13], molecular nanomaterials [14, 15], and organic dyes [16-18]. Unfortunately, these nanomaterials have disadvantages of high toxicity, low emission quantum yields (QYs), poor water solubility, and complicated synthesis procedures that hampered their practical applications [6-18]. Over the past decade, carbon dots (CDs) with their outstanding merits in terms of luminescence, stability, biocompatibility, and low cost, have been intensively studied for potential applications in fluorescent probes, light-emitting devices, biosensors, efficient visible light-active photocatalysts, and so on [19-21]. This new rising member of carbon family is considered to be a potential alternative to semiconductor QDs [22]. Thus, numerous raw materials and various synthetic approaches have been reported for the fabrication of CDs. However, some major drawbacks of these nanomaterials arise from the difficulty in preparing long-wavelength color emission CDs (e.g. red color emission CDs) and multicolor (capable of single wavelength excitation) emissive products [23-25]. Therefore, the development of facile methods for the preparation of water-soluble, biocompatible, and photo-stable, multicolor PL carbon dots, is still highly desirable.

Up to now, there have been only a few publications on the successful synthesis of CDs with tunable PL from blue to red. For instant, Hu and colleagues fabricated a series of CDs by various reagents and concluded that epoxides or hydroxyls on their surfaces were mainly responsible for the resulting PL red shift [26]. Lin et al.

synthesized three types of CDs which are blue, green, and red emission CDs by solvothermally treating different carbon sources and proposed that the observed PL red shift to quantum size effects and the nitrogen content of the CDs [22]. Pang and colleagues produced a series of CDs by modifying the reaction conditions and hypothesized that the PL red-shift to both quantum size effects and surface states [27]. Although there have been successfully synthesized CDs with tunable PL, the conclusions regarding the corresponding mechanisms are still under debate and even contradictory. Furthermore, when various samples with complex compositions were studied together, the derived PL mechanisms were even more complex and not convincing because there were too many factors influencing the PL processes, particularly the different conditions used for producing these carbon dots [28-31].

In this current study, we report a facile one pot solvothermal synthesis of multicolor PL CDs, having blue, cyan, yellow, and red color emissions by using the new precursor, pyromellitic acid (PA) and diamines as nitrogen sources. The as-prepared CDs emit strong and stable PL at around 409, 486, 554, and 618 nm for B-, C-, Y-, and R-NCDs, respectively. Based on the UV-vis and XPS measurements, we proposed that both band gap energies and surface defect have influence on the photoluminescence of the as-prepared carbon dots.

5.2 Experimental

5.2.1 Chemicals

Ethylenediamine (EDA), sodium hydroxide, hydrochloric acid, potassium bromide for FTIR were purchased from Deajung Chemicals and Metals Co. Ltd. Reagent grades of Pyromellitic acid (PA), o-, m-, p-phenylenediamine (o-, m-, and p-PD) were purchased from Aldrich Sigma. Quinine sulfate dihydrate was kindly provided by Wako Pure Chemical Industries, Ltd. Rhodamine 6G and rhodamine B was purchased from Aldrich Sigma. Ethyl alcohol anhydrous special grade and petroleum ether were provided by Samchun Pure Chemical Co. Ltd. All chemicals were used as received without further purification unless otherwise specified. Deionized (DI) water was used throughout this study.

5.2.2 Characterizations

UV-vis spectra were recorded on a UV-vis spectrophotometer (SPECORD 210 PLUS-223F1107) using a quartz cell with a 1 cm optical path. Photoluminescence emission spectra were taken on Cary Eclipse fluorescence spectrophotometer (Agilent Technologies, G9800AA).

Fourier transform infrared (FTIR) spectra were recorded on a FTIR spectrometer (KBr disk method; NEXUS) at wavenumbers of 400-4000 cm^{-1}. Transmission electron microscopy (TEM) images were taken on a JEM-2100 (JEOL) with an operating voltage of 200 kV. X-ray photoelectron spectroscopy (XPS) measurement was performed on an ESCALB-MKII250 photoelectron spectrometer (VG Co.) with Al Kα X-ray radiation as the X-ray source for excitation.

5.2.3 Synthesis of multicolor N-doped carbon dots (MNCDs)

The MCDs were synthesized via a green, facile, and one pot solvothermal method. In a typical process, 30 mg of PA and 60 mg of diamines (EDA, o-PD, m-PD, and p-PD) were added into 60 mL absolute ethanol. The mixture was then transferred to a Teflon-lined stainless-steel autoclave, sealed and placed into siliconit muffle furnace, which is then heated to at 160^{o}C and kept at this temperature for a period time of 12 h. After cooling down to ambient temperature, the obtained solutions were then filtered by filter paper to eliminate large particles. Then, the obtained solutions were purified by petroleum ether via separating funnels as follow: 10 mL of obtained solution was added into 20 mL of petroleum ether in a funnel. Then 100 mL of petroleum ether was added to the funnel, shaken well and separated the upper solution. The process was repeated 3 times to get the purified NCDs.

5.2.4 Determination of quantum yields (QYs).

QY of the MCDs was determined by a widely accepted relative method. Specially, quinine sulfate (QY=54% in 0.1 M H_2SO_4) was selected as the reference for the emission range of 400-480 nm (for B-NCDs herein), rhodamine 6G (QY=95% in ethanol) for the emission range of 480-560 nm (for C-NCDs and Y-NCDs herein), and rhodamine B (QY=56% in ethanol) for the emission range of 580-610 nm (for R-NCDs herein). The QY of a sample was calculated according to the following equation:

$$\emptyset=\emptyset'\times\frac{A'}{I'}\times\frac{I}{A}\times\frac{n^2}{n'^2}$$

where ϕ is the QY of the testing sample, I is the testing sample's integrated emission intensity, n is the refractive index (1.33 for water and 1.36 for ethanol), and A is the optical density. The prime symbol (′) refers to the referenced dye of known QY. To obtain more reliable results, a series of solutions of MCDs and referenced dyes of known QYs were prepared with concentrations adjusted such that the optical absorbance values were between 0-0.1 at 365 nm (or other desired wavelengths). The PL spectra were measured and the PL intensity was integrated. QYs were determined by comparison of the integrated PL intensity *vs* absorbance curves (refractive index, n, had also to be considered).

5.3 Results and discussion

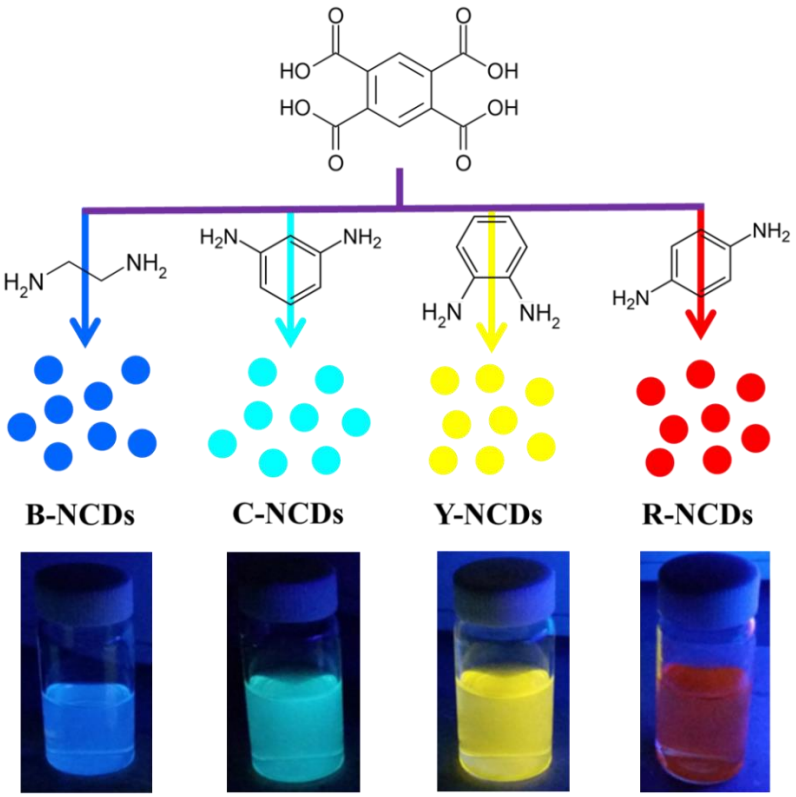

Scheme 5.1 Preparation of MNCDs exhibiting blue, cyan, yellow and red color emission by solvothermal treatment of PA and diamines

The preparation of MNCDs namely B-NCDs, C-NCDs, Y-NCDs and R-NCDs can be facilely accomplished by heating solution of PA and diamines (EDA, m-PD, o-PD, and p-PD, respectively) in an absolute ethanol solution at 160^{o}C for 12 hours in an autoclave and then purification using petroleum ether. The obtained CDs which can be dispersed in water and exhibited blue, cyan, yellow and red color emission under single-wavelength UV irradiation (e.g. λ=365 nm) as shown in Scheme 5.1.

5.3.1. FTIR analysis

It can be seen that all the FTIR spectra of NCDs demonstrate individual absorption peaks around 3378 cm^{-1}, which are corresponding to two types of amino groups, namely primary amine (-NH_2) and secondary amine (-NH-) [32]. There is also a strong stretching vibration band of O-H which is observed at 3214 cm^{-1} [33]. Other strong bands at 1723 and 1122 cm^{-1} are attributed to C=O and C-O stretching vibrations, respectively [32, 34]. In addition, strong bands at 1514 and 1386 cm^{-1} are attributed to C=N and C-N stretching vibrations, successively [35]. Moreover, band at about 1272 cm^{-1} is attributed to NH stretching vibrations and the bands in the region 600-900 cm^{-1} are contributed to NH_2 wagging, subsequently [36].

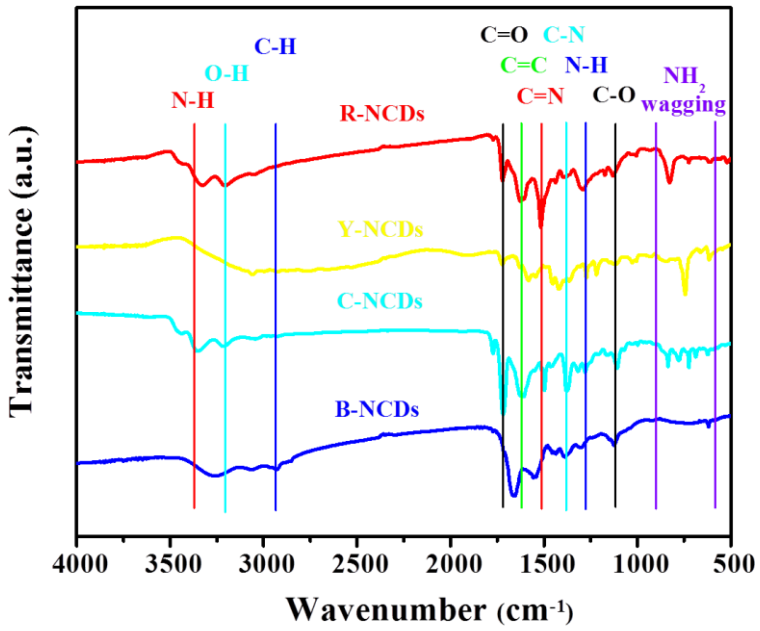

Fig. 5.1 FTIR spectra of B-, C-, Y-, and R-NCDs, respectively

5.3.2 XPS analysis

X-ray photoelectron spectroscopy (XPS) characterizations were used to further investigate the surfaces of these samples. The XPS surveys shown in Figure 5.2 exhibited three typical peaks, which are assigned for C1s, N1s, and O1s. These results indicate that all four MNCDs have the same elemental composition (i.e., C, N, and O) and are nitrogen-doped [37].

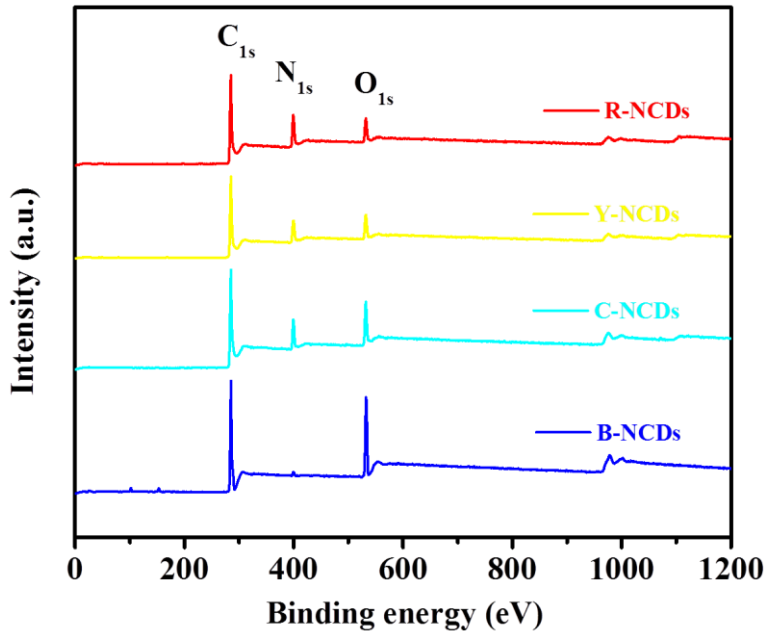

Fig. 5.2 XPS survey of B-, C-, Y-, and R-NCDs, respectively

Sample	C (%)	O (%)	N (%)
B-NCDs	**74.57**	**21.01**	**1.95**
C-NCDs	**75.15**	**12.64**	**12.19**
Y-NCDs	**77.16**	**9.81**	**13.03**
R-NCDs	**75.83**	**8.43**	**15.74**

Table 5.1 Relative contents of C, N and O atoms of B-, C-, Y-, and R-NCDs (determined by XPS)

Figure 5.3 to 5.5 presented the high-resolution spectra of the three elements including C_{1s}, N_{1s}, and O_{1s}. The C_{1s} band in Figure 5.3 can be deconvoluted into four peaks, which are attributed to sp^2 carbons (C=C), sp^3 carbons (C−O/C−N), carbonyl carbons (C=O), and carboxyl carbons (COOH). In Figure 5.4, the N1s band can be deconvoluted into three peaks representation of pyridinic N, amino N, and pyrrolic N, respectively. The O_{1s} band contains two peaks assigned for C=O and C−O, respectively (Figure 5.5). In general, the deconvolution of high resolution XPS spectra for C_{1s}, N_{1s} and O_{1s} demonstrate that they contain the same chemical bonds [32].

It is noticed that from B- to C-, Y- and R-NCDs, percentages of oxygen decreased while that of nitrogen increased steadily as shown in Table 5.1. Clearly, the percentage of O and N in B-NCDs, which is synthesized from aliphatic diamine (EDA), is strongly differ than that of the other three, which are synthesized from aromatic diamines (phenylenediamines). The increase percentages of N in MNCDs may be contributed to the red-shift in PL color emission of MNCDs.

Moreover, the introduction of nitrogen atom in the form of quaternary ammonium salt could also probably create capture centers of excitons analogous to those in carboxyl groups and subsequently lead to changes in the surface states and surface potential of the MNCDs. Therefore, the different surface states derived from doping effects would have a primary influence on the PL properties of the MNCDs.

Taking into account of the XPS characterizations, the relative intensities of blue and red emissions on the oxygen and nitrogen contents are shown in Table 1. It is noticeable that the PL of MNCDs blue-shifted with the increase of oxygen content, whereas they red-shifted when the oxygen gradually decreases. The variation of blue-shifted and red-shifted PL color emissions with nitrogen content is opposite. This may hypothesize that the origin of blue emission is associated to oxygenous related defect states, while that of red emission comes from the nitrogen contained fluorophores. The reason can be explained that the oxygenous related groups, which are mainly hydrophilic ones, such as C=O, OH and COOH, are easily formed in solvents with the presence of aliphatic diamine. In contrast, due to the presence of aromatic diamines, oxygenous related groups are confined, and nitrogen contained fluorophores are easily

formed, leading to the decrease of blue-shifted and the increase of red-shifted PL emission [32].

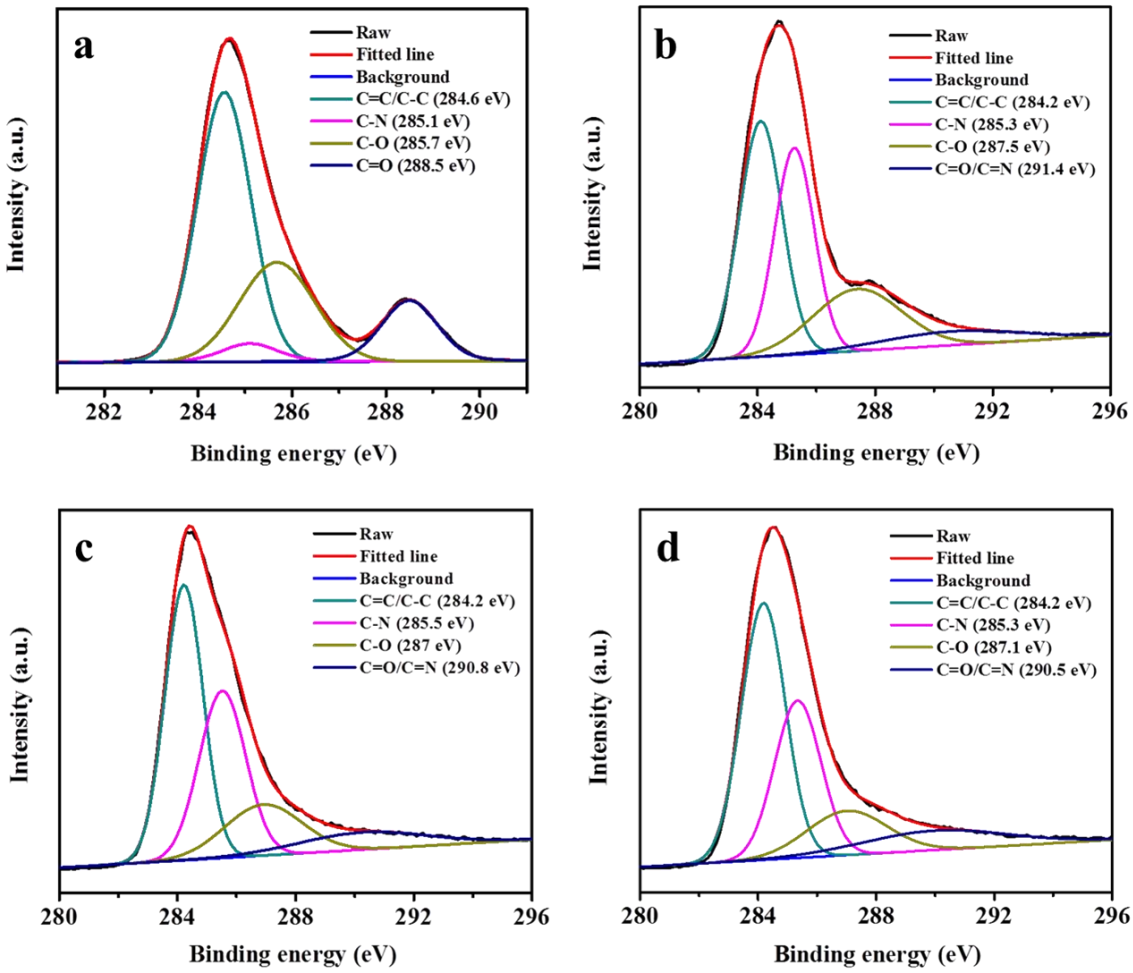

Fig. 5.3 (a-d) High-resolution XPS spectra of C_{1s} of B-, C-, Y-, and R-NCDs, respectively

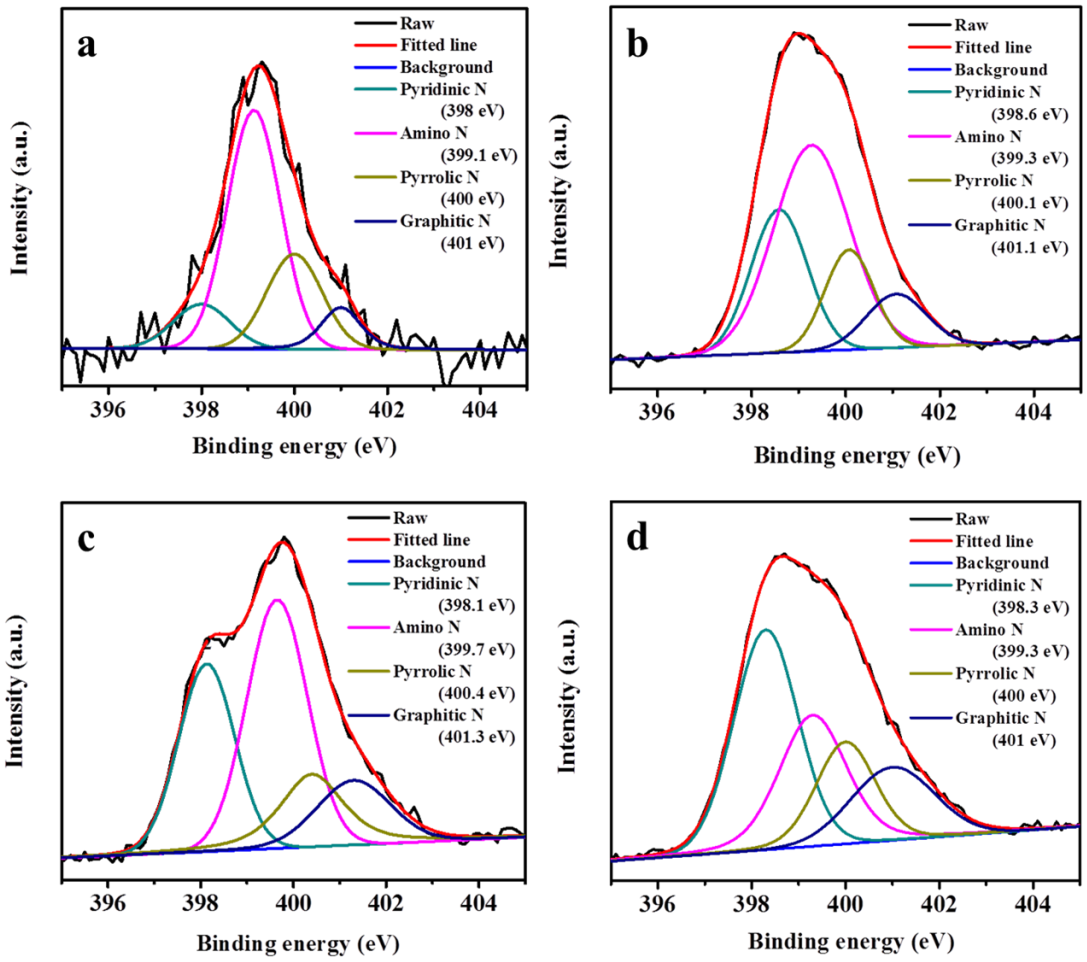

Fig. 5.4 (a-d) High-resolution XPS spectra of N_{1s} of B-, C-, Y-, and R-NCDs, respectively

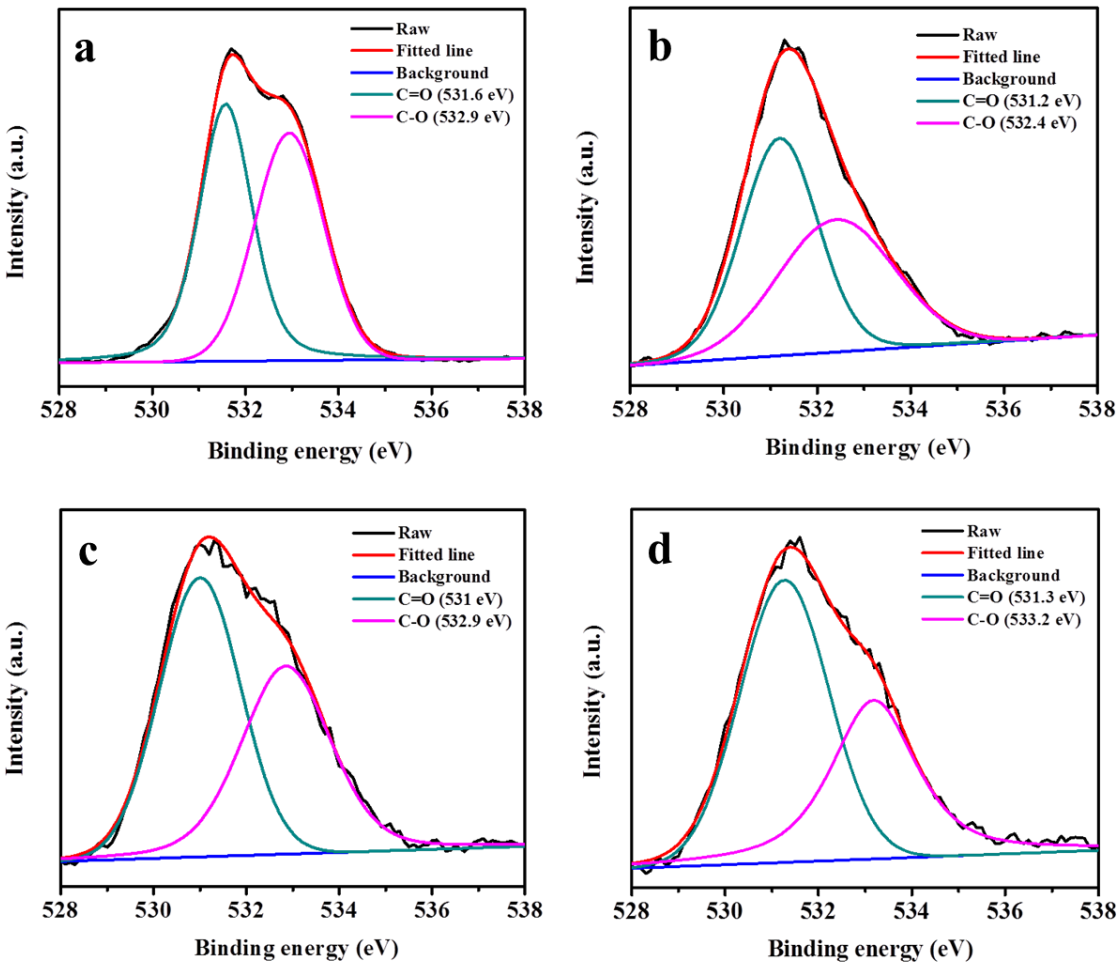

Fig. 5.5 (a-d) High-resolution XPS spectra of O_{1s} of B-, C-, Y-, and R-NCDs, respectively

5.3.3. Optical analysis

5.3.3.1 Absorbance

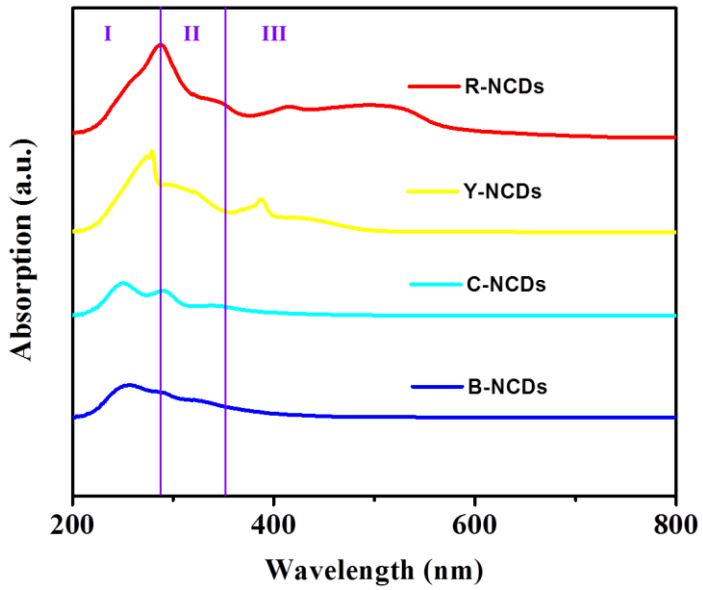

Fig. 5.6 UV–vis absorption spectra of B-, C-, Y-, and R-NCDs, respectively

The UV-vis absorption spectra of the four NCDs demonstrated multiple electronic absorption transitions and can be divided into three bands, for brevity, they are named by band (I), (II) and (III), respectively [32].

According to previous reports, the band (I) from 220 nm to 286 nm could be assigned to intrinsic state (π-π*) transition from the aromatic sp^2 domains (C=C and C=N), which do not typically generate fluorescence. Also, there are bands (II) from 286 to 350 nm comes from defect states (n-π*) which is mainly included oxygenous functional groups C-O and C=O, respectively. In addition, other strong bands (III) from 350 nm to 600 nm was also observed, which was usually assigned to the surface groups transition roughly. The appearance of these bands may be due to states (n-π*) which are attributed to C=N groups [31, 34, 38, 39].

In general, the UV absorption of NCDs is similar to the absorption characteristics of quantum-confined semiconductor quantum dots but quite different from that of previous reported CDs within only the UV region. Also, it indicated that these samples possessed different surface states.

Band gap energies of MNCDs were calculated using the equation: $\boldsymbol{E_g^{opt} = 1240/\lambda_{edge}}$, where λ_{edge} is the onset value of the first excitonic absorption bands in the direction of longer wavelengths [37]. It can be seen that from B- to R-NCDs, the band gap energy decreased steadily from 3.09 eV to 2.10 eV. The decline of band gap energy of MNCDs may contribute to the ref-shift of MNCDs from B- to R-NCDs.

Sample	**λ_{edge} (nm)**	**E_g^{opt} (eV)**
B-NCDs	**401**	**3.09**
C-NCDs	**438**	**2.83**
Y-NCDs	**506**	**2.45**
R-NCDs	**591**	**2.10**

Table 5.2 Estimation of the band gap energy of MNCDs

5.3.3.2 Photoluminescence

The PL properties of the four MNCDs were thoroughly investigated. Figure 2a–d shown their PL spectra with the emission maxima of B-NCDs, C-NCDs, Y-NCDs, and R-NCDs which are centered at about λ = 409, 486, 564 and 618 nm, respectively, in aqueous solution. The PL excitation maxima of the four samples are at around λ = 330, 385, 460 and 490 nm, subsequently.

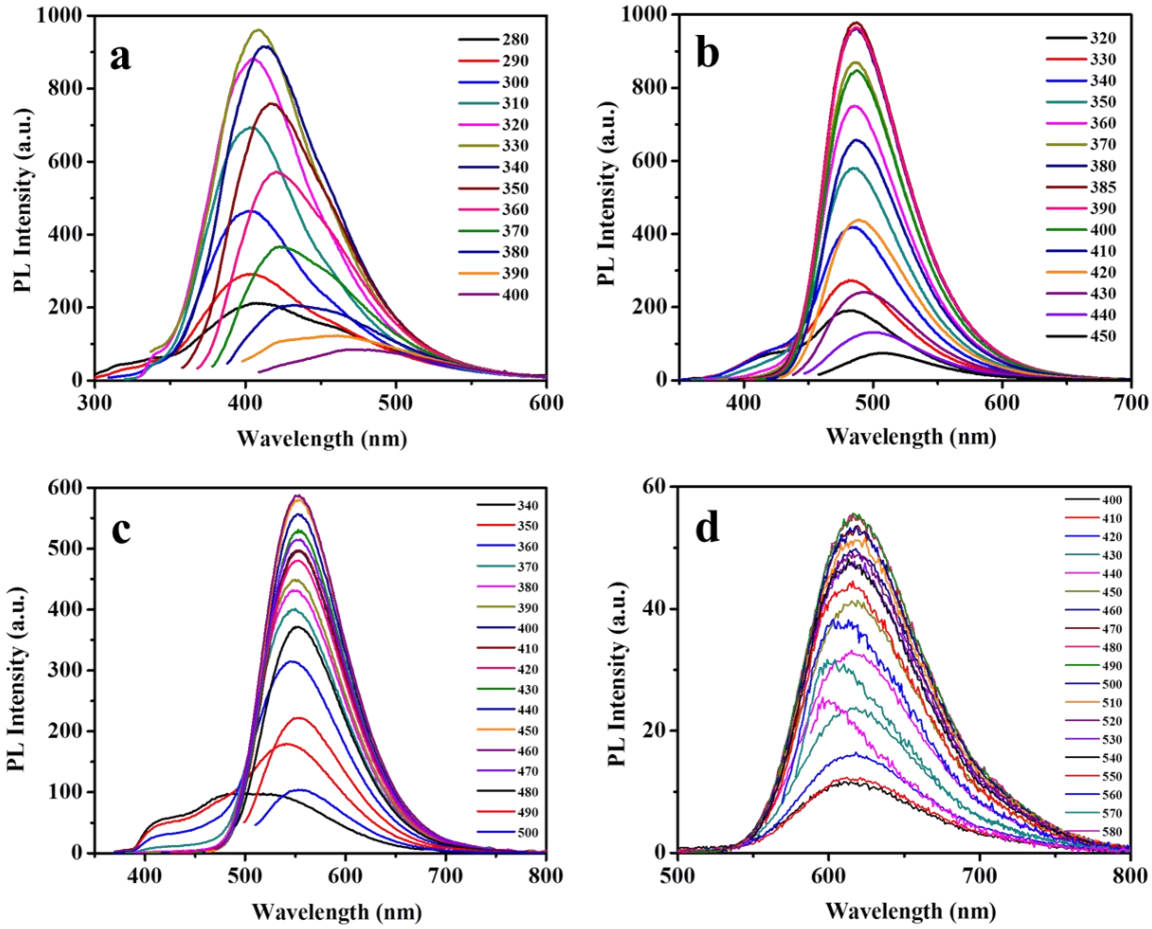

Fig. 5.7 (a-d) PL spectra of B-, C-, Y-, and R-NCDs at different excitation wavelengths

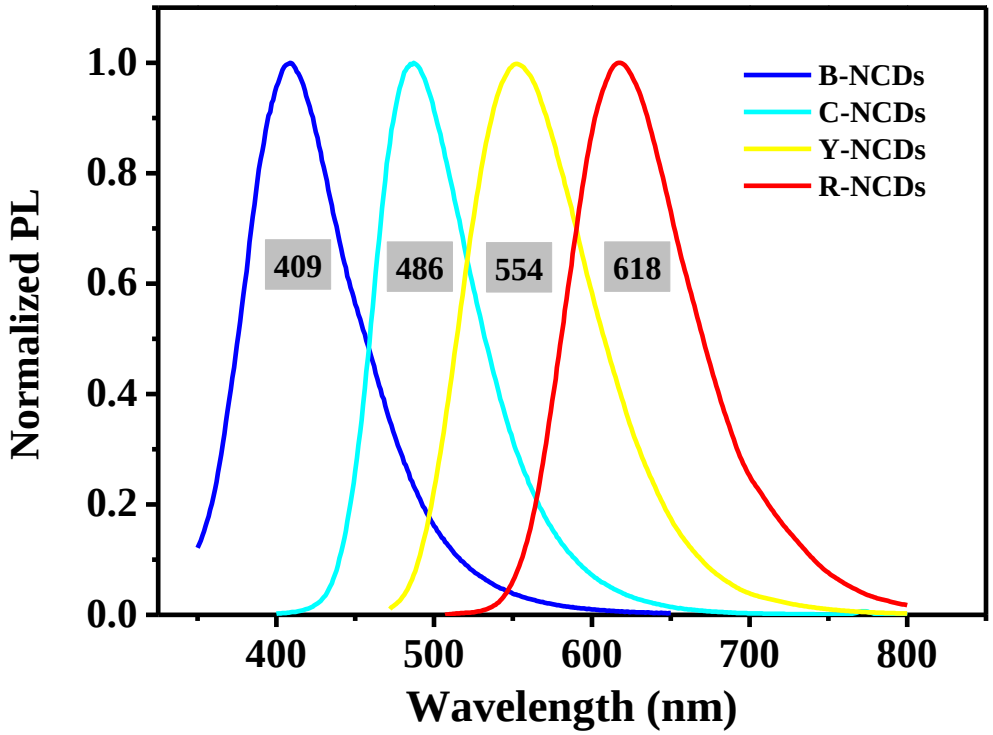

Fig. 5.8 Normalized maxima PL spectra of B-, C-, Y-, and R-NCDs

5.3.4. Photoluminescence mechanism

Till these days, several parameters, such as quantum size effects, surface state effects, different elements doping, molecule state and carbon-core state effects, have been reported to be a key role influence the emission properties of carbon dots. However, the actual mechanism of carbon dots photoluminescence remains under debate and therefore, the amazing PL of CDs continues to motivate scientists to conduct deeper explorations. In the present work, we assumed that not only a single factor affects the photoluminescence of carbon dots but two or more factors may also affect the carbon dots PL. It is possible that both the band gap energies and surface defect have influence on the photoluminescence of the carbon dots.

The first factor which is band gap energies based on UV-vis measurement. From B- to C-, Y- and R-NCDs, the band gap energies decrease steadily leading to the color emission changing from blue to cyan, yellow and red PL color emission [37].

Taking into account of the second factor which is attributed to the ratio of oxygen and nitrogen atom in the MNCDs based on XPS characterization [40]. It is supposed that under the given reaction conditions the MNCDs are N doped, and are highly surface passivated. Furthermore, it can be inferred that the nitrogen sources of diamines play a pivotal role for producing the special MNCDs. Aliphatic diamines (EDA) acted as nitrogen source for doping and passivating agent. However, aromatic diamines (m-, o-, and p-PD) could be considered as the sp^2 domain with a unique amino-substituted rigid carbon skeleton structure, which concomitantly acts as a building block to form intact sp^2 cluster being N doped in the large rigid π-conjugated structure and highly surface passivated with amino at edge sites, which are clearly confirmed by FTIR spectra and deconvoluted high-resolution XPS spectra.

5.4. Conclusion

In this chapter, multicolor emission nitrogen-doped carbon dots (MNCDs) have been successful synthesis via a facile one pot solvothermal treatment of pyromellitic acid (PA) and diamines (EDA, m-, o-, and p-PD). The as-synthesized MNCDs exhibited blue, cyan, yellow and red color emission when the nitrogen sources changing from aliphatic diamine (EDA) to aromatic diamines (m-, o-, and p-PD), respectively. It is supposed that both composition of oxygen and nitrogen containing in MNCDs and band gap energy may contributed to the red-shift of PL emission of the as-prepared MNCDs. This simple strategy offer a promising route for producing multicolor emission carbon dots that could be employed in various applications such as bioimaging and light emitting diodes.

5.5 References

[1] H.H. Gorris, O.S. Wolfbeis, Photon-Upconverting Nanoparticles for Optical Encoding and Multiplexing of Cells, Biomolecules, and Microspheres, Angewandte Chemie International Edition, 52(2013) 3584-600.

[2] M.I.J. Stich, M. Schaeferling, O.S. Wolfbeis, Multicolor Fluorescent and Permeation-Selective Microbeads Enable Simultaneous Sensing of pH, Oxygen, and Temperature, Advanced Materials, 21(2009) 2216-20.

[3] Q. Dou, N.M. Idris, Y. Zhang, Sandwich-structured upconversion nanoparticles with tunable color for multiplexed cell labeling, Biomaterials, 34(2013) 1722-31.

[4] L. Zhu, X. Li, Q. Zhang, X. Ma, M. Li, H. Zhang, et al., Unimolecular Photoconversion of Multicolor Luminescence on Hierarchical Self-Assemblies, Journal of the American Chemical Society, 135(2013) 5175-82.

[5] Y. Tao, C. Yang, J. Qin, Organic host materials for phosphorescent organic light-emitting diodes, Chemical Society Reviews, 40(2011) 2943-70.

[6] L. Qu, X. Peng, Control of Photoluminescence Properties of CdSe Nanocrystals in Growth, Journal of the American Chemical Society, 124(2002) 2049-55.

[7] A.P. Alivisatos, Semiconductor Clusters, Nanocrystals, and Quantum Dots, Science, 271(1996) 933-7.

[8] M. Shim, P. Guyot-Sionnest, n-type colloidal semiconductor nanocrystals, Nature, 407(2000) 981.

[9] J.-C.G. Bunzli, C. Piguet, Taking advantage of luminescent lanthanide ions, Chemical Society Reviews, 34(2005) 1048-77.

[10] F. Wang, X. Liu, Multicolor Tuning of Lanthanide-Doped Nanoparticles by Single Wavelength Excitation, Accounts of Chemical Research, 47(2014) 1378-85.

[11] J. Kido, Y. Okamoto, Organo Lanthanide Metal Complexes for Electroluminescent Materials, Chemical Reviews, 102(2002) 2357-68.

[12] Y. Rong, C. Wu, J. Yu, X. Zhang, F. Ye, M. Zeigler, et al., Multicolor Fluorescent Semiconducting Polymer Dots with Narrow Emissions and High Brightness, ACS Nano, 7(2013) 376-84.

[13] C. Wu, B. Bull, C. Szymanski, K. Christensen, J. McNeill, Multicolor Conjugated Polymer Dots for Biological Fluorescence Imaging, ACS Nano, 2(2008) 2415-23.

[14] Y.S. Zhao, H. Fu, A. Peng, Y. Ma, D. Xiao, J. Yao, Low-Dimensional Nanomaterials Based on Small Organic Molecules: Preparation and Optoelectronic Properties, Advanced Materials, 20(2008) 2859-76.

[15] A. Patra, C.G. Chandaluri, T.P. Radhakrishnan, Optical materials based on molecular nanoparticles, Nanoscale, 4(2012) 343-59.

[16] A. Wakamiya, K. Mori, S. Yamaguchi, 3-Boryl-2,2′-bithiophene as a Versatile Core Skeleton for Full-Color Highly Emissive Organic Solids, Angewandte Chemie International Edition, 46(2007) 4273-6.

[17] D. Yao, S. Zhao, J. Guo, Z. Zhang, H. Zhang, Y. Liu, et al., Hydroxyphenyl-benzothiazole based full color organic emitting materials generated by facile molecular modification, Journal of Materials Chemistry, 21(2011) 3568-70.

[18] E. Kim, M. Koh, B.J. Lim, S.B. Park, Emission Wavelength Prediction of a Full-Color-Tunable Fluorescent Core Skeleton, 9-Aryl-1,2-dihydropyrrolo[3,4-b]indolizin-3-one, Journal of the American Chemical Society, 133(2011) 6642-9.

[19] K. Hola, Y. Zhang, Y. Wang, E.P. Giannelis, R. Zboril, A.L. Rogach, Carbon dots—Emerging light emitters for bioimaging, cancer therapy and optoelectronics, Nano Today, 9(2014) 590-603.

[20] S.N. Baker, G.A. Baker, Luminescent Carbon Nanodots: Emergent Nanolights, Angewandte Chemie International Edition, 49(2010) 6726-44.

[21] S.Y. Lim, W. Shen, Z. Gao, Carbon quantum dots and their applications, Chemical Society Reviews, 44(2015) 362-81.

[22] K. Jiang, S. Sun, L. Zhang, Y. Lu, A. Wu, C. Cai, et al., Red, Green, and Blue Luminescence by Carbon Dots: Full-Color Emission Tuning and Multicolor Cellular Imaging, Angewandte Chemie International Edition, 54(2015) 5360-3.

[23] H. Tetsuka, R. Asahi, A. Nagoya, K. Okamoto, I. Tajima, R. Ohta, et al., Optically Tunable Amino-Functionalized Graphene Quantum Dots, Advanced Materials, 24(2012) 5333-8.

[24] Y. Lu, L. Zhang, H. Lin, The Use of a Microreactor for Rapid Screening of the Reaction Conditions and Investigation of the Photoluminescence Mechanism of Carbon Dots, Chemistry – A European Journal, 20(2014) 4246-50.

[25] S.K. Bhunia, A. Saha, A.R. Maity, S.C. Ray, N.R. Jana, Carbon Nanoparticle-based Fluorescent Bioimaging Probes, Scientific Reports, 3(2013) 1473.

[26] S. Hu, A. Trinchi, P. Atkin, I. Cole, Tunable Photoluminescence Across the Entire Visible Spectrum from Carbon Dots Excited by White Light, Angewandte Chemie International Edition, 54(2015) 2970-4.

[27] L. Bao, C. Liu, Z.-L. Zhang, D.-W. Pang, Photoluminescence-Tunable Carbon Nanodots: Surface-State Energy-Gap Tuning, Advanced Materials, 27(2015) 1663-7.

[28] H. Ding, J.-S. Wei, H.-M. Xiong, Nitrogen and sulfur co-doped carbon dots with strong blue luminescence, Nanoscale, 6(2014) 13817-23.

[29] S. Zhu, Q. Meng, L. Wang, J. Zhang, Y. Song, H. Jin, et al., Highly Photoluminescent Carbon Dots for Multicolor Patterning, Sensors, and Bioimaging, Angewandte Chemie International Edition, 52(2013) 3953-7.

[30] M.J. Krysmann, A. Kelarakis, P. Dallas, E.P. Giannelis, Formation Mechanism of Carbogenic Nanoparticles with Dual Photoluminescence Emission, Journal of the American Chemical Society, 134(2012) 747-50.

[31] S. Zhu, Y. Song, X. Zhao, J. Shao, J. Zhang, B. Yang, The photoluminescence mechanism in carbon dots (graphene quantum dots, carbon nanodots, and polymer dots): current state and future perspective, Nano Research, 8(2015) 355-81.

[32] T. Zhang, J. Zhu, Y. Zhai, H. Wang, X. Bai, B. Dong, et al., A novel mechanism for red emission carbon dots: hydrogen bond dominated molecular states emission, Nanoscale, 9(2017) 13042-51.

[33] H. Zhang, Y. Chen, M. Liang, L. Xu, S. Qi, H. Chen, et al., Solid-Phase Synthesis of Highly Fluorescent Nitrogen-Doped Carbon Dots for Sensitive and Selective Probing Ferric Ions in Living Cells, Analytical Chemistry, 86(2014) 9846-52.

[34] H. Ding, S.-B. Yu, J.-S. Wei, H.-M. Xiong, Full-Color Light-Emitting Carbon Dots with a Surface-State-Controlled Luminescence Mechanism, ACS Nano, 10(2016) 484-91.

[35] S. Qu, D. Zhou, D. Li, W. Ji, P. Jing, D. Han, et al., Toward Efficient Orange Emissive Carbon Nanodots through Conjugated sp2-Domain Controlling and Surface Charges Engineering, Advanced Materials, 28(2016) 3516-21.

[36] S. Srivastava, N.S. Gajbhiye, Carbogenic Nanodots: Photoluminescence and Room-Temperature Ferromagnetism, ChemPhysChem, 12(2011) 2624-32.

[37] F. Yuan, Z. Wang, X. Li, Y. Li, Z.a. Tan, L. Fan, et al., Bright Multicolor Bandgap Fluorescent Carbon Quantum Dots for Electroluminescent Light-Emitting Diodes, Advanced Materials, 29(2017) 1604436-n/a.

[38] L. Wang, S.-J. Zhu, H.-Y. Wang, S.-N. Qu, Y.-L. Zhang, J.-H. Zhang, et al., Common Origin of Green Luminescence in Carbon Nanodots and Graphene Quantum Dots, ACS Nano, 8(2014) 2541-7.

[39] S. Zhu, J. Shao, Y. Song, X. Zhao, J. Du, L. Wang, et al., Investigating the surface state of graphene quantum dots, Nanoscale, 7(2015) 7927-33.

[40] L. Guo, J. Ge, W. Liu, G. Niu, Q. Jia, H. Wang, et al., Tunable multicolor carbon dots prepared from well-defined polythiophene derivatives and their emission mechanism, Nanoscale, 8(2016) 729-34.

Chapter 6

Concluding Remarks and Recommendations for Future Developments

6.1 Concluding remarks

For the work reported in this doctoral dissertation, alternative novel precursors such as caffeine, PA are employed via various methods including thermal heating, hydrothermal and solvothermal methods to synthesize CDs. These obtained CDs are characterized in morphology, compositions and optical properties. It can be noticed that the newly prepared CDs exhibited excellent PL properties in blue or longer wavelength color emission (cyan) with excellent quantum yield. In addition, the as-prepared CDs are applied as photoluminescent platform for chemical sensing of heavy metal ion (Ag^{+}) and toxic organic compound (4-NP). More importantly, the as-prepared CDs also exhibited multicolor emission, that are blue, cyan, yellow and red color emission, under facile and mild solvothermal treatment of pyromellitic acid and various diamines.

The major points drawn from the present work are as follow:

1. Highly fluorescent N and S co-doped CDs with an excellent quantum yield of 69% were fabricated by a facile, one pot solid-state approach using caffeine as a new precursor. It seems that the superior optical characterization of the u-CDs can be attributed to the presence of both ammonium persulfate and urea in the precursors. Although it itself could not react with caffeine to produce CDs, urea combined with ammonium persulfate can facilitate the polymerization and carbonization of caffeine, producing larger as-synthesized CDs with more functional groups on their surface, as shown in TEM and XPS analysis. As a result, the u-CDs exhibited a red-shift in PL emission and a much higher quantum yields compared to that of the o-CDs. Furthermore, the as-prepared CDs can be used as a sensing probe for the label-free, sensitive detection of Ag^{+} ions with high sensitivity and selectivity.

2. Novel precursor, PA, was employed to fabricate brightly pure cyan color emission via a facile hydrothermal method. Moreover, the as prepared CDs exhibited

excitation wavelength in visible light and the emission in pure cyan color is an advantage comparing to other hydrothermal processes which are mostly resulted in blue color emission. It is noticeable that the blue color emission of most reported CDs was induced by ultraviolet (UV) excitation that limits their applications in bio-related fields. Also, the QYs of NCDs was measured to be 75%, which is higher value comparing to previous reports and even comparable with that of excellent N-doped carbon nanodots fabricated by hydrothermal citric acid, a unique molecule for the synthesis of CDs, with EDA in the same conditions. It is supposed that the basic formation mechanism might be similar to that between citric acid and diamine because the PA also has multi-carboxylic acid groups. First, the amide bond can be formed by a reaction between amines of EDA and carboxylic acids of PA. Then, the remaining carboxylic acids and amines in the intermediate structure can react further with other molecules to form polymeric networked structures followed by carbonization and aromatization. Furthermore, the as-prepared carbon dots were applied as nanoprobes for selective and sensitive determine of 4-NP in the presence of alkaline borate buffer, pH 9. It is believed that the formation of a zwitterionic spirocyclic Meisenheimer complex via the combination of NCDs and 4-NP resulted in the re-arrangement of positive and negative charges advanced the energy transfer process that leading to a substantially PL quenching of the NCDs. The effective quenching of NCDs in the presence of 4-NP is illustrated in the linear calibration curve of 4-NP which was obtained in the range of 0.1-100 μM 4-NP ($R^2 = 0.9993$), and the limit of detection (LOD) was calculated to be 17 nM (3.3σ) based on IUPAC standard.

3. Multicolor emission carbon dots which are exhibited blue, cyan, yellow and red color emission were synthesized via a facile one pot solvothemal method at mild temperature. The approach was employed pyromellitic acid as new precursor and various diamines as nitrogen sources. It can be seen that the maxima PL emission of these carbon dots were red-shifted from 409 nm (blue) to 486 nm (cyan), yellow (554 nm) and red (615 nm) when the nitrogen sources were changed from aliphatic diamine (EDA) to aromatic diamines (m-, o-, p-PD), respectively. It is supposed that the size of carbon dots, band gap energy and also the composition of nitrogen in the synthesized carbon dots are important factor contributed to the photoluminescence of carbon dots.

6.2 Recommendations for future developments

Since their accidentally discovery in 2004, luminescent carbon dots have been widely studied. Novel synthesis methods and enormous applications for carbon dots have been developed. However, most of the synthesized carbon dots are employed citric acid and its relatives or natural organic materials as precursors and these carbon dots exhibited blue color emission with low quantum yields that limited their practical applications. Moreover, very few papers reported synthesis of multicolor emission carbon dots and also proposed the mechanism for their photoluminescence properties as discussed in this dissertation. Therefore, it is necessary to further investigate novel green and economic precursors that could effectively fabrication of highly fluorescent carbon dots. The successful of synthesis longer wavelength excitation/emission or multicolor emission carbon dots with high quantum yields would be desirable. Moreover, further studies on mechanism for photoluminescence of carbon dots is remained a challenge for researchers who are interesting in investigating this new rising member of the carbon family.

The successful synthesis of multicolor emission carbon dots is a promising pathway to fabricate newly carbon dots exhibited longer wavelength color emission (e.g. red color) with highly quantum yields. These carbon dots could be applied in the field of electroluminescent light-emitting diodes (LEDs), the subject of intense academic research recently in anticipation for applications in liquid-crystal display (LCDs), full-color displays, and as next generation lightning sources in our daily life.

Although longer wavelength emission and excitation carbon have been successfully synthesized (e.g. cyan color emission at visible light excitation, multicolor emission) there was no application in bio-related fields such as bio-sensing, bio-imaging, and toxicity studies. For this reason, it is a demand that would be desirable to address in an upcoming work in the future.

List of Publications

Dissertation related publications

1. D. K. Dang, C. Sundaram, Y-L. T. Ngo, J. S. Chung, E. J. Kim, S. H. Hur

One pot solid-state synthesis of highly fluorescent N and S co-doped carbon dots and its use as fluorescent probe for Ag^+ detection in aqueous solution

Sensor and Actuator B: Chemical (accepted)

2. D. K. Dang, C. Sundaram, Y-L. T. Ngo, J. S. Chung, E. J. Kim, S. H. Hur

Pyromellitic acid derived highly fluorescent N doped carbon as nanoprobes for sensitive and selective determination of 4-nitrophenol.

(in manuscripts)

3. D. K. Dang, C. Sundaram, Y-L. T. Ngo, J. S. Chung, E. J. Kim, S. H. Hur

Multicolor emission carbon dots derived from pyromellitic acid and diamines via solvothermal method.

(in preparation)

Other publications

4. J. S. Xu, D. K. Dang, V. T. Tran, X. Y. Liu, J. S. Chung, S. H. Hur, W. M. Choi, E. J. Kim, P. A. Kolh

Liquid-phase exfoliation of graphene in organic solvents with addition of naphthalene

Journal of Colloid and Interface Science, Volume 418 (2014) 37-42.

5. J. S. Xu, D. K. Dang, J. S. Chung, S. H. Hur, W. M. Choi, E. J. Kim

Sonochemical fabrication of Cu_2O@C/graphene nanohybrid with a hierarchical architecture

Journal of Solid State Chemistry, Volume 220 (2014), 111-117.

6. D. K. Dang, E. J. Kim

Solvothermal-assisted liquid-phase exfoliation of graphite in a mixed solvent of toluene and oleylamine

Nanoscale Research Letter (2015) 10:6

7. N. B. Trung, T. V. Tam, D. K. Dang, K. F. Babu, E. J. Kim, J. B. Kim, W. M. Choi

Facile synthesis of three-dimensional graphene/nickel oxide nanoparticles composites for high performance supercapacitor electrodes

Chemical Engineering Journal, Volume 264 (2015), 603-609.

8. C. Sundaram, Y-L. T. Ngo, D. K. Dang, L. Sui, E. J. Kim, J. S. Chung, S. H. Hur

Highly enhanced visible light water splitting of CdS by green to blue upconversion

Dalton Transactions, September 13, 2017